UNIVERSITY OF CALIFORNIA,
IRVINE

Impaired T cell immunity in the Elderly via N-glycosylation

DISSERTATION

submitted in partial satisfaction of the requirements
for the degree of

DOCTOR OF PHILOSOPHY

in Biomedical Sciences

by

Ken Luke Hayama

Dissertation Committee:
Professor Michael Demetriou, Chair
Professor Michael McClelland
Professor Eric Pearlman

2020

DEDICATION

To

my parents,

Bakji Cho and Hatsuko Hayama,

and my brother Hiroki Hayama

TABLE OF CONTENTS

	Page
LIST OF FIGURES	iv
LIST OF TABLES	v
ACKNOWLEDGMENTS	vi
CURRICULUM VITAE	viii
ABSTRACT OF THE DISSERTATION	x
CHAPTER 1: Introduction	1
CHAPTER 2: Impaired T cell immunity in the elderly via interleukin-7 driven up-regulation of N-glycan branching	38
CHAPTER 3: Conclusions and Future Discussions	100

LIST OF FIGURES

		Page
Figure 1.1	IL-7 mediated signaling pathways	16
Figure 1.2	N-glycosylation branching pathway	17
Figure 1.3	Biosynthetic hexosamine pathway	18
Figure 2.1	N-glycan branching increases with age in mice	61
Figure 2.2	Lymphocytes from male do not exhibit increased N-glycan Branching with age	63
Figure 2.3	Age dependent increase in N-glycan branching suppresses T cell function and differentiation in mice	65
Figure 2.4	Regulating N-glycan branching in aged human PBMCs promote T cell activity and proliferation	67
Figure 2.5	Genetically regulating N-glycan branching promotes immune response to Salmonella in aged mice	69
Figure 2.6	Regulating N-glycan branching in aged male mice show minimal effect to Salmonella infection	71
Figure 2.7	Regulating IL-7 signaling reduces N-glycan branching to young phenotype	73
Figure 2.8	IL-7 signaling pathway increases with age to promote N-glycan branching	75
Figure 2.9	N-glycan branching increases with age in humans	77
Figure 2.10	Age-dependent increase in N-glycan branching also suppresses T cell activity in humans	79
Figure 2.11	IL-7 synergizes with age-dependent increase in endogenous N-acetylglucosamine to increase N-glycan branching in humans	81
Figure 2.12	Inhibiting N-glycosylation in human cells reverse age-induced suppression of T cell activity by N-glycan branching	83

LIST OF TABLES

		Page
Table 2.1	Female and Male IL-7 Signaling Pathway Genes	85
Table 2.2	Female Only Young vs. Old Naïve DEGs	86
Table 2.3	Male Only Young vs. Old Naïve DEGs	88
Table 2.4	Female and Male Overlapping DEGs	91
Table 2.5	Female Glycosylation and related DEGs	92

ACKNOWLEDGMENTS

I would like to thank my thesis advisor, Dr. Michael Demetriou. He is a scholar who possesses profound scientific insight and a depth of experience in immunology who influenced and promoted my growth throughout my study. I'll always remember his patience and kindness as I was graced with his mentorship. I am truly blessed to have been taken in as a member of his laboratory.

I would also like to thank the members of my advancement and dissertation committees, Dr. Michael McClelland, Dr. Eric Pearlman, Dr. Craig Walsh, and Dr. Manuela Raffatellu. Their guidance and support throughout the years have been beneficial to my research. I am grateful for their support and dedication to provide feedback towards the completion of my study.

I would like to express my gratitude to the following members of the Demetriou lab for their friendship and support: Barbara Newton, Raymond Zhou, Lindsey Araujo, Christie Mortales, Mike Sy, Sung-Uk Lee, Carey Li, and Khachik Khachikyan. I am also indebted to my undergraduate students, Kim Ly, Jasper Hai, Andrew Gong, Philip Lee, and Phuong Tran, who all performed research and experiments diligently. I would especially like to give special thanks to my lab mate Haik Mkhikian, whom has directly influenced and mentored me and guided this study from beginning to end. I would not have made much progress with my research without all the discussions and encouragement from my colleagues.

Lastly, I would like to give thanks to my parents and brother. Growing up my parents always encouraged me to pursue any topic that I am interested in. My brother

gave me the strength to strive towards graduate school by being the role model paving the way and showing anything is possible with hard work. Without their love and support I would not have had the courage and tenacity to pursue higher education in the topics that I love. I am truly grateful for all the opportunities that they have provided me and I hope to instill the same values in my own family.

CURRICULUM VITAE

Ken Luke Hayama

EDUCATION

UNIVERSITY OF CALIFORNIA, IRVINE — **Irvine, CA**
Ph.D. in Biomedical Sciences — 2020

UNIVERSITY OF CALIFORNIA, SAN DIEGO — **San Diego, CA**
B.S. Biochemistry and Cell Biology — 2009

HONORS AND AWARDS

NIH-BEST Professional Development Certificate	2018
American Association of Immunologists Trainee Abstract Award	2017
American Association of Immunologists Trainee	2017
Bio-Techne Go Everywhere Travel Grant March 2017 Recipient	2017
UC Irvine School of Medicine Graduate Travel Award	2017
AAAS/Science Program for Excellence in Science	2015-2017
2nd place poster award – 13th UC Irvine Immunology Fair	2015
Francisco J. Ayala Graduate Teaching Fellowship	2014
Mentoring Excellence Certificate	2014
Howard Hughes Medical Institute Graduate Teaching Fellowship	2013
Howard Hughes Medical Institute Travel Award	2013

PEER-REVIEWED PUBLICATIONS

1. **Hayama KL***, Mkhikian H*, Khachikyan K, Li CF, Zhou RW, Pawling J, Klaus S, Tran PQN, Ly KM, Gong AD, Saryan H, Hai JL, Lee PL, Rafatellu M, Dennis JW, and Demetriou M (2020). Impaired T cell immunity in the elderly via interleukin-7 and n-acetylglucosamine driven up-regulation of N-glycan branching. (To be submitted). * These authors contributed equally to this study
2. Brandt AU, Sy M, Lee SU, Newton B, Bellman-Strobl J, Pawling J, Li CF, Zimmermann H, **Hayama KL**, G Autreen, Rahman A, Yu Z, Kuhle J, Cooper G, Chien C, Scheel M, Dörr J, Wuerfel J, Dennis JW, Paul F, and Demetriou M (2020). N-Acetylglucosamine drives myelination and is associated with neuroprotection in multiple sclerosis. (To be submitted).
3. Mortales CL, Lee SU, Manousadjian A, **Hayama KL**, Demetriou M (2020). N-glycan branching decouples B cell innate and adaptive immunity to control inflammatory demyelination. *iScience* 23(8):101380. PMID: 32745987
4. Zocchi L, Wu SC, Wu J, **Hayama KL** and Benavente CA (2018). The cyclin-dependent kinase inhibitor flavopiridol (alvocidib) inhibits metastasis of human osteosarcoma cells. *Oncotarget* 9(34):23505-23518. PMID: 29805751

5. Tajiri N, Quach DM, Kaneko Y, Wu S, Lee D, Lam T, **Hayama KL**, Hazel TG, Johe K, Wu MC and Borlongan CV (2017). NSI-189, a small molecule with neurogenic properties, exerts behavioral, and neurostructural benefits in stroke rats. *J Cell Physiol* 232(10):2731-2740. PMID: 28181668
6. White CA, Pone EJ, Lam T, Tat C, **Hayama KL**, Li G, Zan H and Casali P (2014). Histone deacetylase inhibitors upregulate B cell microRNAs that silence AID and Blimp-1 expression for epigenetic modulation of antibody and autoantibody responses. *Journal of Immunology* 193(12):5933-50. PMID: 25392531
7. Tajiri N, Quach DM, Kaneko Y, Wu S, Lee D, Lam T, **Hayama KL**, Hazel TG, Johe K, Wu MC and Borlongan CV (2014). Behavioral and histopathological assessment of adult ischemic rat brains after intracerebral transplantation of NSI-566RSC cell lines. *PLoS One* 9(3):e91408. PMID: 24614895
8. Li G, White CA, Lam T, Pone EJ, DC Tran, **Hayama KL**, Zan H, Xu Z and Casali P (2013). Combinatorial H3K9acS10ph histone modifications in IgH locus S regions target 14-3-3 adaptors and AID to specify antibody class switch DNA recombination. *Cell Rep* 5(3):702-714. PMID: 24209747

ABSTRACT OF THE DISSERTATION

Impaired T cell immunity in the Elderly via N-glycosylation

By

Ken Luke Hayama

Doctor of Philosophy in Biomedical Sciences

University of California, Irvine, 2020

Professor Michael Demetriou, Chair

Immunological function declines with age, increasing the susceptibility and severity of infections in the elderly. For example, those who are 65 years of age and older make up around 15% of the U.S. population but represents nearly 90% of the deaths associated with influenza. This age-associated reduction in immunity has been attributed to the dysfunction of both the innate and adaptive immune system. Indeed, functional capacity of T cells is severely diminished and is exacerbated with age. Our lab has revealed that N-linked glycans play a critical role in controlling T cell immunity in mice and humans. Furthermore, irregularity in N-glycosylation as a mechanism for dysfunction of T cells in the elderly has not been examined as of yet.

Here we report N-glycan branching in T cells increases with age in females, leading to T cell hypo-activity and increased susceptibility to infection. Reducing N-glycan branching rejuvenates T cell activation, proliferation and pro-inflammatory T_H17 over anti-inflammatory Treg differentiation in aged female T cells. Susceptibility of aged female mice to *Salmonella typhimurium* invasion/dissemination was reduced by lowering N-glycan branching. A critical metabolic precursor of N-glycosylation and branching is N-

acetylglucosamine (GlcNAc), a common amino sugar that is part of the regular human diet. GlcNAc is endogenous to human serum, increases with age and correlates with N-glycan branching in female > male human T cells. Interleukin-7 (IL-7) signaling synergistically regulates N-glycan branching with environmental GlcNAc. Both adoptive transfer of aged female T cells into young mice and negatively regulating IL-7 reversed aged-dependent increase in N-glycan branching. These results suggest that age-dependent increases of N-glycan branching, via increased supply of GlcNAc and IL-7 signaling, impairs T cell immunity in the elderly females, providing a novel mechanism to supplement current treatments for age-related diseases.

Chapter 1

Introduction

Portions of this chapter are taken from:

Mackall, C.L. et al. Harnessing the biology of IL-7 for therapeutic application. *Nat Rev Immunol* **11**, 330-342 (2011)

Aging is associated with a decline in immune function, leading to an increase in frequency and severity of infection in the elderly. This age-associated immune deficiency has been attributed to dysfunction in both innate and adaptive arms of the immune system. Existing peripheral T and B cells display reduced functional capacity with age. Furthermore, there is a decrease in generating new naïve T and B cells in the elderly. This issue is further exacerbated with the rapidly growing aging population. It is necessary that we develop a fundamental understanding underlying the cellular and molecular basis of immune aging in order to develop appropriate therapeutic measures to prevent age-related bacterial and viral infections such as the ongoing COVID-19 pandemic, and provide insight into the higher incidences of cancer related mortalities within the elderly population.

It has been recognized that the immune system is influenced by aging, but perhaps not always in the same direction[1,2]. Aging of the immune system is characterized by the paradox of two properties that incorporate different sides of the same coin – immunosenescence, which is commonly defined as the deterioration of immune function in relation to age, and inflammaging, which refers to a chronic inflammatory condition including elevated levels of pro-inflammatory chemokines and cytokines[3]. The mechanisms that underlie these age-related defects are not well understood and have been a focus of many recent studies due to advances in cellular and molecular phenotyping[4]. To further our understanding and inspire new ideas and directions towards immune aging this dissertation will introduce and explore the role N-glycosylation plays in T cell immunity of the elderly.

Immunosenescence

People worldwide are living longer, however the increase in lifespan does not coincide with a healthy life including being free from disability and chronic diseases. There is an unavoidable complex process involving a continuous compromise of a normally functioning immune system, suggesting that this immune dysfunction is represented not by a pre-established moment but rather a slow and steady process. This phenomenon called immunosenescence, a term coined by Roy Walford, affects both natural and acquired immunity[5]. Immunosenescence involves a restructuring of innate and adaptive immune functions. There is a decline in immune responses due to dysregulated immune responses, leading to severe consequences to bacterial and viral infections including reduced responses to vaccination[2]. Although innate immunity is considered relatively well preserved in the elderly, adaptive immunity is more susceptible due to age-associated functional decline and antigen burden that an individual is exposed to during their lifetime[6]. Various factors including genetics, nutrition, previous exposure to microorganisms, and steroid hormones differentially modulate the immune system[7-9]. Consequently, infections and cancer occur more frequently within the elderly population.

While the overall number of circulating T cells remains relatively consistent with age, multifaceted changes occur that result in a decline of adaptive immune response with age. Critical changes in T cells that occur with advancement in age include decreased numbers of naïve T cells[10-12], increased population of memory cells[13,14], and decreased cellular proliferation and antigen response[15,16]. The developmental site of T cells, the thymus, atrophies with age, an phenomenon accelerating following onset of puberty[17,18]. This decline is due to defects in thymic stromal cell production of growth

factors and cytokines[19,20]. In an attempt to restore the size of the depleted population of peripheral T cells, existing populations of naïve T cells undergo homeostatic proliferation[21,22]. Thus, while the ratio between naïve and memory T cells begins high at a young age, it gradually reverses with age due to thymic involution combined with life-long immune responses to foreign pathogens. The long-term survival for these remaining T cells are sustained by contact with cytokines and/or peptide-major histocompatibility complex (pMHC)[23,24]. Naïve T cells are sustained largely by interleukin-7 (IL-7), whereas memory T cell homeostasis requires both IL-7 and IL-15[25].

Interleukin-7: mediator of homeostatic proliferation

IL-7 induces homeostatic proliferation of naïve T cells to maintain the naïve pool in adults following involution of the thymus. IL-7 is a member of the common gamma-chain (γc, CD132, IL2Rg) cytokine family, also identified as the IL-2 superfamily[26], which comprises IL-2, IL-4, IL-7, IL-9, IL-15 and IL-21[27] (**Fig. 1.1**). The receptors for these cytokines all share the same common gamma chain (γc, or CD132) while coming with cytokine-specific receptor subunits to form their unique heterodimeric receptor. An exception exists for IL-2R and IL-15R, which comprises a third shared β chain (CD122)[28]. IL-7R comprises CD132 (γc) and its own unique α chain, CD127 (IL7Rα). The interleukins and ectodomains share very little sequence identity with each other, including their binding interfaces. Previous studies have shown that glycosylation does not play a role in complex formation between IL-2, IL-4, IL-6, IL-15, and IL-21 with their receptors[29-33]. IL-7 has three asparagines with six asparagines in the IL-7Rα ectodomain that may be N-glycosylated through their Asn-X-Ser/Thr (NXS/T, X≠P) recognition motif[34]. Although

previous studies have determined that glycosylation does not affect the binding or function of IL-7 to IL-7Rα[35], it has been found that N-glycosylation outside the binding interface of IL-7/IL-7Rα indirectly accelerates the on-rate and binding[36], suggesting other cytokine members may also be influenced indirectly through N-glycosylation. In addition to binding to IL-7, IL-7Rα also associates with thymic stromal lymphopoietin (TSLP) receptor to form a heterodimeric receptor complex that binds to TSLP[37] . TSLP is an IL-7-like cytokine that is also produced by stromal cells, in addition to epithelial cells and fibroblasts in the context of inflammation[38]. Numerous genomic studies have implicated TSLP to allergic diseases including atopic dermatitis and increased risk of asthma[39-42].

IL-7 is mainly secreted by stromal cells in lymphoid organs[43-45]. Current studies suggest that the production of IL-7 mRNA transcripts seem to occur at a fixed constitutive rate and is not influenced by extrinsic stimuli including feedback from IL-7 or the size of lymphocyte population[46,47]. Instead, the amount of available IL-7 is regulated by consumption by innate lymphoid cells (ILCs) and T cells rather than production[48]. Typically, the amount of available IL-7 is sufficient to maintain a finite number of T cells. After the lymphoid compartment is depleted, available T cells would encounter abundant IL-7 and undergo homeostatic proliferation until equilibrium is re-established[46]. This increase in number of mature T cells result from increased proliferation of peripheral naïve T cells rather than from enhanced thymic function[49]. The mechanism of production and availability of IL-7 seems to be unique and unlike other γc family members, such as IL-2 where production increases and decreases with T cell expansion and contraction respectively[50].

Unlike IL-7 where there is a constant level of transcription, the expression of the gene encoding IL-7Rα is increased or decreased depending on the stage in T and B cell development. In addition, IL-7Rα expression in mature T cells are dramatically influenced by external stimuli including cytokines such as IL-7[51]. IL-7 suppresses cell-surface expression of IL-7Rα in T cells by downregulating transcription of the gene encoding IL-7Rα[51]. The amount of IL-7Rα on the cell surface plays a critical role in equilibrium by expressing higher levels in order to receive more signals by IL-7 for survival and proliferation. More IL-7Rα expressed results in more IL-7 consumed, therefore depriving neighboring cells of their signals. Since encountering IL-7 results in T cells transiently downregulating IL-7Rα expression, T cells would stop unnecessary consumption of IL-7, thereby regulating IL-7 availability for nearby cells to maintain a homeostatic population[51,52]. In addition to IL-7, other γc family members such as IL-2, IL-4, and IL-15 and even IL-6 which uses a receptor from a different family suppresses IL-7Rα expression[51]. TCR activation also resulted in inhibited IL-7Rα expression[53-55].

IL-7 signaling pathways

IL-7 signals mainly through two different pathways: Jak-Stat (Janus kinase-Signal transducer and activator of transcription) and PI3K(phosphatidylinositol-3-kinase)/Akt. IL-7 engaging IL-7Rα results in Jak3 selectively binding to the γc chain whereas Jak1 binds to IL-7Rα[56-59]. Mutations in either γc or Jak3 results in severe combined immunodeficiency (SCID) in humans[60-64]. The recruitment of Jak1 and Jak3 induces transphosphorylation which both increases their own intrinsic kinase activity and also the phosphorylation of the Y449 site on IL-7Rα[65,66]. The phosphorylated receptor then

becomes a docking site for Stat5 protein binding via SH2-phosphotyrosine interaction where Stat5 becomes phosphorylated by Jaks and dimerizes through their reciprocal phosphotyrosine-SH2 interaction[67,68]. Stat5 dimers are then exported into the nucleus to bind DNA[69,70]. The suppressor of cytokine signaling-1 (SOCS1) protein inhibits IL-7 signaling by either binding and inhibiting Jak1/3 through their kinase inhibitory region (KIR), binding cytokine receptors to block Stat recruitment, or by functioning as ubiquitin ligases that mediate degradation of the signaling complex[65,71-73]. The absence of IL-7 signaling either by administering an anti-IL-7 neutralizing monoclonal antibody[74], in IL-7$^{-/-}$[75], IL-7Rα$^{-/-}$[76,77], γc$^{-/-}$[78], or Jak3$^{-/-}$[79] mice results in reduced thymic cellularity and lack of homeostatic proliferation.

The N-glycosylation pathway

All eukaryotic cells are surrounded by a dense layer of sugar chains and the proteins and lipids to which they are bound to, resulting in a structure collectively termed as the glycocalyx. The term originates from two Latin terms to describe its arrangement – the first which is “glyco” literally translates to “sweet,” indicating the key building units consisting of various sugars and monosaccharides, such as mannose, glucose, and galactose. These sugars are connected in a plethora of combinations which vary in number, size, and complexity, forming the sugar conjugates known as glycans. Glycans are bound to proteins or lipids, resulting in a diverse array of glycoproteins, proteoglycans, and glycolipids. The term “calyx” translates into “outer coverings or husk.” This indicates the location as to where these sugars reside – extracellular to the cell membrane. With a dynamic and complex variety of cell-surface glycoproteins, the glycocalyx can vary in size

up to 100 nanometers thick, a size ten times wider than the plasma membrane. The glycocalyx dominates cell surface topology, suggesting that these glycans play a significant role in regulating cellular communication and function.

Two major classes of glycoproteins are defined accordingly to what the glycan is attached to on the protein. If the glycan is attached via nitrogen (N) in the asparagine side chain, then it is defined as N-glycans. On the other hand, if the glycan is attached via oxygen (O) located within a serine or threonine side chain, then it is defined as an O-glycan. A majority of cell surface receptors and transporters are co- and post-translationally modified with these N-linked and O-linked glycans in the endoplasmic reticulum (ER) with further modifications occurring within the Golgi apparatus[80,81]. Modifications of these glycans are achieved by a series of sequential glycohydrolase and glycosyltransferase-mediated reactions resulting in multiple glycoforms that differ in binding avidity to sugar-binding proteins such as galectins (**Fig. 1.2**).

N-glycosylation of proteins begins with the transfer of a pre-assembled glycan, $Glc_3Man_9GlcNAc_2$ (three glucoses, nine mannoses, and two N-acetylglucosamines), by oligosaccharyltransferases within the endoplasmic reticulum to the asparagine (Asn) residue of Asn-X-Ser/Thr (NXS/T, X≠P) motifs[82]. The newly added glycan is then modified by the removal of three glucose molecules by glucosidase I (GI) and glucosidase II (GII). Further modifications occur during transit through the Golgi via removal of mannose (Man) residues from the trimmed glycan, $Man_9GlcNAc_2$, by Mannosidase I (MI). This results in the remaining $Man_5GlcNAc_2$ glycan structure which is the starting substrate for the first N-acetylglucosaminyltransferase (Mgat) enzyme (**Fig. 1.2**)[83].

The Golgi N-acetylglucosaminyltransferase enzymes I, II, IV and V (encoded by Mgat1, Mgat2, Mgat4a/b and Mgat5) act in a sequential order to initiate N-glycan branching by catalyzing the addition of N-acetylglucosamine (GlcNAc) from uridine diphosphate N-acetylglucosamine (UDP-GlcNAc) onto mannose molecules to form N-glycan intermediates. The first N-glycan intermediate is formed through the addition of GlcNAc by Mgat1, creating a mono-antennary N-glycan structure[84]. Mannosidase II (MII) modifies this initial structure by removing two mannoses to make room for Mgat2 to add an additional GlcNAc to form a bi-antennary N-glycan structure. Mgat4 and Mgat5 may further modify these N-glycans by catalyzing the addition of another GlcNAc molecule onto mannoses, resulting in a tri- and tetra-antennary N-glycan structure respectively. Although these Golgi branching enzymes utilize the common sugar-nucleotide substrate GlcNAc, they do so with declining efficiency such that both Mgat4 and Mgat5 activity are limited by the metabolic production of UDP-GlcNAc. Thus, activity of Golgi enzymes and the availability of substrates combine to determine the degree of N-glycan branching. These GlcNAc branches can be extended with the addition of galactose (Gal) by galactosyltransferase-3 (GalT3) to form the disaccharide N-acetyllactosamine (LacNAc). These LacNAc units are binding ligands for galectin family of sugar binding proteins and can be extended to synthesize poly-N-LacNAc via alternating actions of the addition of GlcNAc by β1,3-N-acetylglucosaminyltransferase-2 (β_3GnT2, an i-extension enzyme iGnT) and galactose by GalT3[85,86]. LacNAc branches and/or extensions can be further modified or terminated through fucosylation and sialylation[80,87-89]. The plant lectin L-PHA (*Phaseolus vulgaris, leukoagglutinin*) specifically binds to β1,6 branched N-glycans, a product of Mgat5, and can be utilized as a sensitive marker for determining levels of N-

glycan branching at the cell surface. Another plant lectin, LEA (Lycopersicon esculentum), recognizes and binds to poly-N-LacNAc structures and can be utilized to assess the degree of branching extension.

Regulation of N-glycan branching by the hexosamine biosynthetic pathway

The hexosamine biosynthetic pathway competes with glycolysis for available glucose to synthesize the sugar-nucleotide uridine diphosphate-N-acetylglucosamine (UDP-GlcNAc), the substrate utilized by the Golgi branching enzymes (**Fig. 1.3**). This pathway merges with glycolysis by utilizing fructose-6-phosphate to form glucosamine-6-phosphate. Although glucose is mainly metabolized through glycolysis, about 2-5% enters the hexosamine pathway to synthesize UDP-GlcNAc *de novo*. Only a small percentage of fructose-6-phosphate is converted to glucosamine-6-phosphate due to the rate-limiting enzyme glutamine fructose-6-phosphate amidotransferase (GFAT). Alternatively, GlcNAc can also be directly salvaged into the hexosamine pathway via phosphorylation by N-acetyl glucosamine kinase (NAGK) to generate UDP-GlcNAc, thereby bypassing the rate-limiting first step of the hexosamine biosynthetic pathway.

In addition to differing Golgi enzyme activity responsible for N-glycan modifications, regulating biosynthesis of UDP-GlcNAc supply through the hexosamine pathway results in a versatile and dynamic glycoforms differing between the same proteins. Since N-glycan branching is dependent on the supply of UDP-GlcNAc via the hexosamine pathway, metabolic supplementation with GlcNAc should enhance N-glycan branching. Indeed, supplementing cells with GlcNAc with/without uridine has been shown to effectively increase surface N-glycan branching[90]. Furthermore, GlcNAc can be used

alone or with other immune-regulatory drugs as it has been used as a dietary supplement for years without reported adverse effects[91]. GlcNAc enters the cells through micropinocytosis, a process that is dependent upon the rate of membrane turnover. Therefore, GlcNAc efficiency of enhancing surface N-glycan branching is increased in rapidly proliferating cells that display high amounts of membrane turnover in comparison to resting cells.

The galectin-glycoprotein lattice

Galectins are a family of carbohydrate binding proteins that are ubiquitously expressed at the cell surface. Each of these galectins have a carbohydrate recognition domain (CRD) which binds to LacNAc units on glycans[92]. In mammals, there are 15 known galectins that interact with multivalent glycan ligands on glycoproteins to form molecular lattices. These soluble galectins have been categorized into three structural groups defined as prototypical, tandem-repeat, and chimeric galectins[93,94]. The first prototypical group contains a single CRD and consists of galectin-1, -2, -5, -7, -10, -11, -13, -14, and -15. Although they possess a single CRD, they frequently dimerize, similar to tandem-repeat galectins which contain two CRDs and consists of galectin-4, -6, -8, -9, and -12[95]. The chimeric galectin -3 contains a single CRD that can form a pentamer in the presence of multivalent ligands[96].

The binding avidity between galectins and glycoproteins is proportional to the number of LacNAc units that is determined by the number of N-glycan sites, the degree of N-glycan branching (mono- to tetra-antennary) and the degree of branching extension of poly-N-LacNAc. The aforementioned is regulated by the expression and efficiency of

Golgi enzymes and their respective substrates. Thus, binding avidity between galectins and glycoproteins increase in proportion to LacNAc content produced by N-glycan Golgi enzymes, a factor established by genetic (enzyme expression and activity) and metabolic (UDP-GlcNAc substrate quantity) factors. Galectins binding to N-glycan ligands via LacNAc structures forms the galectin-glycoprotein lattice which regulates receptors and transporters via lateral movement, clustering, membrane localization and cell surface retention/endocytosis[97].

Regulating T cell growth and signaling by N-glycan branching

The plasticity of T cell immune response is regulated by an intricate interplay of co-stimulatory and co-inhibitory signals to benefit the host while preventing any aberrant behaviors. T cell activation and proliferation is initiated through the clustering of a threshold number of T cell receptors (TCRs) at a specialized contact site, an immunological synapse, where the TCRs recognize foreign peptides bound to the major histocompatibility complex (MHC) site displayed on the surface of the antigen-presenting cell (APC)[98-100]. The number of TCRs required for clustering to initiate T cell activation is decreased by co-stimulatory signaling by CD28 to CD80/CD86 on APCs[101,102]. The galectin-glycoprotein lattice however negatively regulates T cell activation through the binding of multivalent galectins, such as galectin-1 and galectin-3, to N-glycans of the TCR complex by limiting lateral movement and clustering in response to ligands. The binding affinity of TCR for peptide-MHC is similar to that of galectins to LacNAc units in N-glycans, suggesting that the peptide-MHC complex must overcome galectin-TCR interactions in order to induce T cell response[103]. Indeed, by reducing N-glycan branching

through deletion of N-glycan Golgi enzymes Mgat1, Mgat2, Mgat5, or poly-LacNAc extending β3GnT2 reduces binding avidity of galectins to TCRs, resulting in robust T cell activation[104-110] but also promotes dysregulation of T cell activation and autoimmune disorders[110-112]. Consistent with the aforementioned, removal of the encoded N-glycan sites within the TCR also results in an increase in T cell activation[113]. Collectively, N-glycan branching defines the limits of TCR affinity for peptide-MHC interactions essential for T cell activation.

Regulating the T cell response through inhibitory signaling is critical for T cell self-tolerance and growth arrest. Cytotoxic T-lymphocyte associated protein 4 (CTLA-4, CD152) is an inhibitory receptor that is expressed at the cell surface 4-5 days after T cell activation to induce growth arrest[114]. CTLA-4 competes with CD28 for CD80/CD86 co-stimulatory ligands expressed on APCs to negatively influence T cell proliferation. Transcriptional levels and intracellular stores of CTLA-4 increase in proportion to TCR signaling during early T cell activation. However, endosomal trafficking limits expression of CTLA-4 on the cell surface, resulting in it being predominantly found within the endosomes. On the other hand, CD28 is constitutively expressed on the cell surface of T cells, although it has a weaker avidity to CD80/CD86 in comparison to CTLA-4. In addition, CTLA-4 has a low number of N-glycan sites (two NXS/T motifs, where X≠P) and is therefore highly sensitive to metabolic supplement of UDP-GlcNAc and upregulation of N-glycan branching. Indeed, T cells deficient in Mgat5 have decreased levels of CTLA-4[105]. However, strong co-stimulation with CD28 and enhanced surface N-glycans through supplementation of UDP-GlcNAc resulted in similar surface levels of CTLA-4 in activated $Mgat5^{-/-}$ and $Mgat5^{+/+}$ T cells[83,115,116]. Galectins bound to upregulated N-glycans attached

to CTLA-4 enhanced surface retention by opposing endocytic loss, thereby promoting and sustaining growth arrest signaling. In addition to CTLA-4, programmed cell death protein 1 (PD-1) is an immune checkpoint inhibitor that fine-tunes T cell responses and is a major regulator of T cell exhaustion[117]. Our lab has shown that N-glycan branching markedly enhances PD-1 surface expression and blocking N-glycan branching with small molecule inhibitor kifunensine (which targets MI) in human $CD4^+$ T cells reduces expression of PD-1 on the cell surface (unpublished data). Notably, the expression of PD-1 increases on T cells of older individuals and inhibiting it partially restores T cell functional competence[118-120]. Blocking immune suppression via CTLA-4 and PD-1 are currently popular FDA approved treatments for cancer immunotherapy[121-123].

Following growth arrest, activated T cells differentiate into effector T cells dependent on induction of certain transcription factors in response to TCR signal strength[124,125] coupled with cytokines produced and secreted by an activated innate immune system. Under non-polarizing conditions (i.e. absence of exogenous cytokines), N-glycan branching promotes differentiation of $CD4^+$ T cells into anti-inflammatory T_H2 cells (secretes IL-4) while inhibiting pro-inflammatory T_H1 cells (secrets IFNγ)[126,127]. Blocking N-glycan branching via Mgat1 deletion eliminates the ability of CD4+ T cells to differentiate into Tregs[104]. N-glycan branching drives induced Treg differentiation by promoting IL-2Rα (CD25) surface expression and signaling in blasting $CD4^+$ T cells. In addition, N-glycan branching also critically suppresses pro-inflammatory T_H17 differentiation[104]. T_H17 inducing cytokines (TGFβ+IL-6+IL-23) down-regulates branching in blasting $CD4^+$ T cells, resulting in lowered IL-2Rα surface expression and associated IL-2 signaling to promote T_H17 differentiation over iTreg. Reversing lowered branching

caused by T_H17 induction by supplementing GlcNAc blocks T_H17 differentiation and induces a cell fate switch to iTregs by restoring IL-2Rα and thus IL-2 signaling.

T cell dysfunction is influenced by many factors including disruption of glycosylation at the cell surface. Our lab has shown that in T cells, N-glycan branching globally influences T cell activation and differentiation. Given the importance of N-glycan branching in negatively regulating T cell function it is a surprise that nothing is known of their role in immune senescence. Here we explore for the first time how N-glycan branching is involved in T cell immune responses in the elderly.

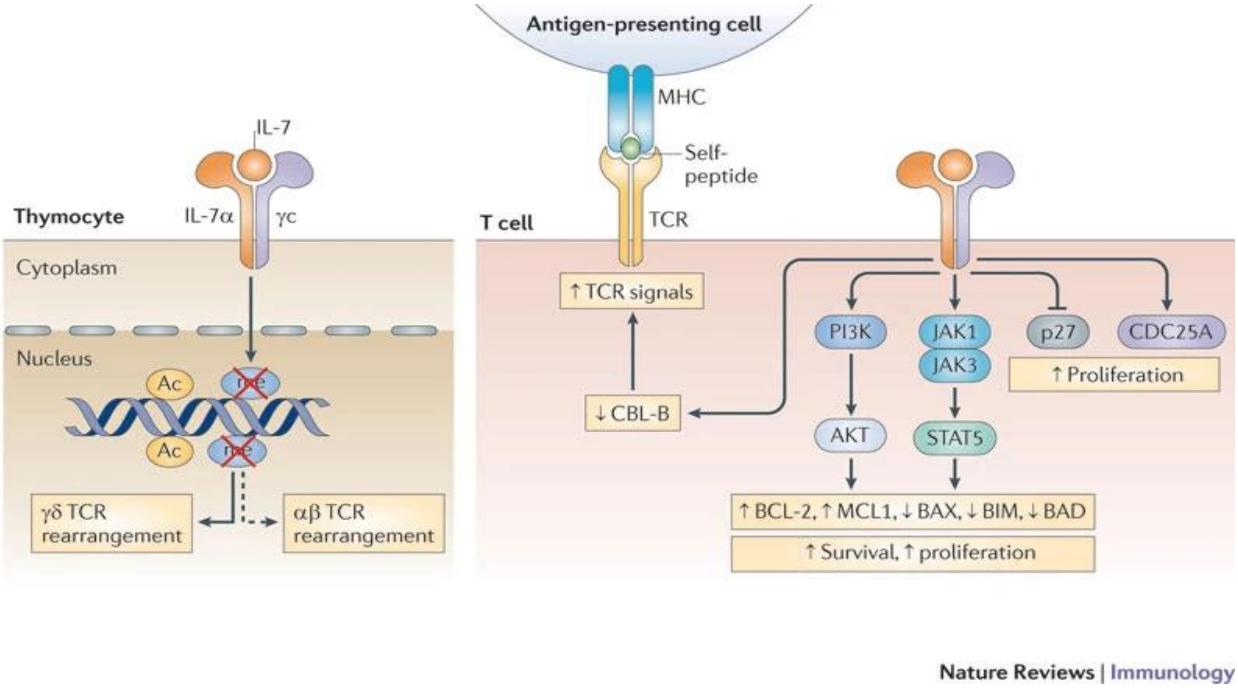

Figure 1.1 IL-7 mediated signaling pathways. IL-7 signals through the IL-7 receptor, a heterodimer consisting of IL-7Rα and the common γ chain. During T cell development within the thymus, IL-7 signaling participates in TCR gene rearrangement by histone acetylation and DNA demethylation. After maturation, IL-7 mediated signaling initiates downstream signaling pathways by interacting with JAK1, JAK3, and PI3K, resulting in the phosphorylation and activation of STAT5. This results in up and downregulated expression of multiple genes responsible for survival and proliferation. IL-7 signaling can also leads to reduced expression of p27 and increased expression of CDC25A, resulting in further upregulation of proliferation. Some of the effects of IL-7 can also be substituted for by having IL-7Rα complexed with thymic stromal lymphopoietin (TSLP) receptor (TSLPR). Abbreviations: MHC, Major Histocompatibility Complex; IL-7, Interleukin-7; IL-7α, Interleukin-7α (also known as CD127); γc, common cytokine receptor γ–chain (also known as CD132); TCR, T cell receptor; Ac, histone acetylation; me, DNA demethylation; γδ TCR, gamma delta T cell receptor; αβ TCR, alpha beta T cell receptor; CBL-C, Casitas B-lineage lymphoma B; PI3K, phosphoinositide 3-kinase (PI3K); JAK1, Janus kinase 1; JAK3, Janus kinase 3; p27, cyclin-dependent kinase inhibitor 1b (also known as $p27^{Kip1}$); CDC25A, cell division cycle 25 homologue A; AKT, protein kinase B; STAT5, signal transducer and activator of transcription 5; BCL-2, B cell lymphoma 2; MCL1, myeloid cell leukemia sequence 1; BAX, BCL-2-associated X protein; BIM, BCL-2-interacting mediator of cell death; BAD, BCL-2 antagonist of cell death.
Image © Mackall C.L. et al. *Nature Reviews Immunology* **Volume 11**, pages 330-342 (2011)

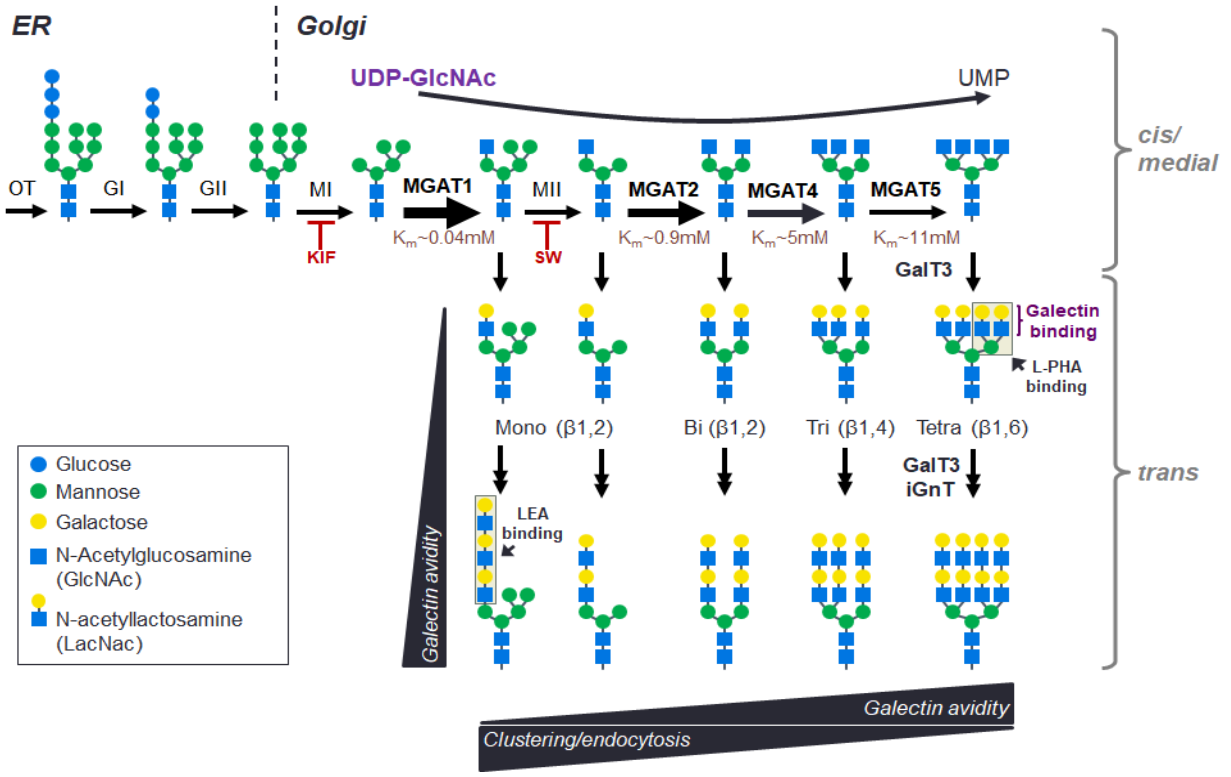

Figure 1.2 N-glycosylation branching pathway. Oligosaccharyltransferase transfers a pre-assembled glycan, $Glc_3Man_9GlcNAc_2$, to the NxS/T motifs (Asp-X-Ser-Thr where X ≠ Pro) on glycoproteins within the endoplasmic reticulum (ER). These glycans are further modified by mannosidases (MI and MII) and N-acetylglucosaminyltransferase (Mgat) enzymes, which act sequentially to generated N-glycans that display increasing avidities for galectins. Mgat1, 2, 4, and 5 utilizes the same sugar-nucleotide donor, UDP-GlcNAc, but with declining efficiency such that both Mgat4 and Mgat5 are limited for branching by the metabolic production of UDP-GlcNAc. Galactosyltransferase 3 (GalT3) and iGnT further extends the branches by adding galactose to GlcNAc, creating N-acetyllactosamine (LacNAc) which can be bound by galectins. Small molecular inhibitors kifunensine (KIF) and swainsonine (SW) can be used to eliminate or reduce branching respectively. Plant lectins L-PHA (*Phaseolus vulgaris*, leukoagglutinin) and LEA (*Lycopersicon Esculentum* lectin) binding sites are also shown. Abbreviations: OT, oligosaccharyltransferase; GI, glucosidase I; GII, glucosidase II; MI, mannosidase I; MII, mannosidase II; Mgat, N-acetylglucosaminyltransferase; GalT3, Galactosyltransferase 3; iGnT, i-branching enzyme b-1,3-N-acetylglucosaminyltransferase; KIF, kifunensine; SW, swainsonine; GlcNAc, N-acetyl glucosamine; UDP, uridine diphosphate; UMP, uridine monophosphate; Km, Michaelis constant of the enzyme.

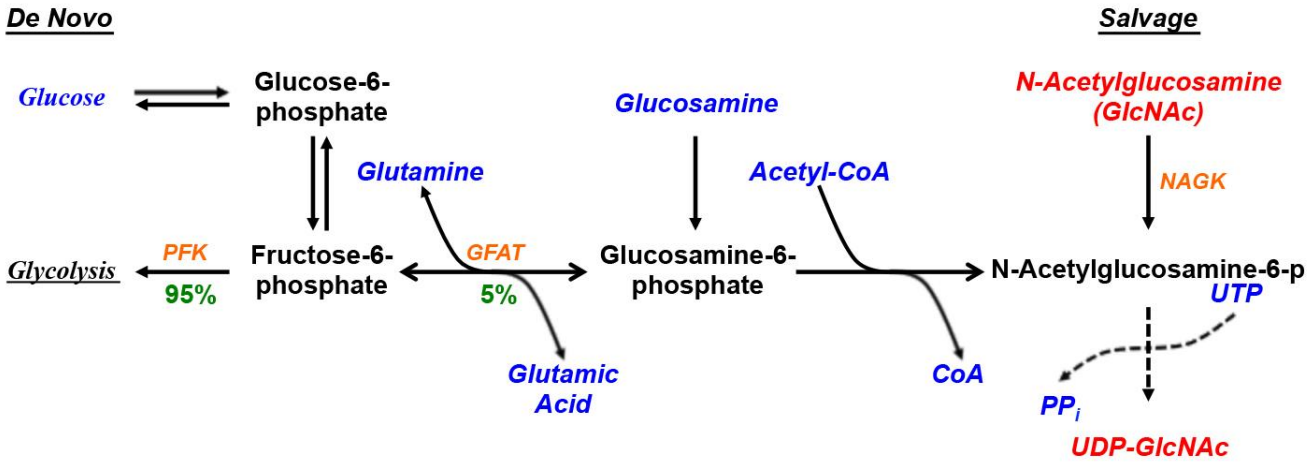

Figure 1.3 Hexosamine Biosynthetic Pathway. Glucose enters the cell *de novo* through a glucose transporter and is metabolized. After being converted into fructose-6-phosphate, the substrate has an option of continuing through glycolysis. However, the hexosamine biosynthetic pathway merges from here to form glucosamine-6-phosphate by the rate-limiting enzyme glutamine fructose-6-phosphate amidotransferase (GFAT) by utilizing glutamine as an amino donor[128]. To produce N-acetylglucosamine-6-phosphate, Glucosamine-6-phosphate can either be acetylated or GlcNAc can be salvaged via micropinocytosis and enter the hexosamine pathway by N-acetylglucosamine kinase (NAGK). N-acetylglucosamine-6-phosphate is further isomerized to N-acetylglucosamine-1-phosphate and is ultimately activated into UDP-N-acetylglucosamine (UDP-GlcNAc), the common precursor for glycosylation. Abbreviations: PFK, phosphofructokinase; GFAT, glutamine fructose-6-phosphate amidotransferase; CoA, coenzyme A; GlcNAc, N-acetylglucosamine; NAGK, N-acetylglucosamine kinase; UTP, uridine triphosphate; PPi, inorganic pyrophosphate; UDP, uridine diphosphate.

References

1 Solana, R. *et al.* Innate immunosenescence: effect of aging on cells and receptors of the innate immune system in humans. *Semin Immunol* **24**, 331-341, doi:10.1016/j.smim.2012.04.008 (2012).

2 Montgomery, R. R. & Shaw, A. C. Paradoxical changes in innate immunity in aging: recent progress and new directions. *J Leukoc Biol* **98**, 937-943, doi:10.1189/jlb.5MR0315-104R (2015).

3 Fagiolo, U. *et al.* Increased cytokine production in mononuclear cells of healthy elderly people. *Eur J Immunol* **23**, 2375-2378, doi:10.1002/eji.1830230950 (1993).

4 Gruver, A. L., Hudson, L. L. & Sempowski, G. D. Immunosenescence of ageing. *J Pathol* **211**, 144-156, doi:10.1002/path.2104 (2007).

5 Walford, R. L. The Immunologic Theory of Aging. *Gerontologist* **4**, 195-197, doi:10.1093/geront/4.4.195 (1964).

6 Nikolich-Zugich, J. The twilight of immunity: emerging concepts in aging of the immune system. *Nat Immunol* **19**, 10-19, doi:10.1038/s41590-017-0006-x (2018).

7 Caruso, C., Accardi, G., Virruso, C. & Candore, G. Sex, gender and immunosenescence: a key to understand the different lifespan between men and women? *Immun Ageing* **10**, 20, doi:10.1186/1742-4933-10-20 (2013).

8 Accardi, G. & Caruso, C. Immune-inflammatory responses in the elderly: an update. *Immun Ageing* **15**, 11, doi:10.1186/s12979-018-0117-8 (2018).

9 Pawelec, G. Hallmarks of human "immunosenescence": adaptation or dysregulation? *Immun Ageing* **9**, 15, doi:10.1186/1742-4933-9-15 (2012).

10 Goronzy, J. J., Fang, F., Cavanagh, M. M., Qi, Q. & Weyand, C. M. Naive T cell maintenance and function in human aging. *J Immunol* **194**, 4073-4080, doi:10.4049/jimmunol.1500046 (2015).

11 Lazuardi, L. *et al.* Age-related loss of naive T cells and dysregulation of T-cell/B-cell interactions in human lymph nodes. *Immunology* **114**, 37-43, doi:10.1111/j.1365-2567.2004.02006.x (2005).

12 Moro-Garcia, M. A., Alonso-Arias, R. & Lopez-Larrea, C. When Aging Reaches CD4+ T-Cells: Phenotypic and Functional Changes. *Front Immunol* **4**, 107, doi:10.3389/fimmu.2013.00107 (2013).

13 De Paoli, P., Battistin, S. & Santini, G. F. Age-related changes in human lymphocyte subsets: progressive reduction of the CD4 CD45R (suppressor inducer) population. *Clin Immunol Immunopathol* **48**, 290-296, doi:10.1016/0090-1229(88)90022-0 (1988).

14 Utsuyama, M. *et al.* Differential age-change in the numbers of CD4+CD45RA+ and CD4+CD29+ T cell subsets in human peripheral blood. *Mech Ageing Dev* **63**, 57-68, doi:10.1016/0047-6374(92)90016-7 (1992).

15 Chou, J. P. & Effros, R. B. T cell replicative senescence in human aging. *Curr Pharm Des* **19**, 1680-1698, doi:10.2174/138161213805219711 (2013).

16 Weng, N. P. Aging of the immune system: how much can the adaptive immune system adapt? *Immunity* **24**, 495-499, doi:10.1016/j.immuni.2006.05.001 (2006).

17 Dorshkind, K., Montecino-Rodriguez, E. & Signer, R. A. The ageing immune system: is it ever too old to become young again? *Nat Rev Immunol* **9**, 57-62, doi:10.1038/nri2471 (2009).

18 Haynes, B. F., Sempowski, G. D., Wells, A. F. & Hale, L. P. The human thymus during aging. *Immunol Res* **22**, 253-261, doi:10.1385/IR:22:2-3:253 (2000).

19 Ki, S. *et al.* Global transcriptional profiling reveals distinct functions of thymic stromal subsets and age-related changes during thymic involution. *Cell Rep* **9**, 402-415, doi:10.1016/j.celrep.2014.08.070 (2014).

20 Tibbetts, T. A., DeMayo, F., Rich, S., Conneely, O. M. & O'Malley, B. W. Progesterone receptors in the thymus are required for thymic involution during pregnancy and for normal fertility. *Proc Natl Acad Sci U S A* **96**, 12021-12026, doi:10.1073/pnas.96.21.12021 (1999).

21 Goldrath, A. W. & Bevan, M. J. Selecting and maintaining a diverse T-cell repertoire. *Nature* **402**, 255-262, doi:10.1038/46218 (1999).

22 Surh, C. D. & Sprent, J. Homeostatic T cell proliferation: how far can T cells be activated to self-ligands? *J Exp Med* **192**, F9-F14, doi:10.1084/jem.192.4.f9 (2000).

23 Sprent, J. & Surh, C. D. Normal T cell homeostasis: the conversion of naive cells into memory-phenotype cells. *Nat Immunol* **12**, 478-484, doi:10.1038/ni.2018 (2011).

24 Sprent, J. & Surh, C. D. Cytokines and T cell homeostasis. *Immunol Lett* **85**, 145-149, doi:10.1016/s0165-2478(02)00221-3 (2003).

25 Becklund, B. R. *et al.* The aged lymphoid tissue environment fails to support naive T cell homeostasis. *Sci Rep* **6**, 30842, doi:10.1038/srep30842 (2016).

26 Kondo, M. *et al.* Functional participation of the IL-2 receptor gamma chain in IL-7 receptor complexes. *Science* **263**, 1453-1454, doi:10.1126/science.8128231 (1994).

27 Kinter, A. L. *et al.* The common gamma-chain cytokines IL-2, IL-7, IL-15, and IL-21 induce the expression of programmed death-1 and its ligands. *J Immunol* **181**, 6738-6746, doi:10.4049/jimmunol.181.10.6738 (2008).

28 Waldmann, T. A. The shared and contrasting roles of IL2 and IL15 in the life and death of normal and neoplastic lymphocytes: implications for cancer therapy. *Cancer Immunol Res* **3**, 219-227, doi:10.1158/2326-6066.CIR-15-0009 (2015).

29 Rickert, M., Boulanger, M. J., Goriatcheva, N. & Garcia, K. C. Compensatory energetic mechanisms mediating the assembly of signaling complexes between interleukin-2 and its alpha, beta, and gamma(c) receptors. *J Mol Biol* **339**, 1115-1128, doi:10.1016/j.jmb.2004.04.038 (2004).

30 Hage, T., Sebald, W. & Reinemer, P. Crystal structure of the interleukin-4/receptor alpha chain complex reveals a mosaic binding interface. *Cell* **97**, 271-281, doi:10.1016/s0092-8674(00)80736-9 (1999).

31 Matsumoto, M. *et al.* On-column refolding and characterization of soluble human interleukin-15 receptor alpha-chain produced in Escherichia coli. *Protein Expr Purif* **31**, 64-71, doi:10.1016/s1046-5928(03)00143-8 (2003).

32 Zhang, J. L., Foster, D. & Sebald, W. Human IL-21 and IL-4 bind to partially overlapping epitopes of common gamma-chain. *Biochem Biophys Res Commun* **300**, 291-296, doi:10.1016/s0006-291x(02)02836-x (2003).

33 Dela Cruz, C. S. *et al.* N-linked glycosylation is required for optimal function of Kaposi's sarcoma herpesvirus-encoded, but not cellular, interleukin 6. *J Exp Med* **199**, 503-514, doi:10.1084/jem.20031205 (2004).

34 McElroy, C. A. *et al.* Structural reorganization of the interleukin-7 signaling complex. *Proc Natl Acad Sci U S A* **109**, 2503-2508, doi:10.1073/pnas.1116582109 (2012).

35 Goodwin, R. G. *et al.* Human interleukin 7: molecular cloning and growth factor activity on human and murine B-lineage cells. *Proc Natl Acad Sci U S A* **86**, 302-306, doi:10.1073/pnas.86.1.302 (1989).

36 McElroy, C. A., Dohm, J. A. & Walsh, S. T. Structural and biophysical studies of the human IL-7/IL-7Ralpha complex. *Structure* **17**, 54-65, doi:10.1016/j.str.2008.10.019 (2009).

37 Durum, S. K. IL-7 and TSLP receptors: twisted sisters. *Blood* **124**, 4-5, doi:10.1182/blood-2014-05-574327 (2014).

38 Ziegler, S. F. *et al.* The biology of thymic stromal lymphopoietin (TSLP). *Adv Pharmacol* **66**, 129-155, doi:10.1016/B978-0-12-404717-4.00004-4 (2013).

39 Torgerson, D. G. *et al.* Meta-analysis of genome-wide association studies of asthma in ethnically diverse North American populations. *Nat Genet* **43**, 887-892, doi:10.1038/ng.888 (2011).

40 Hirota, T. *et al.* Genome-wide association study identifies three new susceptibility loci for adult asthma in the Japanese population. *Nat Genet* **43**, 893-896, doi:10.1038/ng.887 (2011).

41 Sun, L. D. *et al.* Genome-wide association study identifies two new susceptibility loci for atopic dermatitis in the Chinese Han population. *Nat Genet* **43**, 690-694, doi:10.1038/ng.851 (2011).

42 Gao, P. S. *et al.* Genetic variants in thymic stromal lymphopoietin are associated with atopic dermatitis and eczema herpeticum. *J Allergy Clin Immunol* **125**, 1403-1407 e1404, doi:10.1016/j.jaci.2010.03.016 (2010).

43 Mazzucchelli, R. I. *et al.* Visualization and identification of IL-7 producing cells in reporter mice. *PLoS One* **4**, e7637, doi:10.1371/journal.pone.0007637 (2009).

44 Hara, T. *et al.* Identification of IL-7-producing cells in primary and secondary lymphoid organs using IL-7-GFP knock-in mice. *J Immunol* **189**, 1577-1584, doi:10.4049/jimmunol.1200586 (2012).

45 Onder, L. *et al.* IL-7-producing stromal cells are critical for lymph node remodeling. *Blood* **120**, 4675-4683, doi:10.1182/blood-2012-03-416859 (2012).

46 Fry, T. J. & Mackall, C. L. The many faces of IL-7: from lymphopoiesis to peripheral T cell maintenance. *J Immunol* **174**, 6571-6576, doi:10.4049/jimmunol.174.11.6571 (2005).

47 Mazzucchelli, R. & Durum, S. K. Interleukin-7 receptor expression: intelligent design. *Nat Rev Immunol* **7**, 144-154, doi:10.1038/nri2023 (2007).

48 Martin, C. E. *et al.* Interleukin-7 Availability Is Maintained by a Hematopoietic Cytokine Sink Comprising Innate Lymphoid Cells and T Cells. *Immunity* **47**, 171-182 e174, doi:10.1016/j.immuni.2017.07.005 (2017).

49 Chu, Y. W. *et al.* Exogenous IL-7 increases recent thymic emigrants in peripheral lymphoid tissue without enhanced thymic function. *Blood* **104**, 1110-1119, doi:10.1182/blood-2003-10-3635 (2004).

50 Bachmann, M. F. & Oxenius, A. Interleukin 2: from immunostimulation to immunoregulation and back again. *EMBO Rep* **8**, 1142-1148, doi:10.1038/sj.embor.7401099 (2007).

51 Park, J. H. *et al.* Suppression of IL7Ralpha transcription by IL-7 and other prosurvival cytokines: a novel mechanism for maximizing IL-7-dependent T cell survival. *Immunity* **21**, 289-302, doi:10.1016/j.immuni.2004.07.016 (2004).

52 Munitic, I. *et al.* Dynamic regulation of IL-7 receptor expression is required for normal thymopoiesis. *Blood* **104**, 4165-4172, doi:10.1182/blood-2004-06-2484 (2004).

53 Schluns, K. S., Kieper, W. C., Jameson, S. C. & Lefrancois, L. Interleukin-7 mediates the homeostasis of naive and memory CD8 T cells in vivo. *Nat Immunol* **1**, 426-432, doi:10.1038/80868 (2000).

54 Franchimont, D. *et al.* Positive effects of glucocorticoids on T cell function by up-regulation of IL-7 receptor alpha. *J Immunol* **168**, 2212-2218, doi:10.4049/jimmunol.168.5.2212 (2002).

55 Kaech, S. M. *et al.* Selective expression of the interleukin 7 receptor identifies effector CD8 T cells that give rise to long-lived memory cells. *Nat Immunol* **4**, 1191-1198, doi:10.1038/ni1009 (2003).

56 Suzuki, K. *et al.* Role of common cytokine receptor gamma chain (gamma(c))-and Jak3-dependent signaling in the proliferation and survival of murine mast cells. *Blood* **96**, 2172-2180 (2000).

57 Suzuki, K. *et al.* Janus kinase 3 (Jak3) is essential for common cytokine receptor gamma chain (gamma(c))-dependent signaling: comparative analysis of gamma(c), Jak3, and gamma(c) and Jak3 double-deficient mice. *Int Immunol* **12**, 123-132, doi:10.1093/intimm/12.2.123 (2000).

58 Migone, T. S. *et al.* Functional cooperation of the interleukin-2 receptor beta chain and Jak1 in phosphatidylinositol 3-kinase recruitment and phosphorylation. *Mol Cell Biol* **18**, 6416-6422, doi:10.1128/mcb.18.11.6416 (1998).

59 Rodig, S. J. *et al.* Disruption of the Jak1 gene demonstrates obligatory and nonredundant roles of the Jaks in cytokine-induced biologic responses. *Cell* **93**, 373-383, doi:10.1016/s0092-8674(00)81166-6 (1998).

60 Cao, X. *et al.* Defective lymphoid development in mice lacking expression of the common cytokine receptor gamma chain. *Immunity* **2**, 223-238, doi:10.1016/1074-7613(95)90047-0 (1995).

61 DiSanto, J. P., Muller, W., Guy-Grand, D., Fischer, A. & Rajewsky, K. Lymphoid development in mice with a targeted deletion of the interleukin 2 receptor gamma chain. *Proc Natl Acad Sci U S A* **92**, 377-381, doi:10.1073/pnas.92.2.377 (1995).

62 Ohbo, K. *et al.* Functional analysis of the human interleukin 2 receptor gamma chain gene promoter. *J Biol Chem* **270**, 7479-7486, doi:10.1074/jbc.270.13.7479 (1995).

63 Baird, A. M., Lucas, J. A. & Berg, L. J. A profound deficiency in thymic progenitor cells in mice lacking Jak3. *J Immunol* **165**, 3680-3688, doi:10.4049/jimmunol.165.7.3680 (2000).

64 Nosaka, T. *et al.* Defective lymphoid development in mice lacking Jak3. *Science* **270**, 800-802, doi:10.1126/science.270.5237.800 (1995).

65 Jiang, Q. *et al.* Cell biology of IL-7, a key lymphotrophin. *Cytokine Growth Factor Rev* **16**, 513-533, doi:10.1016/j.cytogfr.2005.05.004 (2005).

66 Jiang, Q. *et al.* Distinct regions of the interleukin-7 receptor regulate different Bcl2 family members. *Mol Cell Biol* **24**, 6501-6513, doi:10.1128/MCB.24.14.6501-6513.2004 (2004).

67 Delespine-Carmagnat, M., Bouvier, G. & Bertoglio, J. Association of STAT1, STAT3 and STAT5 proteins with the IL-2 receptor involves different subdomains of the IL-2 receptor beta chain. *Eur J Immunol* **30**, 59-68, doi:10.1002/1521-4141(200001)30:1<59::AID-IMMU59>3.0.CO;2-1 (2000).

68 Chen, J., Sadowski, H. B., Kohanski, R. A. & Wang, L. H. Stat5 is a physiological substrate of the insulin receptor. *Proc Natl Acad Sci U S A* **94**, 2295-2300, doi:10.1073/pnas.94.6.2295 (1997).

69 Foxwell, B. M., Beadling, C., Guschin, D., Kerr, I. & Cantrell, D. Interleukin-7 can induce the activation of Jak 1, Jak 3 and STAT 5 proteins in murine T cells. *Eur J Immunol* **25**, 3041-3046, doi:10.1002/eji.1830251109 (1995).

70 Lin, J. X. *et al.* The role of shared receptor motifs and common Stat proteins in the generation of cytokine pleiotropy and redundancy by IL-2, IL-4, IL-7, IL-13, and IL-15. *Immunity* **2**, 331-339, doi:10.1016/1074-7613(95)90141-8 (1995).

71 Yasukawa, H. *et al.* The JAK-binding protein JAB inhibits Janus tyrosine kinase activity through binding in the activation loop. *EMBO J* **18**, 1309-1320, doi:10.1093/emboj/18.5.1309 (1999).

72 Yoshimura, A., Suzuki, M., Sakaguchi, R., Hanada, T. & Yasukawa, H. SOCS, Inflammation, and Autoimmunity. *Front Immunol* **3**, 20, doi:10.3389/fimmu.2012.00020 (2012).

73 Yoshimura, A. & Yasukawa, H. JAK's SOCS: a mechanism of inhibition. *Immunity* **36**, 157-159, doi:10.1016/j.immuni.2012.01.010 (2012).

74 Grabstein, K. H. *et al.* Inhibition of murine B and T lymphopoiesis in vivo by an anti-interleukin 7 monoclonal antibody. *J Exp Med* **178**, 257-264, doi:10.1084/jem.178.1.257 (1993).

75 von Freeden-Jeffry, U. *et al.* Lymphopenia in interleukin (IL)-7 gene-deleted mice identifies IL-7 as a nonredundant cytokine. *J Exp Med* **181**, 1519-1526, doi:10.1084/jem.181.4.1519 (1995).

76 Peschon, J. J. *et al.* Early lymphocyte expansion is severely impaired in interleukin 7 receptor-deficient mice. *J Exp Med* **180**, 1955-1960, doi:10.1084/jem.180.5.1955 (1994).

77 Maki, K. *et al.* Interleukin 7 receptor-deficient mice lack gammadelta T cells. *Proc Natl Acad Sci U S A* **93**, 7172-7177, doi:10.1073/pnas.93.14.7172 (1996).

78 Malissen, M., Pereira, P., Gerber, D. J., Malissen, B. & DiSanto, J. P. The common cytokine receptor gamma chain controls survival of gamma/delta T cells. *J Exp Med* **186**, 1277-1285, doi:10.1084/jem.186.8.1277 (1997).

79 Park, S. Y. *et al.* Developmental defects of lymphoid cells in Jak3 kinase-deficient mice. *Immunity* **3**, 771-782, doi:10.1016/1074-7613(95)90066-7 (1995).

80 Kornfeld, R. & Kornfeld, S. Assembly of asparagine-linked oligosaccharides. *Annu Rev Biochem* **54**, 631-664, doi:10.1146/annurev.bi.54.070185.003215 (1985).

81 Schachter, H. The 'yellow brick road' to branched complex N-glycans. *Glycobiology* **1**, 453-461, doi:10.1093/glycob/1.5.453 (1991).

82 Trombetta, E. S. The contribution of N-glycans and their processing in the endoplasmic reticulum to glycoprotein biosynthesis. *Glycobiology* **13**, 77R-91R, doi:10.1093/glycob/cwg075 (2003).

83 Grigorian, A. *et al.* Control of T Cell-mediated autoimmunity by metabolite flux to N-glycan biosynthesis. *J Biol Chem* **282**, 20027-20035, doi:10.1074/jbc.M701890200 (2007).

84 Kumar, R. & Stanley, P. Transfection of a human gene that corrects the Lec1 glycosylation defect: evidence for transfer of the structural gene for N-acetylglucosaminyltransferase I. *Mol Cell Biol* **9**, 5713-5717, doi:10.1128/mcb.9.12.5713 (1989).

85 Ujita, M. *et al.* Poly-N-acetyllactosamine synthesis in branched N-glycans is controlled by complemental branch specificity of I-extension enzyme and beta1,4-galactosyltransferase I. *J Biol Chem* **274**, 16717-16726, doi:10.1074/jbc.274.24.16717 (1999).

86 Ujita, M. *et al.* Regulation of I-branched poly-N-acetyllactosamine synthesis. Concerted actions by I-extension enzyme, I-branching enzyme, and beta1,4-

galactosyltransferase I. *J Biol Chem* **274**, 9296-9304, doi:10.1074/jbc.274.14.9296 (1999).

87 Banerjee, S. *et al.* The evolution of N-glycan-dependent endoplasmic reticulum quality control factors for glycoprotein folding and degradation. *Proc Natl Acad Sci U S A* **104**, 11676-11681, doi:10.1073/pnas.0704862104 (2007).

88 Helenius, A. & Aebi, M. Roles of N-linked glycans in the endoplasmic reticulum. *Annu Rev Biochem* **73**, 1019-1049, doi:10.1146/annurev.biochem.73.011303.073752 (2004).

89 Kowarik, M. *et al.* N-linked glycosylation of folded proteins by the bacterial oligosaccharyltransferase. *Science* **314**, 1148-1150, doi:10.1126/science.1134351 (2006).

90 Grigorian, A. & Demetriou, M. Manipulating cell surface glycoproteins by targeting N-glycan-galectin interactions. *Methods Enzymol* **480**, 245-266, doi:10.1016/S0076-6879(10)80012-6 (2010).

91 Chen, J. K., Shen, C. R. & Liu, C. L. N-acetylglucosamine: production and applications. *Mar Drugs* **8**, 2493-2516, doi:10.3390/md8092493 (2010).

92 Hirabayashi, J. *et al.* Oligosaccharide specificity of galectins: a search by frontal affinity chromatography. *Biochim Biophys Acta* **1572**, 232-254, doi:10.1016/s0304-4165(02)00311-2 (2002).

93 Liu, F. T. Galectins: novel anti-inflammatory drug targets. *Expert Opin Ther Targets* **6**, 461-468, doi:10.1517/14728222.6.4.461 (2002).

94 Liu, F. T., Patterson, R. J. & Wang, J. L. Intracellular functions of galectins. *Biochim Biophys Acta* **1572**, 263-273, doi:10.1016/s0304-4165(02)00313-6 (2002).

95 Stowell, S. R. *et al.* Dimeric Galectin-8 induces phosphatidylserine exposure in leukocytes through polylactosamine recognition by the C-terminal domain. *J Biol Chem* **283**, 20547-20559, doi:10.1074/jbc.M802495200 (2008).

96 Ahmad, N. *et al.* Galectin-3 precipitates as a pentamer with synthetic multivalent carbohydrates and forms heterogeneous cross-linked complexes. *J Biol Chem* **279**, 10841-10847, doi:10.1074/jbc.M312834200 (2004).

97 Dennis, J. W., Nabi, I. R. & Demetriou, M. Metabolism, cell surface organization, and disease. *Cell* **139**, 1229-1241, doi:10.1016/j.cell.2009.12.008 (2009).

98 Grakoui, A. *et al.* The immunological synapse: a molecular machine controlling T cell activation. *Science* **285**, 221-227, doi:10.1126/science.285.5425.221 (1999).

99 Monks, C. R., Freiberg, B. A., Kupfer, H., Sciaky, N. & Kupfer, A. Three-dimensional segregation of supramolecular activation clusters in T cells. *Nature* **395**, 82-86, doi:10.1038/25764 (1998).

100 Viola, A. & Lanzavecchia, A. T cell activation determined by T cell receptor number and tunable thresholds. *Science* **273**, 104-106, doi:10.1126/science.273.5271.104 (1996).

101 Sansom, D. M. CD28, CTLA-4 and their ligands: who does what and to whom? *Immunology* **101**, 169-177, doi:10.1046/j.1365-2567.2000.00121.x (2000).

102 Shi, Z. *et al.* Importance of CD80/CD86-CD28 interactions in the recognition of target cells by CD8+CD122+ regulatory T cells. *Immunology* **124**, 121-128, doi:10.1111/j.1365-2567.2007.02747.x (2008).

103 Hirabayashi, J. & Kasai, K. The family of metazoan metal-independent beta-galactoside-binding lectins: structure, function and molecular evolution. *Glycobiology* **3**, 297-304, doi:10.1093/glycob/3.4.297 (1993).

104 Araujo, L., Khim, P., Mkhikian, H., Mortales, C. L. & Demetriou, M. Glycolysis and glutaminolysis cooperatively control T cell function by limiting metabolite supply to N-glycosylation. *Elife* **6**, doi:10.7554/eLife.21330 (2017).

105 Demetriou, M., Granovsky, M., Quaggin, S. & Dennis, J. W. Negative regulation of T-cell activation and autoimmunity by Mgat5 N-glycosylation. *Nature* **409**, 733-739, doi:10.1038/35055582 (2001).

106 Dennis, J. W., Lau, K. S., Demetriou, M. & Nabi, I. R. Adaptive regulation at the cell surface by N-glycosylation. *Traffic* **10**, 1569-1578, doi:10.1111/j.1600-0854.2009.00981.x (2009).

107 Lee, S. U. *et al.* N-glycan processing deficiency promotes spontaneous inflammatory demyelination and neurodegeneration. *J Biol Chem* **282**, 33725-33734, doi:10.1074/jbc.M704839200 (2007).

108 Mkhikian, H. *et al.* Genetics and the environment converge to dysregulate N-glycosylation in multiple sclerosis. *Nat Commun* **2**, 334, doi:10.1038/ncomms1333 (2011).

109 Mkhikian, H. *et al.* Golgi self-correction generates bioequivalent glycans to preserve cellular homeostasis. *Elife* **5**, doi:10.7554/eLife.14814 (2016).

110 Zhou, R. W. *et al.* N-glycosylation bidirectionally extends the boundaries of thymocyte positive selection by decoupling Lck from Ca(2)(+) signaling. *Nat Immunol* **15**, 1038-1045, doi:10.1038/ni.3007 (2014).

111 Grigorian, A. & Demetriou, M. Mgat5 deficiency in T cells and experimental autoimmune encephalomyelitis. *ISRN Neurol* **2011**, 374314, doi:10.5402/2011/374314 (2011).

112 Li, C. F. *et al.* Hypomorphic MGAT5 polymorphisms promote multiple sclerosis cooperatively with MGAT1 and interleukin-2 and 7 receptor variants. *J Neuroimmunol* **256**, 71-76, doi:10.1016/j.jneuroim.2012.12.008 (2013).

113 Kuball, J. *et al.* Increasing functional avidity of TCR-redirected T cells by removing defined N-glycosylation sites in the TCR constant domain. *J Exp Med* **206**, 463-475, doi:10.1084/jem.20082487 (2009).

114 Alegre, M. L., Frauwirth, K. A. & Thompson, C. B. T-cell regulation by CD28 and CTLA-4. *Nat Rev Immunol* **1**, 220-228, doi:10.1038/35105024 (2001).

115 Grigorian, A., Torossian, S. & Demetriou, M. T-cell growth, cell surface organization, and the galectin-glycoprotein lattice. *Immunol Rev* **230**, 232-246, doi:10.1111/j.1600-065X.2009.00796.x (2009).

116 Lau, K. S. *et al.* Complex N-glycan number and degree of branching cooperate to regulate cell proliferation and differentiation. *Cell* **129**, 123-134, doi:10.1016/j.cell.2007.01.049 (2007).

117 Lee, J., Ahn, E., Kissick, H. T. & Ahmed, R. Reinvigorating Exhausted T Cells by Blockade of the PD-1 Pathway. *For Immunopathol Dis Therap* **6**, 7-17, doi:10.1615/ForumImmunDisTher.2015014188 (2015).

118 Chen, L. & Flies, D. B. Molecular mechanisms of T cell co-stimulation and co-inhibition. *Nat Rev Immunol* **13**, 227-242, doi:10.1038/nri3405 (2013).

119 Elias, R., Morales, J., Rehman, Y. & Khurshid, H. Immune Checkpoint Inhibitors in Older Adults. *Curr Oncol Rep* **18**, 47, doi:10.1007/s11912-016-0534-9 (2016).

120 Vigano, S., Perreau, M., Pantaleo, G. & Harari, A. Positive and negative regulation of cellular immune responses in physiologic conditions and diseases. *Clin Dev Immunol* **2012**, 485781, doi:10.1155/2012/485781 (2012).

121 Callahan, M. K. & Wolchok, J. D. At the bedside: CTLA-4- and PD-1-blocking antibodies in cancer immunotherapy. *J Leukoc Biol* **94**, 41-53, doi:10.1189/jlb.1212631 (2013).

122 Seidel, J. A., Otsuka, A. & Kabashima, K. Anti-PD-1 and Anti-CTLA-4 Therapies in Cancer: Mechanisms of Action, Efficacy, and Limitations. *Front Oncol* **8**, 86, doi:10.3389/fonc.2018.00086 (2018).

123 Wei, S. C., Duffy, C. R. & Allison, J. P. Fundamental Mechanisms of Immune Checkpoint Blockade Therapy. *Cancer Discov* **8**, 1069-1086, doi:10.1158/2159-8290.CD-18-0367 (2018).

124 Tao, X., Constant, S., Jorritsma, P. & Bottomly, K. Strength of TCR signal determines the costimulatory requirements for Th1 and Th2 CD4+ T cell differentiation. *J Immunol* **159**, 5956-5963 (1997).

125 Tao, X., Grant, C., Constant, S. & Bottomly, K. Induction of IL-4-producing CD4+ T cells by antigenic peptides altered for TCR binding. *J Immunol* **158**, 4237-4244 (1997).

126 Grigorian, A. *et al.* N-acetylglucosamine inhibits T-helper 1 (Th1)/T-helper 17 (Th17) cell responses and treats experimental autoimmune encephalomyelitis. *J Biol Chem* **286**, 40133-40141, doi:10.1074/jbc.M111.277814 (2011).

127 Morgan, R. *et al.* N-acetylglucosaminyltransferase V (Mgat5)-mediated N-glycosylation negatively regulates Th1 cytokine production by T cells. *J Immunol* **173**, 7200-7208, doi:10.4049/jimmunol.173.12.7200 (2004).

128 Marshall, S., Bacote, V. & Traxinger, R. R. Discovery of a metabolic pathway mediating glucose-induced desensitization of the glucose transport system. Role of hexosamine biosynthesis in the induction of insulin resistance. *J Biol Chem* **266**, 4706-4712 (1991).

Chapter 2

Impaired T cell immunity in the elderly via interleukin-7 driven up-regulation of N-glycan branching

Summary

Impaired T cell immunity in the elderly increase's mortality from infectious disease. The branching of Asparagine (N) - linked glycans serves as a critical negative regulator of T cell immunity. Here we report that branching in female > male and naïve > memory T cells increases with age. Reversing this increase rejuvenates T cell function and limits severity of *Salmonella* infection. Naïve T cells are generated by the thymus in adult mice, but by interleukin-7 (IL-7) driven homeostatic proliferation in adult humans. Co-incident with thymic involution in old mice, IL-7 signaling increased in female naïve T cells, which in turn increased branching. Serum levels of N-acetylglucosamine, a rate limiting metabolite for branching, increased with age in humans and synergized with IL-7 to raise branching. Thus, in the elderly naïve T cell generation via IL-7 combines with rising N-acetylglucosamine to secondarily suppress function via branching. Targeting this pathway may reduce severity of infections like COVID-19 in the elderly.

Introduction

Aging is associated with diminishing immune functional response, contributing to the increased morbidity and mortality rate from neoplastic diseases and infections. Within the United States approximately 90% of influenza associated deaths occur among adults over the age of 65, despite this age group representing only 15% of the population[1-4]. The vulnerability of the elderly to infectious agents have been recently highlighted with the emergence of SARS-CoV-2, the virus responsible for the COVID-19 pandemic[5]. This increase in morbidity and mortality among elderly patients extends toward common bacterial infections including *Salmonella* gastroenteritis[6]. With the elderly population rapidly increasing in numbers, interventions that effectively rejuvenate the immune response is essential to prevent or regulate age-related pathologies to maintain or improve the health status of society.

Age-associated decline in immune function, or immune senescence, has been attributed to the dysfunction of both the innate and adaptive arms of the immune system. The generation of naïve T and B lymphocytes decline with age, whereas the functional capacity of existing peripheral T and B cells are largely reduced among the elderly[7,8]. Previous transcriptomic profiling of aging in naïve and memory $CD4^+$ T cells from mice through microarray data analysis provide potential molecular targets which may drive age-related functional decline in aged immune cells[9-11]. In addition, global gene expression profiling in humans show conserved alternations between mouse and human data sets where dysregulation of basal NF-κB may contribute to IL-7 responsiveness in aging[12-14]. Despite the identification of multiple contributing deficiencies in immune

senescence, the molecular underpinnings of age-dependent impairment of T cell functions are not well understood.

Asn (N) – linked glycans plays a critical role in regulating T cell immunity in mice and humans[15-19]. Virtually all cell surface and secreted proteins are co- and post-translationally modified by the addition of complex carbohydrates in the ER/Golgi secretory pathway. These glycans impart substantial molecular information that is not encoded by the genome, thus providing an avenue for versatility by not being restricted to abide by genetic templates. Previous studies done in our lab have revealed that sugar binding proteins, such as galectins, bind to glycans on TCRs and other receptors and transporters at the cell surface, forming a molecular lattice that controls clustering, signaling and endocytosis of these proteins to affect cell growth, differentiation and thus immune response in mice and humans[15-27]. In T cells, N-glycan branching cooperates with the galectin lattice to negatively regulate TCR clustering and signaling[15,16], promotes surface retention of CTLA-4, PD-1 and transforming growth factor-β receptor (TβR) type I and II[16,26,28], inhibits T_H1 and T_H17 while promoting T_H2 and induced T regulatory (iTreg) cell differentiation[20,21,24] and suppresses development of autoimmunity[15,22,23] in mice and humans. N-glycan branching is metabolically regulated by Golgi branching enzymes utilizing a common sugar-nucleotide substrate, UDP-GlcNAc. However, they do so with declining efficiency such that metabolic production of UDP-GlcNAc is limited for branching by Mgat4 and 5[16]. Thus, metabolic changes regulating biosynthesis of UDP-GlcNAc have profound effects on N-glycan branching.

Given the importance of N-glycan branching in negatively regulating T cell function and that immune function declines with age, we investigated whether N-glycan production

increases with age. Indeed, we demonstrate here that aging in female humans and mice is associated with increases in N-glycan branching in T cells and that reversing this phenotype rejuvenates T cell activity. Furthermore, this age-associated increase is driven by the IL-7 pathway, thus providing a potential therapeutic target for immune senescence.

Materials and Methods

Mice and human subjects

C57BL/6J (000664), *Mgat2*$^{f/f}$ (006892), *Lck-Cre* (003802), and *Cd45.1* Pep Boy (002014) mice were obtained from Jackson Laboratory. Young and aged C57BL/6 mice were obtained from the National Institute of Aging (NIA) maintained at Charles River Laboratories (Wilmington, MA, USA). Upon arrival mice were allowed to acclimate to the new environment for at least one week prior to the start of an experiment. To acquire mouse plasma, blood was collected in sterile tubes containing 0.1M EDTA as an anticoagulant.

All human subjects are Caucasian (non-Hispanic) and include both male and females. Individuals with cancer, uncontrolled medical disease or any other inflammatory syndrome were excluded. Human whole blood was collected from healthy individuals through the Research Blood Donor Program serviced by the Institute for Clinical & Translational Science (ICTS) or through The 90+ Study at the University of California, Irvine (UCI). All procedures with human subjects were approved by the Institutional Review Board of the University of California, Irvine.

T cell isolation and culture

For all *in vitro* mouse experiments, erythrocytes were depleted from splenic or lymph node cell suspensions by incubation with red blood cell (RBC) lysis buffer followed by negative selection using EasySep™ Naïve CD4+ T Cell Isolation Kit or EasySep™ CD4+ T Cell Isolation Kit (STEMCELL Technologies) according to manufacturer's instructions and supplemented with or without 20µg/mL biotinylated Phaseolus Vulgaris Leucoagglutinin (L-PHA, Vector Labs) to deplete non-*Mgat2* deleted cells. Freshly harvested cells were cultured ($2x10^5$-$5x10^6$ cells) in RPMI-1640 (Thermo Fisher Scientific) supplemented with 10% heat inactivated fetal bovine serum (Sigma Aldrich), 2µM L-glutamine (Gibco), 100U/mL penicillin/streptomycin (Gibco), and 50µM β-mercaptoethanol (Gibco) as previously described [15,16,19].

Human peripheral blood mononuclear cells (PBMCs) isolated by density gradient centrifugation over Histopaque-1077 (Sigma-Aldrich) or Lymphoprep (StemCell Technologies) were stimulated with plate-bound anti-CD3 (OKT3, eBioscience) plus soluable anti-CD28 (CD28.2, eBioscience) in media as described above. PBMCs were pre-treated with or without 5μM KIF 2 days prior to stimulation if indicated. For pharmacological treatments, cells were incubated with GlcNAc (40mM added daily, Wellesley Therapeutics), kifunensine (5uM, Glycosyn), recombinant human IL-7 (0.5ug-1.5ug, R&D Systems), and/or anti-mouse/human IL-7 antibody (clone M25; 5-15ug, BioXCell) as indicated. T_H17 and iTreg induction were performed as previously described[20].

Flow Cytometry

Flow cytometry experiments were performed as previously described [15,19]. Mouse antibodies for surface, intracellular and phospho-flow staining to CD69 (H1.2F3), IL17 (eBio17B7), CD4 (RM4-5), CD8α (53-6.7), CD19 (1D3), Foxp3 (Fjk-16s), CD44 (IM7), CD62L (MEL-14), CD3 (145-2C11 and 17A2), IL7Rα (A7R34), Rat IgG2a kappa Isotype Control (eBR2a), Phospho-STAT5 (SRBCZX), Mouse IgG1 kappa Isotype Control (P3.6.2.8.1) were purchased from eBioscience. In addition, CD45RA (HI100), CD4 (RM4-5) and CCR7 (4B12) were purchased for human cells. DyLight 649 conjugated Streptavidin (SA-5649) and both Fluorescein labeled and biotinylated L-PHA were purchased from Vector Labs. Anti-mouse CD45.1 (A20) and CD45.2 (104), and anti-human CD45RO (UCHL1) and CD8 (SK1) were purchased from BioLegend. Proliferation was assessed by staining cells with CellTrace CFSE proliferation kit (Thermo Fisher Scientific). Flow cytometry experiments were performed with the BD FACSAria Fusion Sorter, LSR II, Invitrogen Attune NxT Flow Cytometer, or ACEA Novocyte Flow Cytometer and analyzed following appropriate compensation using FlowJo software.

Mouse experiments

Mice were pre-treated with streptomycin (0.1 ml of a 200 mg/ml solution in sterile water) intragastrically prior to mock-infection or inoculation with a mixture of salmonella (*Salmonella typhimurium, IR715 strain ATCC14028*, 5×10^8 CFU/animal). At 72 hours after infection, mice were euthanized and the cecum, Peyer's patches, mesenteric lymph nodes, and spleen were collected for analysis of immune cells. Analysis of bacterial dissemination were performed through serial 10-fold dilutions plated for enumerating bacterial CFUs on agar plates.

Lymphocytes were prepared from pooled inguinal lymph nodes and splenocytes and purified for naïve CD4+ T cells from CD45.2 C56BL/6 donor mice as described above then injected intravenously by tail vein in 200µl of phosphate-buffered saline (PBS) into CD45.1 congenic C57BL/6 recipient mice.

For *in vivo* IL-7 treatment, mice were i.p. injected with either 200µl of PBS or rhIL-7/M25 cytokine/antibody complex (R&D Systems and BioXCell) every two days. Before injection, the cytokine/antibody complex were generated through co-incubation for 30 mins at room temperature. GlcNAc was administered orally by adding GlcNAc to their drinking water at 1mg/ml. Fresh GlcNAc was given daily for the duration of the experiment.

For IL-7 blockade experiments, mice were i.p. injected with 1-1.5mg of mouse IgG1 isotype control antibody (MOPC-21, BioXCell) or anti-mouse/human IL-7 (M25, BioXCell) in 200µl of PBS three times at 2 day intervals per week as indicated.

RNA extraction, library prep, and sequencing

Lymphocytes were prepared from pooled lymph nodes (axillary, brachial, cervical, inguinal) and splenocytes then purified for CD4+ T cells through negative selection by EasySep™ CD4+ T cell Isolation Kit (STEMCELL Technologies). Cell suspensions are then stained and FACS-sorted for either naïve (CD3+CD4+CD25-CD62L+CD44-) or memory (CD3+CD4+CD25-CD62L-CD44+) populations by BD FACSAria Fusion Sorter. Total RNA were then isolated using RNeasy Plus Micro Kit (Qiagen) and analyzed for RNA integrity number (RIN) by Agilent Bioanalyzer 2100. RIN of all samples was

determined to be ≥9.0. Subsequently, 125ng of total RNA was used for library prep through NEBNext Poly(A) mRNA Magnetic Isolation Module before using NEBNext Ultra II DNA Library Prep Kit for Illumina. Collected samples was cleaned with AMPure XP beads (Beckman Coulter) to make RNA into strand specific cDNA libraries with multiplexing barcodes from NEBNext Multiplex Oligos for Illumina (Index Primers Set 1 and 2). RNASeq libraries were then analyzed by qPCR (KAPA Biosystem), normalized to 2nM and pooled for multiplexing in equal volumes, then underwent paired-end 100-bp sequencing run on HiSeq 4000 (Illumina). Statistical analysis for differential gene expression was performed using DESeq2.

LC-MS/MS analysis

Human serum samples for metabolomics analysis were prepared as described previously[29]. Metabolites from 50µl of serum were extracted by the addition of 200µl of ice-cold extraction solvent (40% acetonitrile, 40% methanol, and 20% water). Thereafter the samples were shaken at 4°C for 1 hour at 1400rpm in a Thermomixer R (Eppendorf) and then centrifuged at 4°C for 10 minutes at ~18,000 x g in an Eppendorf microcentrifuge. The supernatant were transferred to fresh tubes and evaporated in a Speedvac (Acid-Resistant CentriVap Vacuum Concentrators, Labconco). The dry-extract samples were stored at -80°C.

The dry eluted metabolites were resuspended in 100ul of water containing internal standards D^7-Glucose at 0.2mg/mL and H-Tyrosine at 0.02mg/ml. Eluted metabolites were analyzed in negative mode at the optimal polarity in MRM mode on electrospray ionization (ESI) triple-quadrupole mass spectrometer (AB Sciex 4000Qtrap, Toronto, ON, Canada). Standard curves were prepared by adding increasing concentrations of GlcNAc or N-Acetyl-D-[UL-$^{13}C_6$]glucosamine (Omicron Biochemicals) to 50µl aliquot of control serum. Raw data were imported to MultiQuant software (AB Sciex, Version 2.1) for peak analysis and manual peak confirmation. The resulting data including area ratio is then exported to Excel and analyzed with MetaboAnalyst 3.0.

Statistical analysis

All experimental data from *in vitro* and *in vivo* studies were analyzed for significance from at least three independent experiments. Correlation of age, sex, and serum GlcNAc were analyzed with a linear regression model for age. Correlations of serum GlcNAc levels with L-PHA staining on different cell populations were also analyzed with linear regression models. Statistical analyses were calculated with Prism software (GraphPad). *P* values were from two- or one-tailed unpaired *t*-tests unless specified otherwise.

Results

N-glycan branching increases with age in female mouse T cells

To explore whether N-glycan branching increases with age, we initially compared L-PHA binding (*Phaseolus vulgaris, leukoagglutinin*) in splenic mouse T cells from young (~4-5 months) and old (~20-23 months) adult mice. L-PHA binds to β1,6GlcNAc-branched N-glycans and is utilized as a sensitive quantitative marker for N-glycan branching[15]. Indeed, flow cytometry revealed an increase in female $CD4^+$ T cells, with differences in naïve > central memory > effector memory populations (**Fig. 2.1A-C, 2.2A**). Remarkably, naïve $CD4^+$ T cells displayed nearly a 2-fold increase in L-PHA binding, whereas only a ~20% difference is sufficient to alter T cell function and risk for developing inflammatory diseases[22,23]. In comparison, L-PHA binding in old male $CD4^+$ T cells was not elevated (**Fig. 2.1D**) and was lower than old female CD4+ T cells, indicating that branching specifically increased in elderly female but not male mice relative to young mice (**Fig. 2.2B,C)**. This extended to male $CD8^+$ T cells displaying no difference, whereas female $CD8^+$ naïve T cells demonstrated a modest increase in L-PHA binding but not in the memory subsets (**Fig. 2.1E,F)**.

$CD19^+$ B cells in both young and old females and males displayed little difference in N-glycan branching (**Fig. 2.2D**). Age-associated thymic involution involves a decrease in cellularity, ultimately resulting in a reduction in naïve T cell output[30-32]. Although N-glycan branching regulates T cell production and development from the thymus[19], single and double positive thymocytes demonstrated no age-associated differences in L-PHA binding (**Fig. 2.2E**). This indicates that the increase in N-glycan branching in old naïve female T cells occurs in the periphery rather than from alterations in thymocyte

development. Together, these data indicate an increase in N-glycan branching with age in female but not male mouse T cells, with the most striking differences being displayed within the naïve $CD4^+$ T cell subsets.

Age-associated increase in N-glycan branching suppresses T cell function

N-glycan branching negatively regulates TCR clustering and signaling, thus limiting T cell immune response. As N-glycan branching increases with age, we explored T cell activation thresholds by comparing induction of the T cell activation marker CD69 in response to anti-CD3 antibody. Indeed, $CD4^+$ T cells from aged female mice were hypo-reactive in comparison to young $CD4^+$ T cells (**Fig. 2.3A**). This effect was reversed by supplementing the cells with mannosidase I inhibitor kifunensine (KIF), which blocks N-glycan branching[18], thus confirming that the elevated levels in N-glycan branching in old T cells inhibited ligand induced TCR signaling (**Fig. 2.3A, Fig. 2.4A**). We further confirmed this phenotype by examining aged mice with T cell specific deletion of the Mgat2 Golgi branching enzyme (i.e. *Mgat2*$^{fl/fl}$*lck-cre* mice). T cells lacking *Mgat2* results in N-glycans with a single branch that is extended by poly-N-acetyllactosamine[17]. Indeed, old *Mgat2* deficient $CD4^+$ T cells display up-regulation of CD69 relative to age-matched control $CD4^+$ T cells (**Fig. 2.3B**). Consistent with these results, proliferation of old female $CD4^+$ T cells was also rejuvenated by decreasing branching with KIF or by genetic deletion of *Mgat2* (**Fig. 2.3C**).

In addition to limiting TCR activity, N-glycan branching suppresses inflammatory T cell responses by inhibiting pro-inflammatory T_H17 differentiation while promoting anti-inflammatory Treg differentiation[20,21]. Therefore, the age-associated increase in N-glycan

branching is expected to reduce inflammatory responses by T cells. Indeed, reversing age-associated increases in N-glycan branching in old female $CD4^+$ T cells via KIF or *Mgat2* deletion enhanced T_H17 differentiation while reducing Treg induction (**Fig. 2.3D,E**). Together, these results indicate that age-induced increase in N-glycan branching functionally suppresses T cell activity in females.

Reversing age-induced increases in N-glycan branching rejuvenates immunity to *Salmonella typhimurium*

In immune-competent hosts, non-typhoidal salmonella induces a robust T_H17 response and a localized self-limited infection within the bowel mucosa[33,34]. However, salmonella infection in the elderly results in reduced T_H17 induction and dissemination outside of the bowel mucosa[6,35]. To assess whether the age-associated increase in N-glycan branching suppresses T cell function *in vivo*, we explored an infection model with non-typhoidal salmonella (*Salmonella typhimurium*). We infected old wild type female mice with a virulent strain of salmonella (IR715), resulting in two deaths and significant dissemination from the bowel mucosa to the Peyer's patches, mesenteric lymph nodes (MLN), and the spleen (**Fig. 2.5A-C**). In contrast, infecting age-matched T cell specific *Mgat2* deficient female mice in parallel resulted in no deaths and significantly reduced dissemination to Peyer's patches, MLN, and the spleen (**Fig. 2.5A-C**). Luminal content of IR715 did not differ between wild type and *Mgat2* deficient old female mice, suggesting a defect in dissemination of IR715 (**Fig 2.6A**). Consistent with previous data indicating a lack of increase in N-glycan branching in old male T cells, deletion of *Mgat2* did not significantly alter IR715 dissemination and luminal content in old male mice (**Fig. 2.5D-F,**

Fig. 2.6B). In addition, our *in vitro* data indicates age-dependent increase in N-glycan branching suppresses T_H17 while enhancing Treg responses where infected *Mgat2* deficient old female mice displayed increased IL-17^+ cells and reduced FoxP3^+ cells with the bowel compared to infected wild type control mice. Collectively, age-dependent increase in N-glycan branching promotes *Salmonella typhimurium* dissemination by limiting T_H17 response and promoting Treg responses *in vivo*.

IL-7 signaling pathway increases with age to raise N-glycan branching

Age-dependent increase in N-glycan branching in old naïve female T cells may arise from cell-intrinsic and/or cell-extrinsic factors. To assess this, we normalized the environment of naïve $CD4^+$ T cells from young and old female mice to eliminate external factors. Indeed, culturing cells in the same media for three days was sufficient to markedly reduce the difference in N-glycan branching between young and old female naïve $CD4^+$ T cells (**Fig. 2.7A**). Similarly, adoptively transferring old naïve CD4+ T cells that express CD45.2 into young recipient CD45.1 female mice for two weeks resulted in significantly reduced differences in N-glycan branching between young and old naïve CD4+ T cells (**Fig. 2.7B, 2.8A**). Together, these data suggest that cell extrinsic factors in the environment of aged female mice primarily drive age-associated increases in N-glycan branching.

To determine whether environmental driven changes in N-glycan branching is associated with changes in gene expression profiles of old female mice, we performed high throughput RNA sequencing (RNA-Seq) analysis on cell sorted young and old naïve CD4+ T cells from female and male mice (**Fig. 2.8B**). Of the 158 and 192 differentially

expressed genes (DEGs) between young and old naïve CD4+ T cells in females and males, respectively, only 44 overlapped (**Fig. 2.8C, Table 2.1-2.4**). In addition, there were no differences observed in gene expression of N-glycan branching enzymes or other relevant genes involved in glycosylation (**Table 2.5**), which we confirmed by performing quantitative PCR for critical Golgi enzymes involved in N-glycan branching (**Fig. 2.8D**). However, among the highest DEGs in females but not males included three within the IL-7 signaling pathway (**Table 2.1**), namely reduced expression of IL7Rα (CD127) and increased expression of Suppressor of cytokine signaling 3 (Socs3) and Janus kinase 3 (Jak3). In contrast, other IL-7 signaling pathway genes were unchanged (**Table 2.1**). To confirm this RNA-seq data, we examined IL7Rα surface expression on naïve $CD4^+$ T cells in females. Indeed, IL7Rα (CD127) protein is reduced in old female naïve $CD4^+$ T cells relative to young female mice (**Fig. 2.7C**). Reduced IL7Rα and increased inhibitory Socs3 in old female mice is likely secondary to excessive IL-7 signaling[36,37]. Indeed, old naïve but not memory female T cells displayed increased basal expression of phosphorylated-STAT5 relative to young controls (pSTAT5, **Fig. 2.7D**).

To examine whether increased levels of IL-7 signaling may enhance N-glycan branching, we cultured young and old naïve $CD4^+$ T cells with recombinant IL-7. Indeed, supplementing IL-7 *in vitro* significantly increased N-glycan branching in both young and old naïve $CD4^+$ T cells (**Fig. 2.7E,F**). To confirm whether the same effects can be achieved *in vivo*, we administered IL-7 complexed with the anti-IL-7 monoclonal antibody M25 clone into young female mice. The IL-7/M25 complex significantly augments cytokine potency *in vivo* and improves IL-7 half-life[38,39]. Indeed, enhancing IL-7 signaling *in vivo*

by administering the IL-7/M25 complex at two different doses significantly raised N-glycan branching levels in naïve $CD4^+$ T cells in young female mice (**Fig. 2.7G**).

IL-7 has a short serum half-life in mice (~2 hrs)[38] and is not detectable by ELISA in the serum of old female mice (data not shown). Therefore, to investigate whether excessive IL-7 signaling *in vivo* raises N-glycan branching in naïve T cells of old female mice, we injected antagonistic doses of anti-IL-7 antibody (M25) to block endogenous IL-7 signaling. Indeed, two weeks of IL-7 antagonism with M25 treatment reduced N-glycan branching levels in old naïve female $CD4^+$ T cells to levels seen in young cells in both blood and the spleen (**Fig. 2.7H,I**). Furthermore, IL7Rα protein expression was partially restored following treatment in old naïve $CD4^+$ T cells (**Fig. 2.8E**). As two weeks treatment to inhibit IL-7 signaling may have been too short to fully reverse the down-regulated expression of IL7Rα, we repeated the treatment for four weeks. Four weeks of M25 treatment reduced N-glycan branching similar to two weeks of treatment (**Fig. 2.8F,G**) as well as reversed the reduction in IL7Rα protein expression and elevated pSTAT5 levels previously observed (**Fig. 2.7J,K**). This confirms that excessive IL-7 signaling *in vivo* is responsible for both reduced IL7Rα and elevated basal pSTAT5 expression in old female mice. Together, our data indicates that increased basal IL-7 signaling in old female mice to induce homeostatic maintenance of the naïve $CD4^+$ T cell population as a consequence of thymic involution due to age, secondarily raises N-glycan branching in naïve CD4+ T cells to diminish T cell function in old female mice.

IL-7 synergizes with N-acetylglucosamine to raise N-glycan branching in old human naïve T cells

In contrast to mice, where thymic involution occurs very late in life, in humans thymic production of naïve T cells begin decreasing from birth and significantly declines by puberty before ceasing at young adulthood[31,40-42]. Therefore, humans become highly dependent on IL-7 mediated homeostatic proliferation to maintain a naïve $CD4^+$ T cell pool at much younger age compared with mice. Given this difference, we investigated whether N-glycan branching also increases with age in human T cells by examining females and males ranging in age from 19 to 98 years old. Surprisingly, we observed similar phenotypes as in mice, with age-dependent increases in N-glycan branching in $CD4^+$ T cells > $CD8^+$ T cells and $CD19^+$ B cells, with significantly bigger differences seen in females than male and naïve over memory subset populations (**Fig. 2.9A-F, 2.10A-D**). Restricting analysis to ages between 19 and 65 showed similar results in female $CD4^+$ T cells, indicating that the data is not skewed by those above 90 years of age and instead indicates a gradual and consistent increase in N-glycan branching with age (**Fig. 2.10E,F**). As seen in mice, age-associated increases in N-glycan branching suppressed T cell activity, as treating old female PBMCs with KIF to inhibit N-glycan branching rejuvenated ligand-induced T cell activation and proliferation (**Fig. 2.12A,B**).

Our lab has previously reported that short-term treatment of $CD4^+$ T cells (mixed naïve and memory populations) for 3 days with recombinant IL-7 lowers branching, which is opposite of what we have observed with mouse naïve $CD4^+$ T cells. However, this analysis did not consider gender differences or naïve versus memory T cells. In addition, homeostatic maintenance of the naïve T cell pool involves prolonged exposure to IL-7 *in vivo*, therefore we repeated these experiments for 6 days and analyzed naïve female $CD4^+$ and $CD8^+$ T cells at rest. This revealed that exogenous IL-7 induced little, if any,

increase in N-glycan branching in naïve $CD4^+$ T cells and a small increase in naïve $CD8^+$ T cells.

Our lab has previously shown that IL-7 regulates mRNA expression of the *Mgat1* branching enzyme in human T cells[17], where increased expression of IL-7 can either raise or lower N-glycan branching depending on the metabolic supply of UDP-GlcNAc. N-glycan branching enzymes all utilize the common sugar-nucleotide substrate UDP-GlcNAc, but they do so with declining efficiency such that Mgat4 and Mgat5 are limited for branching by the metabolic production of UDP-GlcNAc. This is due to the Km of Mgat4 and Mgat5 being ~100-200 fold worse than Mgat1 (~0.04 mM). Thus, when UDP-GlcNAc supply is limiting, increasing Mgat1 activity lowers branching by hoarding UDP-GlcNAc away from Mgat4 and Mgat5. Together, this suggests that IL-7 induced increase in Mgat1 activity may synergize with age-dependent increase in UDP-GlcNAc to increase N-glycan branching. Supplementing T cells from mice or humans with GlcNAc raises UDP-GlcNAc levels and N-glycan branching[16,22,28]. Strikingly, endogenous levels of GlcNAc in human serum markedly increase with age in both females and males (**Fig. 2.11A,B**). However, this increase in endogenous serum GlcNAc levels only positively correlated with N-glycan branching in female naïve $CD4^+$ T cells but not males (**Fig. 2.11C,D**), consistent with age-dependent increase in N-glycan branching being greater in females than in males. In addition, co-incubating resting female peripheral blood monocytes (PBMCs) with GlcNAc and IL-7 for 6 or 9 days synergistically increased N-glycan branching in female naïve $CD4^+$ T cells (**Fig. 2.11E,F, 2.12C,D**) while only having an additive effect for effector memory $CD4^+$ T cells (**Fig. 2.12E,F**). Together, our data suggests that elevated IL-7 signaling as a consequence of homeostatic maintenance of the naïve T cell pool in

humans synergizes with age-dependent increase in serum GlcNAc to raise N-glycan branching and suppress T cell activity in naïve > memory and female > male.

Discussion

Our current understanding of immune senescence implicates changes within the adaptive immune system, particularly within T cell populations, as the primary determinant of declining immune function with age. Despite our limited mechanistic understanding of immune senescence, the need to demonstrate direct association between immune cell function and clinical outcomes are required to keep pace with the rapidly aging global population. Here we demonstrate that IL-7 driven upregulation of N-glycan branching in female naïve $CD4^+$ T cells contributes to age-dependent immune dysfunction. This is a novel molecular mechanism not previously linked to immune senescence and provides a new avenue for therapeutic targeting. We have demonstrated that inhibiting N-glycan branching either pharmacologically with kifunensine *in vitro* or via genetic disruption of the branching enzyme Mgat2 rejuvenates immune function in aged T cells. This extends to rejuvenating immune response in an *in vivo* model of *Salmonella typhimurium* infection. Most importantly, our findings point to clear sex discrepancies between old male and female naïve $CD4^+$ T cells. Though previous studies have examined transcriptome changes in aged T cell subsets[11,14], this is the first study to our knowledge that specifically examines sex specific changes. Among the relatively few DEG's identified between young and old naïve $CD4^+$ T cells, less than 30% of these overlapped between males and females (**Table 2.2-2.4**), suggesting that immune senescence between sexes is mechanistically different. Immune function differences between males and females are well documented, such as increased risk in women for autoimmune diseases[43,44] or increased morbidity and mortality by SARS-CoV-2 among men[45]. Other aging associated sex differences are also becoming increasingly

appreciated. For instance, while immune responses to vaccination are consistently higher in females than males throughout childhood and adulthood, this trend is reversed in aged individuals for the pneumococcal and Td/Tdap vaccines (Klein and Flanagan, 2016). This reversal is consistent with the female specific increase in N-glycan branching observed in this study. Furthermore, while females demonstrate higher antibody titers to influenza vaccination throughout life and in old age, elderly males produce higher affinity antibodies than elderly females[46], with the latter more dependent on T cell help. Cumulatively, such sex differences imply that effective interventions of immune senescence in the elderly may require sex-specific strategies.

The mechanism underlying sex-specific increase in N-glycan branching in naïve T cell with age is unclear. Sex chromosome or sex hormone mediated mechanisms are most likely to be involved. Among the IL-7 pathway genes, only the gene encoding IL2rγ, a subunit of the IL-7 receptor, is present on the X-chromosome. However, we did not detect aging associated changes in its gene expression. Sex hormones on the other hand have been previously linked to the IL-7 pathway. In particular, ovariectomy in young female mice was reported to result in higher tissue levels of IL-7, an effect which was reversed by administration of estrogen[47,48]. Thus, IL-7 driven increases in naïve $CD4^+$ T cell branching may be secondary to age associated reduction in estrogen level in females. By comparison, although sex hormone levels also decrease with age in men, the rate of decrease is much slower[49] and may not decrease sufficiently to trigger increased IL-7 production.

Early reports of T cell hypo-reactivity in the elderly used mixed populations. In analyses of distinct T cell subsets, functional defects have persisted in naïve $CD4^+$ T cells

but have been brought into question for other subsets[50,51]. Interestingly, this pattern parallels the magnitude of N-glycan branching observed in this study, with $CD4^+$ > $CD8^+$ and naive > memory. Critically, our findings reveal that increases in N-glycan branching with age are driven by cell extrinsic factors *in vivo* and quickly reversed when the environment is normalized. Therefore *in vitro* studies, particularly proliferation studies requiring several days of cell culture, will lead to normalization of branching and will therefore underestimate the true extent of functional impairment. In this regard, *in vivo* studies and short-term *in vitro* assays, such as signaling assays in response to TCR stimulation, are likely more accurate measures. However, as aging associated defects have been described in the innate and adaptive arms of the immune system as well as lymphoid tissue architecture, *in vivo* studies need to be interpreted with caution. To overcome this issue, we used T cell specific branching deficiency (*Mgat2*$^{fl/fl}$*lck-cre* mice) in an *in vivo* model of *Salmonella typhimurium* infection. Indeed, in aged female mice, Mgat2 deficiency significantly rejuvenated immune function while leading to no improvement in aged males.

Our previous work revealed that IL7Rα deficient young mice had higher levels of N-glycan branching in a mixed population of $CD4^+$ T cells than wild-type littermates[17]. Our current study showed seemingly contradictory results – *in vivo* blocking of IL-7 with a neutralizing antibody (M25) resulted in lowered N-glycan branching whereas supplementing with IL-7 increased N-glycan branching. This discrepancy is likely secondary to a number of technical differences between the two studies. Our earlier studies analyzed splenic $CD4^+$ T cells as a whole whereas our study focused on distinguishing between naïve and memory $CD4^+$ T cell populations. Since memory T cells

have significantly higher levels of N-glycan branching than naïve T cells, population differences skewed towards memory over naïve in IL7Ra deficient mice[36,52] may have accounted for the observed increase in branching. The receptor for thymic stromal lymphopoietin (TSLP) is also absent since it is a heterodimer formed with IL7Rα as a subunit, consequentially resulting in absent TSLP signaling that may contribute to higher branching in IL7Rα deficient mice. Since IL7Rα mutants dramatically effect T cell development in the thymus, higher branching levels may also be a secondary effect of development. Distinguishing and pursuing these effects may shed more light on IL-7's role and effect on N-glycan branching.

Collectively, our findings provide a novel potential therapeutic target for immune senescence in females. Reversing age-dependent increases in N-glycan branching rejuvenate T cell immunity. Although there are known pharmacological inhibitors, further studies are required to test for toxicity for human use. Using these agents may merit exploration prior to vaccinations or during infection to improve T cell response in elderly females. IL-7 has been a popular non-specific target due to its property to generate T cell receptor diversity[53] and promote clonal expansion of mature thymocytes prior to entering the naïve T cell pool[54]. Treatment of old mice with IL-7 could potentially reverse age-dependent thymic involution[55,56] as well as induce homeostatic proliferation to replenish the peripheral naïve T cell pools. Although rejuvenating the naïve T cell population is attractive, our data indicates that this will lead to increased N-glycan branching and reduced functional competence. Thus, IL-7 therapy would be most effective in combination with N-glycan targeting agents that block the IL-7 induced increase in N-glycan branching.

Figure 2.1 N-glycan branching increases with age in mice

(A and B) Splenic T cells were analyzed for CD62L and CD44 by flow cytometry (C-F) Flow cytometry analysis of (C and E) female and (D and F) male mouse splenic cells for L-PHA binding, gating on naïve (CD62L+CD44-), central memory (CD62L+CD44+), or effector memory (CD62L-CD44-) as shown in A and B. Normalized geometric mean fluorescence intensity (MFI) is shown. Each aged mouse was normalized to its young control. P-values in (C-F) were determined using two-tailed t-test analysis. Error bars indicate mean ± s.e.m.

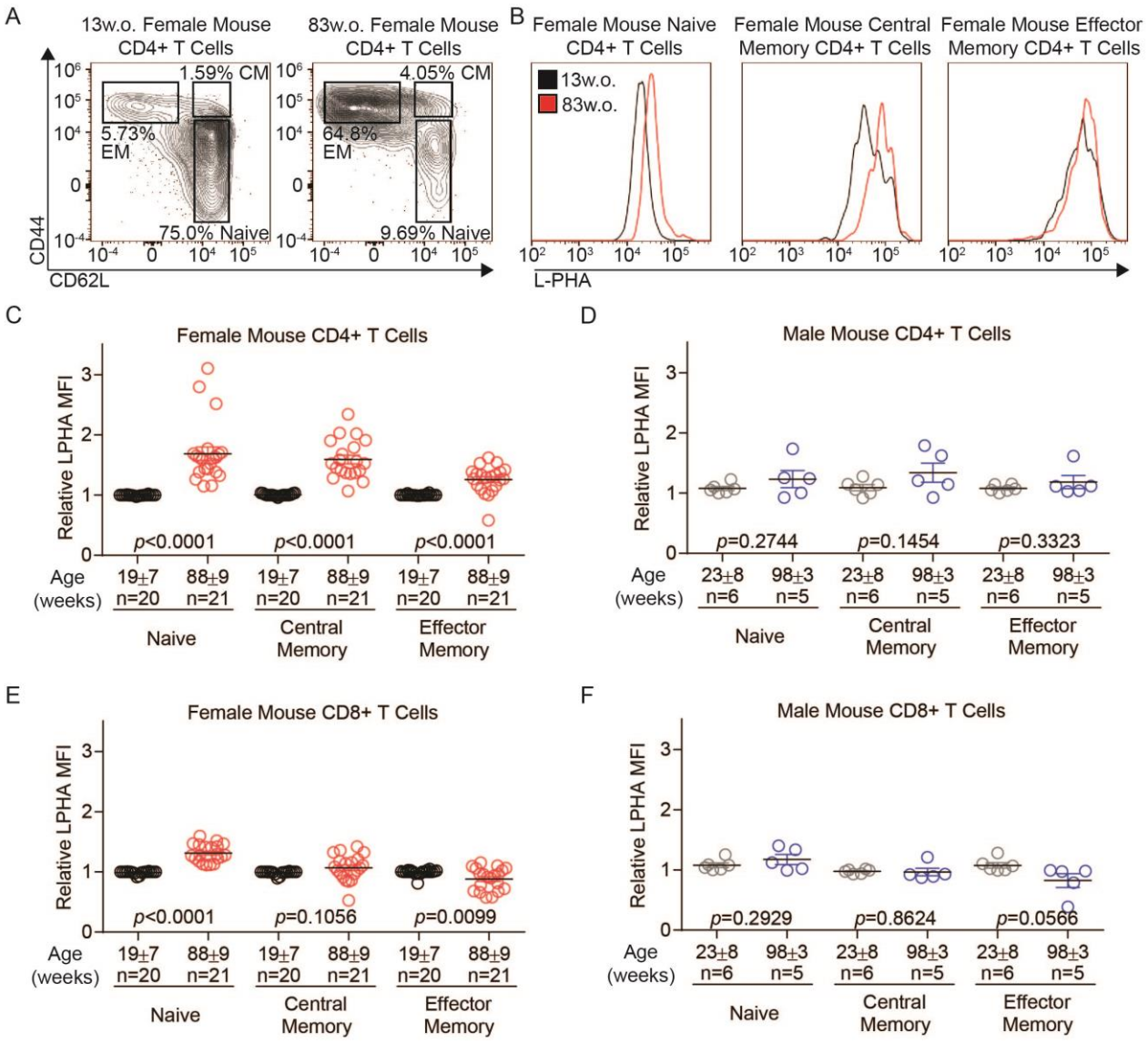
A
13w.o. Female Mouse CD4+ T Cells
83w.o. Female Mouse CD4+ T Cells
1.59% CM
5.73% EM
75.0% Naive
4.05% CM
64.8% EM
9.69% Naive
CD44
CD62L
B
Female Mouse Naive CD4+ T Cells
Female Mouse Central Memory CD4+ T Cells
Female Mouse Effector Memory CD4+ T Cells
13w.o.
83w.o.
L-PHA
C
Female Mouse CD4+ T Cells
Relative LPHA MFI
p<0.0001
p<0.0001
p<0.0001
Age (weeks)
19±7 n=20
88±9 n=21
Naive
Central Memory
Effector Memory
D
Male Mouse CD4+ T Cells
Relative LPHA MFI
p=0.2744
p=0.1454
p=0.3323
Age (weeks)
23±8 n=6
98±3 n=5
Naive
Central Memory
Effector Memory
E
Female Mouse CD8+ T Cells
Relative LPHA MFI
p<0.0001
p=0.1056
p=0.0099
Age (weeks)
19±7 n=20
88±9 n=21
Naive
Central Memory
Effector Memory
F
Male Mouse CD8+ T Cells
Relative LPHA MFI
p=0.2929
p=0.8624
p=0.0566
Age (weeks)
23±8 n=6
98±3 n=5
Naive
Central Memory
Effector Memory

Figure 2.1

Figure 2.2 Lymphocytes from male do not exhibit increased N-glycan branching with age

(A) Naïve CD4+ T cells isolated from lymph nodes in young and aged female mice were analyzed for N-glycan branching. (B) Naïve CD4+ T cells from male mice were analyzed for L-PHA binding by flow cytometry. (C and D) Naïve (CD62L+CD44-) CD4+ T cells and CD19+ B cells were directly compared and analyzed for N-glycan branching by L-PHA binding. (E) Thymocytes from female mice were analyzed for L-PHA binding by flow cytometry. Normalized geometric mean fluorescence intensity (MFI) is shown. Each aged mouse was normalized to its young control per experiment. P-values were determined using two-tailed T test. Error bars indicate mean ± s.e.m.

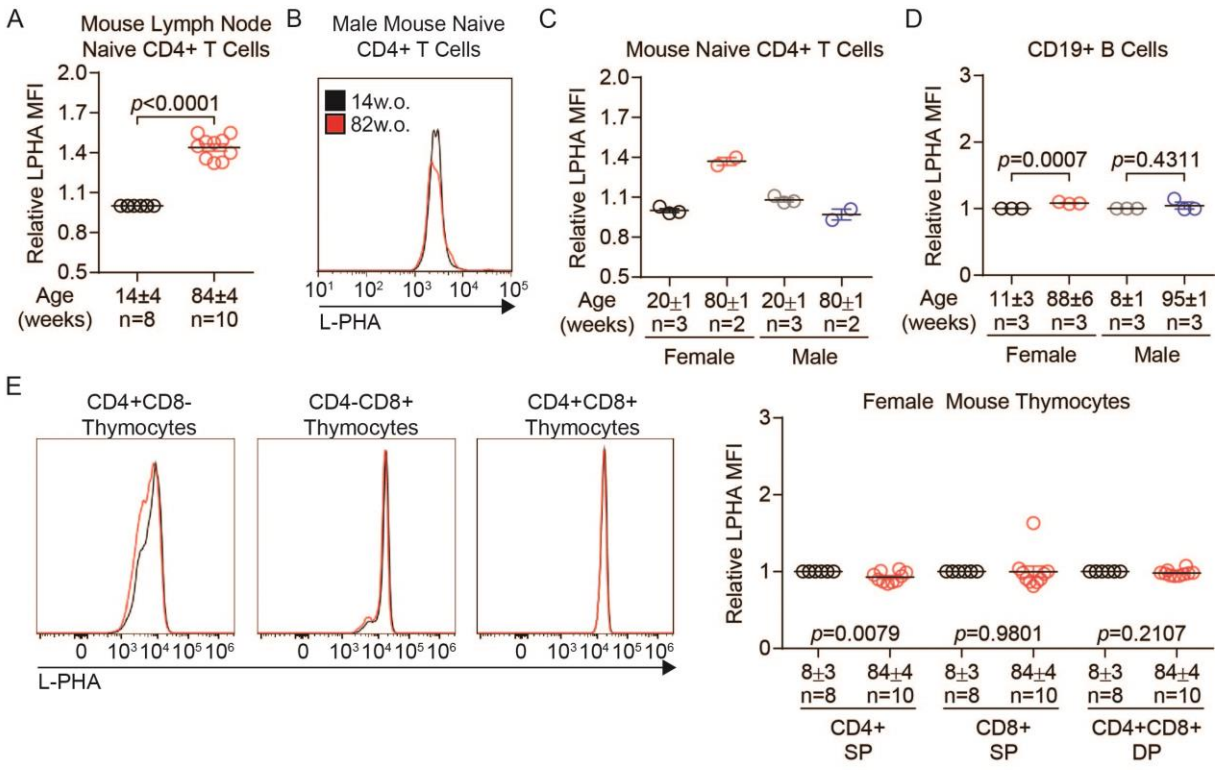
A
Mouse Lymph Node
Naive CD4+ T Cells
Relative LPHA MFI
p<0.0001
Age (weeks)
14±4 n=8
84±4 n=10
B
Male Mouse Naive
CD4+ T Cells
14w.o.
82w.o.
L-PHA
C
Mouse Naive CD4+ T Cells
Relative LPHA MFI
Age (weeks)
20±1 n=3
80±1 n=2
20±1 n=3
80±1 n=2
Female
Male
D
CD19+ B Cells
Relative LPHA MFI
p=0.0007
p=0.4311
Age (weeks)
11±3 n=3
88±6 n=3
8±1 n=3
95±1 n=3
Female
Male
E
CD4+CD8- Thymocytes
CD4-CD8+ Thymocytes
CD4+CD8+ Thymocytes
L-PHA
Female Mouse Thymocytes
Relative LPHA MFI
p=0.0079
p=0.9801
p=0.2107
8±3 n=8
84±4 n=10
CD4+ SP
CD8+ SP
CD4+CD8+ DP

Figure 2.2

Figure 2.3 Age dependent increase in N-glycan branching suppresses T cell function and differentiation in mice

(A-C) Representative flow cytometric analysis of purified splenic CD4+ T cells from the indicated female mouse and strain stimulated by anti-CD3 in the presence or absence of 5μM kifunensine as indicated for (A and B) 24 hours to analyze for activation marker CD69 or (C) 72 hours to assess proliferation by CFSE dilution. (D and E) Flow analysis of purified mouse splenic CD4+ T cells activated with anti-CD3 and anti-CD28 for 4 days with T_H17 (TGFβ+IL-6+IL-23) or iTreg (TGFβ) inducing conditions. Data show one experiment representative of at least three independent experiments. Error bars indicate mean ± s.e.m.

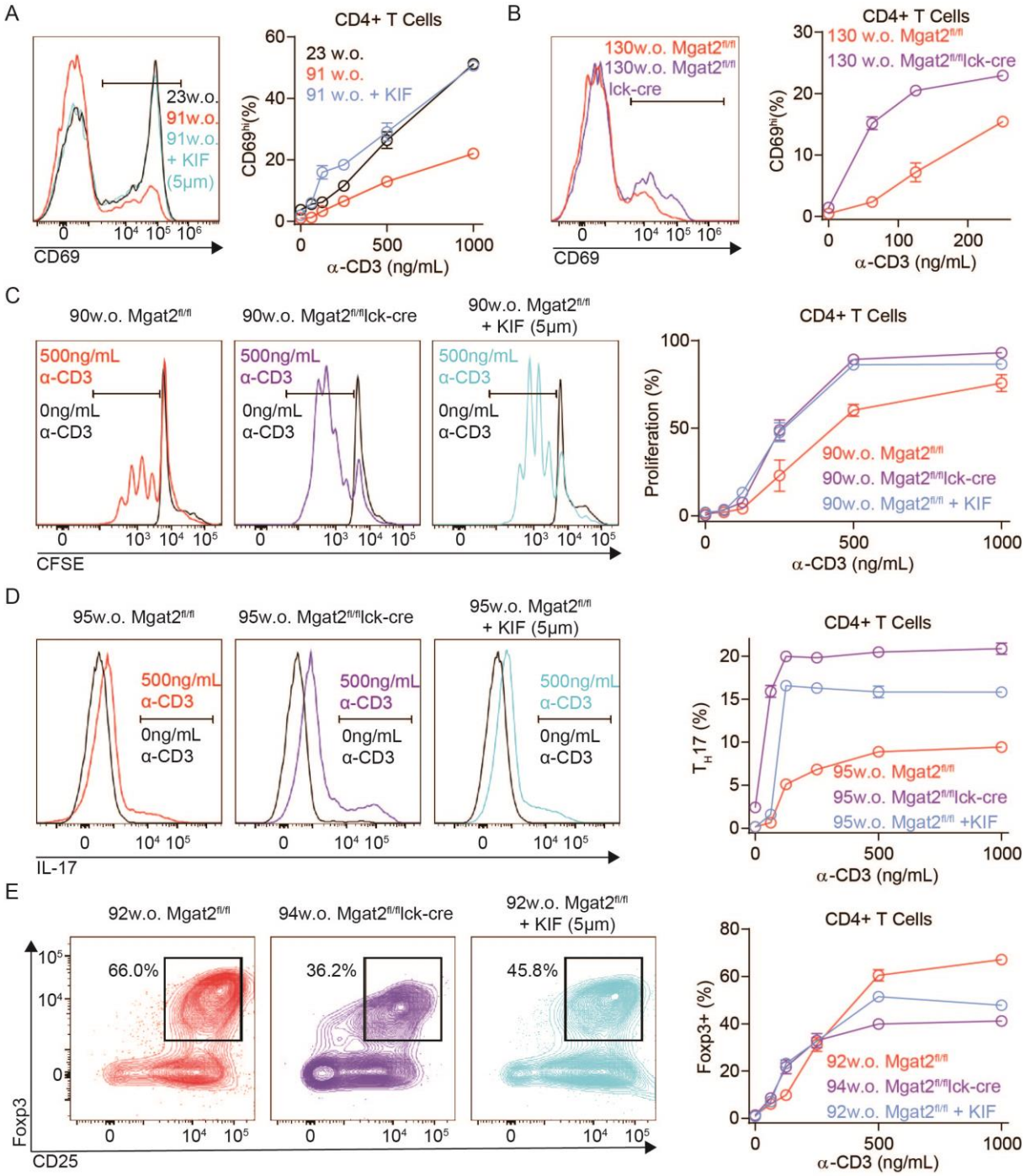
A
CD4+ T Cells
23w.o.
91w.o.
91w.o. + KIF (5μm)
CD69
23 w.o.
91 w.o.
91 w.o. + KIF
CD69hi(%)
α-CD3 (ng/mL)
B
130w.o. Mgat2fl/fl
130w.o. Mgat2fl/fl lck-cre
CD69
CD4+ T Cells
130 w.o. Mgat2fl/fl
130 w.o. Mgat2fl/fl lck-cre
CD69hi(%)
α-CD3 (ng/mL)
C
90w.o. Mgat2fl/fl
90w.o. Mgat2fl/fl lck-cre
90w.o. Mgat2fl/fl + KIF (5μm)
500ng/mL α-CD3
0ng/mL α-CD3
CFSE
CD4+ T Cells
Proliferation (%)
90w.o. Mgat2fl/fl
90w.o. Mgat2fl/fl lck-cre
90w.o. Mgat2fl/fl + KIF
α-CD3 (ng/mL)
D
95w.o. Mgat2fl/fl
95w.o. Mgat2fl/fl lck-cre
95w.o. Mgat2fl/fl + KIF (5μm)
500ng/mL α-CD3
0ng/mL α-CD3
IL-17
CD4+ T Cells
TH17 (%)
95w.o. Mgat2fl/fl
95w.o. Mgat2fl/fl lck-cre
95w.o. Mgat2fl/fl +KIF
α-CD3 (ng/mL)
E
92w.o. Mgat2fl/fl
94w.o. Mgat2fl/fl lck-cre
92w.o. Mgat2fl/fl + KIF (5μm)
66.0%
36.2%
45.8%
Foxp3
CD25
CD4+ T Cells
Foxp3+ (%)
92w.o. Mgat2fl/fl
94w.o. Mgat2fl/fl lck-cre
92w.o. Mgat2fl/fl + KIF
α-CD3 (ng/mL)

Figure 2.3

Figure 2.4 Regulating N-glycan branching in aged human PBMCs promotes T cell activity and proliferation

(A) Flow cytometric analysis of purified memory CD4+ T cells from female mice stimulated by anti-CD3 in the presence or absence of 5μM kifunensine for 24 hours. Data show one experiment representative of at least three independent experiments. Error bars indicate mean ± s.e.m.

A

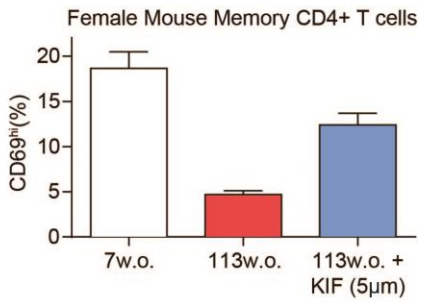
Female Mouse Memory CD4+ T cells
CD69hi(%)
20
15
10
5
0
7w.o.
113w.o.
113w.o. +
KIF (5μm)

Figure 2.4

Figure 2.5 Genetically regulating N-glycan branching promotes immune response to Salmonella in aged mice

Wild Type (WT) and Mgat2$^{-/-}$ mice were pre-treated with streptomycin (0.1ml of a 200mg/ml solution in sterile water) intragastrically prior to inoculation with S. Typhimurium ($5x10^8$ colony forming units per mouse). (A-F) Colony forming units (CFU) in Peyer's patches (A and D), mesenteric lymph nodes (MLN; B and E) and spleen (C and F) were determined at 72 hours after infection in female (A-C) and male (D-F) mice. Normalized proportion of (G) T_H17+ and (H) Foxp3+ cells within the gut were detected by flow cytometry. P-values are calculated by unpaired one-tailed t-test with (A) or without (B-F) Welch's correction. Error bars indicate mean ± s.e.m.

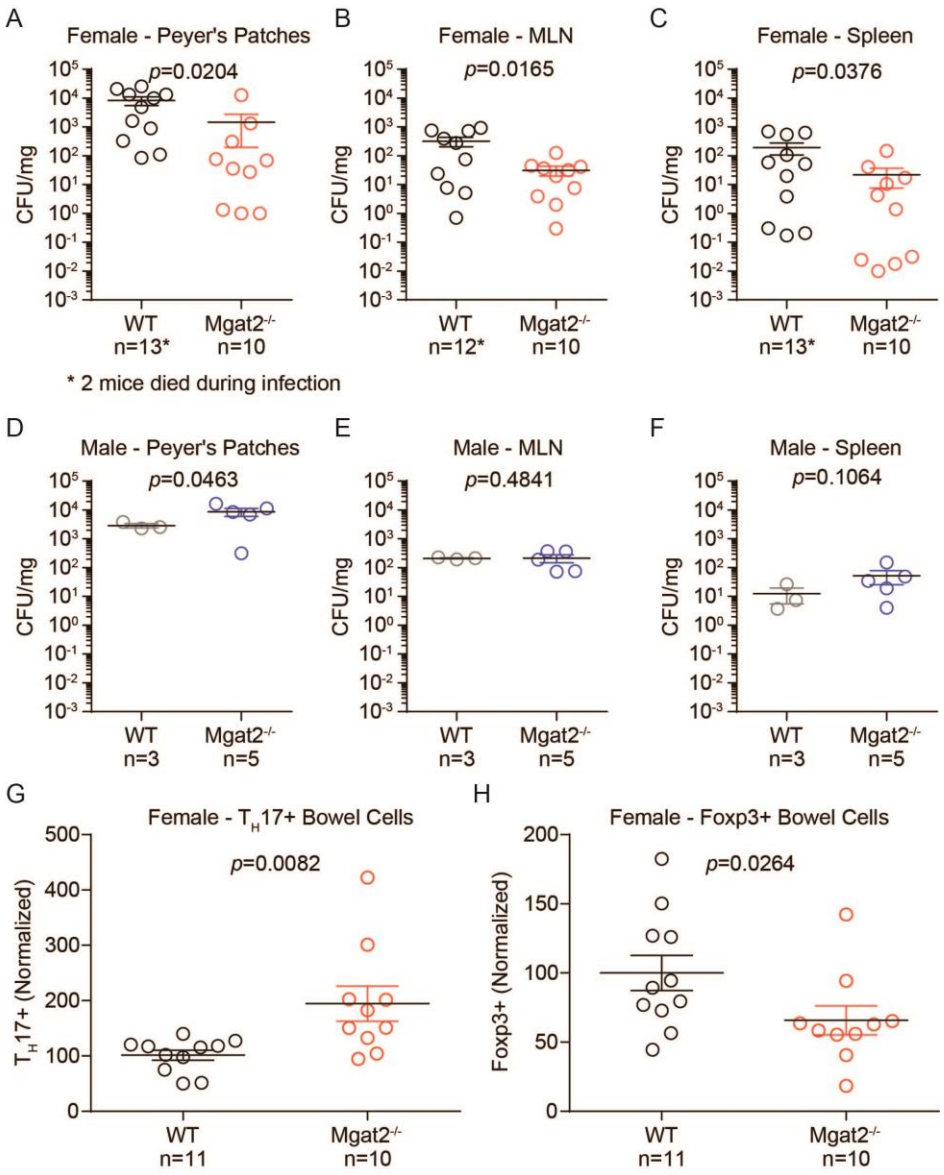
A
Female - Peyer's Patches
p=0.0204
CFU/mg
WT n=13*
Mgat2-/- n=10
B
Female - MLN
p=0.0165
WT n=12*
Mgat2-/- n=10
C
Female - Spleen
p=0.0376
WT n=13*
Mgat2-/- n=10
* 2 mice died during infection
D
Male - Peyer's Patches
p=0.0463
WT n=3
Mgat2-/- n=5
E
Male - MLN
p=0.4841
F
Male - Spleen
p=0.1064
G
Female - TH17+ Bowel Cells
p=0.0082
TH17+ (Normalized)
WT n=11
Mgat2-/- n=10
H
Female - Foxp3+ Bowel Cells
p=0.0264
Foxp3+ (Normalized)

Figure 2.5

Figure 2.6 Regulating N-glycan branching in aged male mice show minimal effect to Salmonella infection

Wild Type (WT) and Mgat2$^{-/-}$ mice were pre-treated with streptomycin (0.1ml of a 200mg/ml solution in sterile water) intragastrically prior to inoculation with S. Typhimurium ($5x10^8$ colony forming units per mouse). (A and B) Colony forming units (CFU) in the cecal content (CC) in (A) female and (B) male mice were determined 72 hours after infection. P-values are calculated by unpaired one-tailed t-test. Error bars indicate mean ± s.e.m.

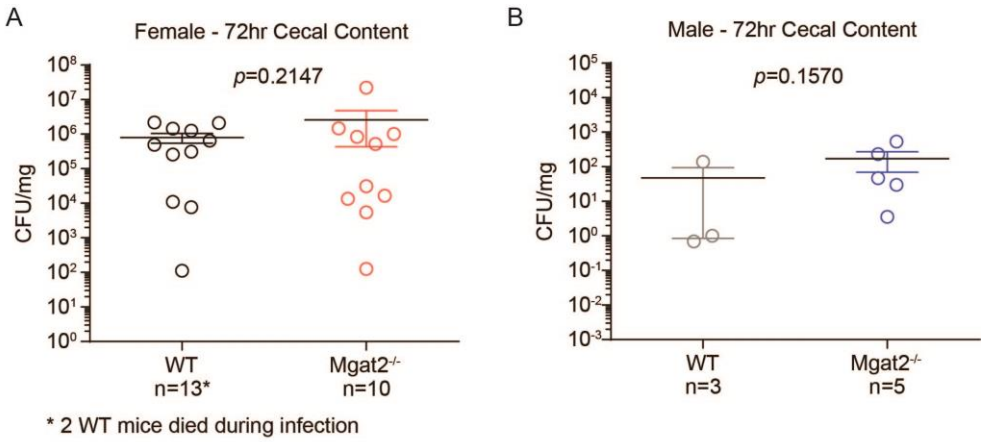
A
Female - 72hr Cecal Content
p=0.2147
CFU/mg
WT
n=13*
Mgat2-/-
n=10
* 2 WT mice died during infection
B
Male - 72hr Cecal Content
p=0.1570
CFU/mg
WT
n=3
Mgat2-/-
n=5

Figure 2.6

Figure 2.7 Regulating IL-7 signaling reduces N-glycan branching to young phenotype

(A) Flow cytometric analysis of freshly isolated naïve CD4+ T cells from the spleen of female mice *ex vivo* and incubated in complete media for 72 hours after isolation. (B) CD45.2+ naïve CD4+ T cells adoptively transferred into young female CD45.1+ mice analyzed by flow cytometry pre- and post-transfer. (C and D) Flow cytometric analysis of (C) IL7rα and (D) pSTAT5 *ex vivo* in female mice. (E and F) L-PHA flow cytometry of naïve CD4+ T cells from female mice treated with or without rhIL-7 (50ng/ml). (G) Mice received intraperitoneal injections of either isotype control (1.5μg) or rhIL-7/M25 on days 1, 3, and 5. On day 7, spleen were harvested and analyzed by LPHA flow cytometry. (H) Mice received intraperitoneal injections of either isotype control (1.5mg) or anti-mouse/human IL-7 (M25, 1.5mg) antibody 3 times a week for two weeks and had both blood drawn from the tail-tip for weekly assessment of N-glycan branching on naïve CD4+ T cells. (I) On day 14, spleens were harvested and LPHA was determined by flow cytometry. (J and K) Flow cytometric analysis of (J) IL7rα and (K) pSTAT5 of mice treated with either isotype control (1.5mg) or anti-mouse/human IL-7 (M25, 1.5mg) antibody 3 times a week for four weeks. P-values in (A) were determined using one-sided Mann-Whitney test. Error bars indicate mean ± s.e.m.

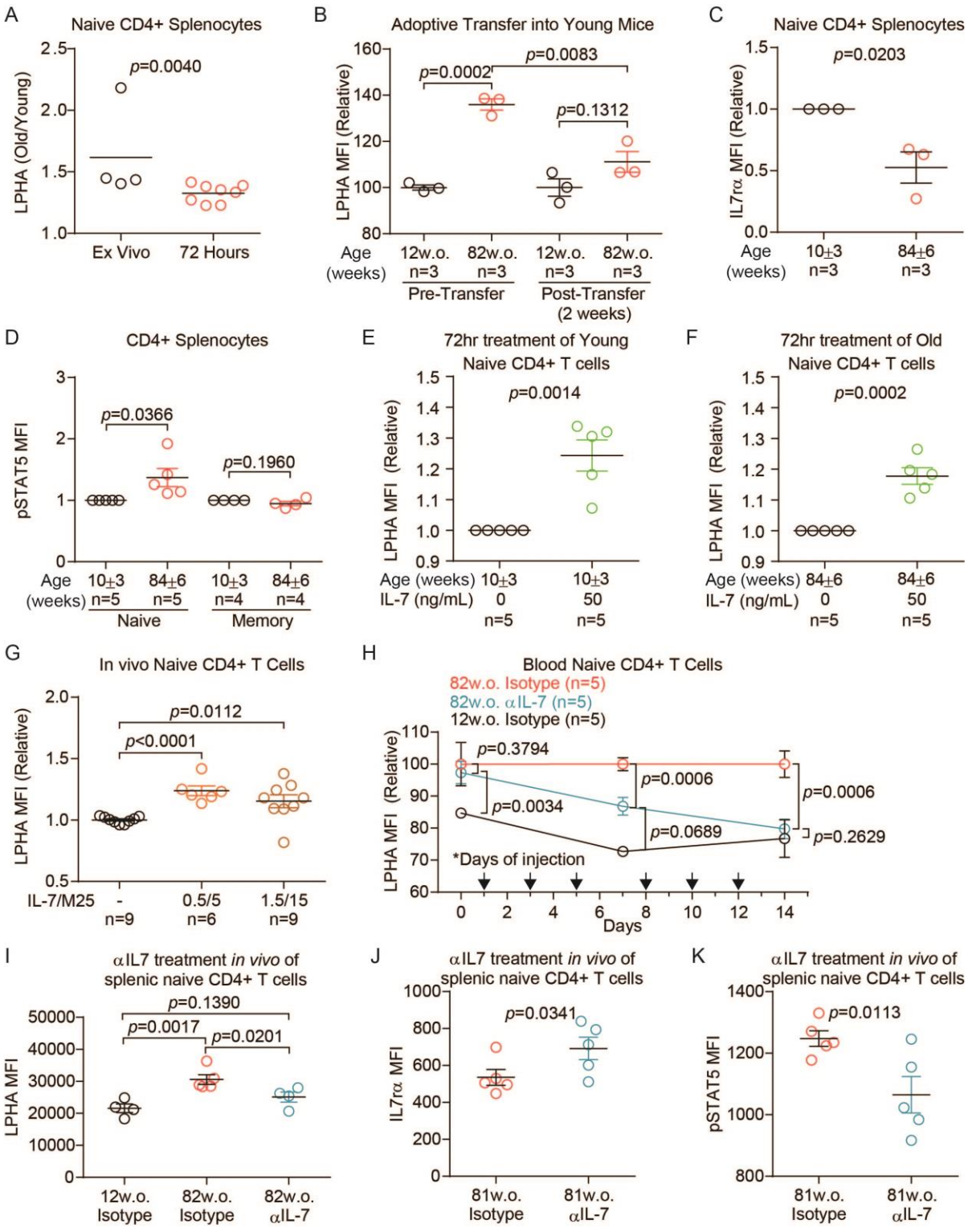
A
Naive CD4+ Splenocytes
LPHA (Old/Young)
p=0.0040
Ex Vivo
72 Hours
B
Adoptive Transfer into Young Mice
LPHA MFI (Relative)
p=0.0002
p=0.0083
p=0.1312
Age (weeks)
12w.o. n=3
82w.o. n=3
12w.o. n=3
82w.o. n=3
Pre-Transfer
Post-Transfer (2 weeks)
C
Naive CD4+ Splenocytes
IL7rα MFI (Relative)
p=0.0203
Age (weeks)
10±3 n=3
84±6 n=3
D
CD4+ Splenocytes
pSTAT5 MFI
p=0.0366
p=0.1960
Age (weeks)
10±3 n=5
84±6 n=5
10±3 n=4
84±6 n=4
Naive
Memory
E
72hr treatment of Young Naive CD4+ T cells
LPHA MFI (Relative)
p=0.0014
Age (weeks) 10±3
IL-7 (ng/mL) 0 n=5
10±3 50 n=5
F
72hr treatment of Old Naive CD4+ T cells
LPHA MFI (Relative)
p=0.0002
Age (weeks) 84±6
IL-7 (ng/mL) 0 n=5
84±6 50 n=5
G
In vivo Naive CD4+ T Cells
LPHA MFI (Relative)
p=0.0112
p<0.0001
IL-7/M25
- n=9
0.5/5 n=6
1.5/15 n=9
H
Blood Naive CD4+ T Cells
82w.o. Isotype (n=5)
82w.o. αIL-7 (n=5)
12w.o. Isotype (n=5)
LPHA MFI (Relative)
p=0.3794
p=0.0006
p=0.0034
p=0.0689
p=0.0006
p=0.2629
*Days of injection
Days
I
αIL7 treatment in vivo of splenic naive CD4+ T cells
LPHA MFI
p=0.1390
p=0.0017
p=0.0201
12w.o. Isotype
82w.o. Isotype
82w.o. αIL-7
J
αIL7 treatment in vivo of splenic naive CD4+ T cells
IL7rα MFI
p=0.0341
81w.o. Isotype
81w.o. αIL-7
K
αIL7 treatment in vivo of splenic naive CD4+ T cells
pSTAT5 MFI
p=0.0113
81w.o. Isotype
81w.o. αIL-7

Figure 2.7

Figure 2.8 IL-7 signaling pathway increases with age to promote N-glycan branching

(A) Representative flow cytometry plots of CD45.2+ donor cells in CD45.1+ recipient mice. (B) Analysis of sorted cells prior to RNA isolation and library prep for RNA-seq (C) Number of differentially expressed genes (DEGs) between young and aged naïve CD4+ T cells in female, male, or both. (D) qPCR of critical Golgi branching enzymes in female mice. (E) Mice received intraperitoneal injections of either isotype control (1.5mg) or anti-mouse/human IL-7 (M25, 1.5mg) antibody 3 times a week for two weeks and had their spleen harvested and analyzed for IL7rα. (F) Mice received intraperitoneal injections of either isotype control (1.5mg) or anti-mouse/human IL-7 (M25, 1.5mg) antibody 3 times a week for four weeks and had blood drawn from the tail-tip for weekly assessment of N-glycan branching on naïve CD4+ T cells. (G) On day 28, spleens were harvested and LPHA was determined by flow cytometry. P-values are calculated by unpaired one-tailed t-test. Error bars indicate mean ± s.e.m.

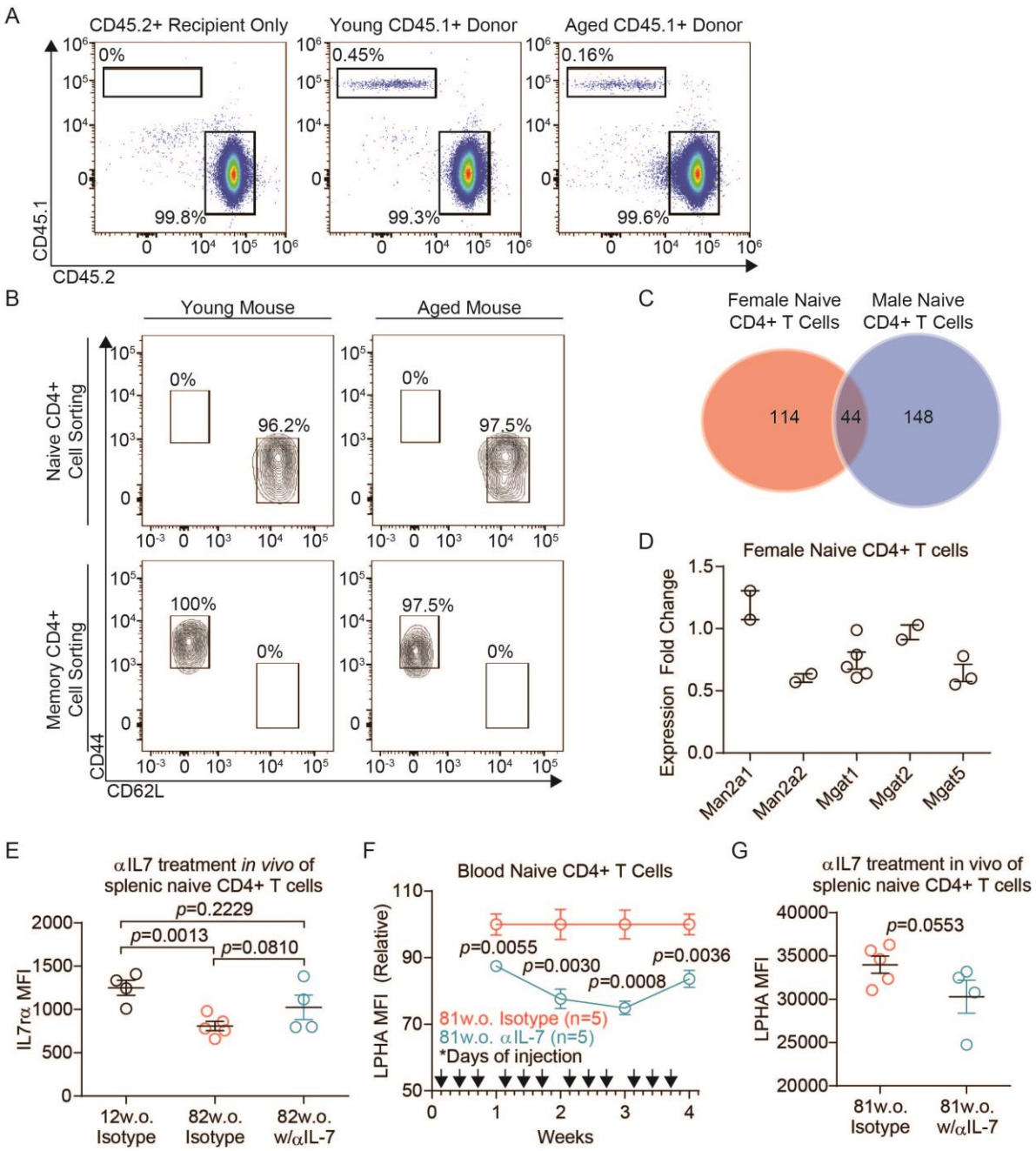
A
CD45.2+ Recipient Only
Young CD45.1+ Donor
Aged CD45.1+ Donor
0%
99.8%
0.45%
99.3%
0.16%
99.6%
CD45.1
CD45.2
B
Young Mouse
Aged Mouse
Naive CD4+ Cell Sorting
Memory CD4+ Cell Sorting
0%
96.2%
97.5%
100%
CD44
CD62L
C
Female Naive CD4+ T Cells
Male Naive CD4+ T Cells
114
44
148
D
Female Naive CD4+ T cells
Expression Fold Change
Man2a1
Man2a2
Mgat1
Mgat2
Mgat5
E
αIL7 treatment in vivo of splenic naive CD4+ T cells
p=0.2229
p=0.0013
p=0.0810
IL7rα MFI
12w.o. Isotype
82w.o. Isotype
82w.o. w/αIL-7
F
Blood Naive CD4+ T Cells
LPHA MFI (Relative)
p=0.0055
p=0.0030
p=0.0008
p=0.0036
81w.o. Isotype (n=5)
81w.o. αIL-7 (n=5)
*Days of injection
Weeks
G
αIL7 treatment in vivo of splenic naive CD4+ T cells
p=0.0553
LPHA MFI
81w.o. Isotype
81w.o. w/αIL-7

Figure 2.8

Figure 2.9 N-glycan branching increases with age in humans

(A-D) Human PBMCs from (A, C and D) females and (B) males were analyzed for L-PHA by flow cytometry in (A and B) CD4+ T cells, (C) CD8+ T cells, and CD19+ (D) B cells. (E) CD4+ T cells were further gated into naïve (CD45RA+CD45RO-) and memory (CD45RA-CD45RO+). (F) N-glycan branching was assessed for naïve and memory CD4+ T cells. Human data are from PBMCs isolated from healthy individuals as indicated in materials and methods. P-values were determined using linear regression analysis. Error bars indicate mean ± s.e.m.

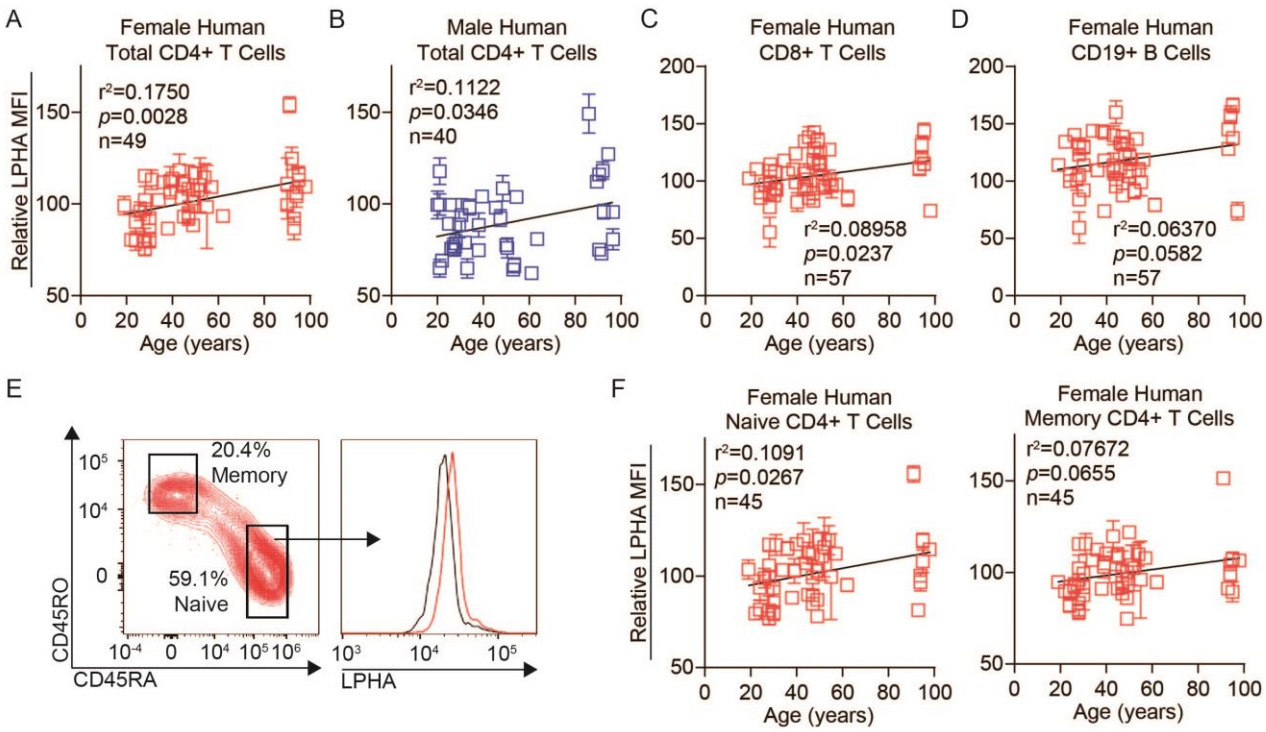
A
Female Human
Total CD4+ T Cells
r²=0.1750
p=0.0028
n=49
Relative LPHA MFI
Age (years)
B
Male Human
Total CD4+ T Cells
r²=0.1122
p=0.0346
n=40
Age (years)
C
Female Human
CD8+ T Cells
r²=0.08958
p=0.0237
n=57
Age (years)
D
Female Human
CD19+ B Cells
r²=0.06370
p=0.0582
n=57
Age (years)
E
20.4%
Memory
59.1%
Naive
CD45RO
CD45RA
LPHA
F
Female Human
Naive CD4+ T Cells
r²=0.1091
p=0.0267
n=45
Relative LPHA MFI
Age (years)
Female Human
Memory CD4+ T Cells
r²=0.07672
p=0.0655
n=45
Age (years)

Figure 2.9

Figure 2.10 Age-dependent increase in N-glycan branching also suppresses T cell activity in humans

(A-F) Human PBMCs from males were analyzed for LPHA by flow cytometry with further gating onto (A) CD8+ T cells, (B) CD19+ B cells, (C) naïve (CD45RA+CD45RO-) and (D) memory (CD45RA-CD45RO+) CD4+ T cells. (E and F) Total CD4+ T cells stained from (E) females and (F) males under the age of 65 were analyzed by LPHA flow cytometry. Human data are from PBMCs isolated from healthy individuals as indicated in materials and methods. P-values were determined using linear regression analysis. Error bars indicate mean ± s.e.m.

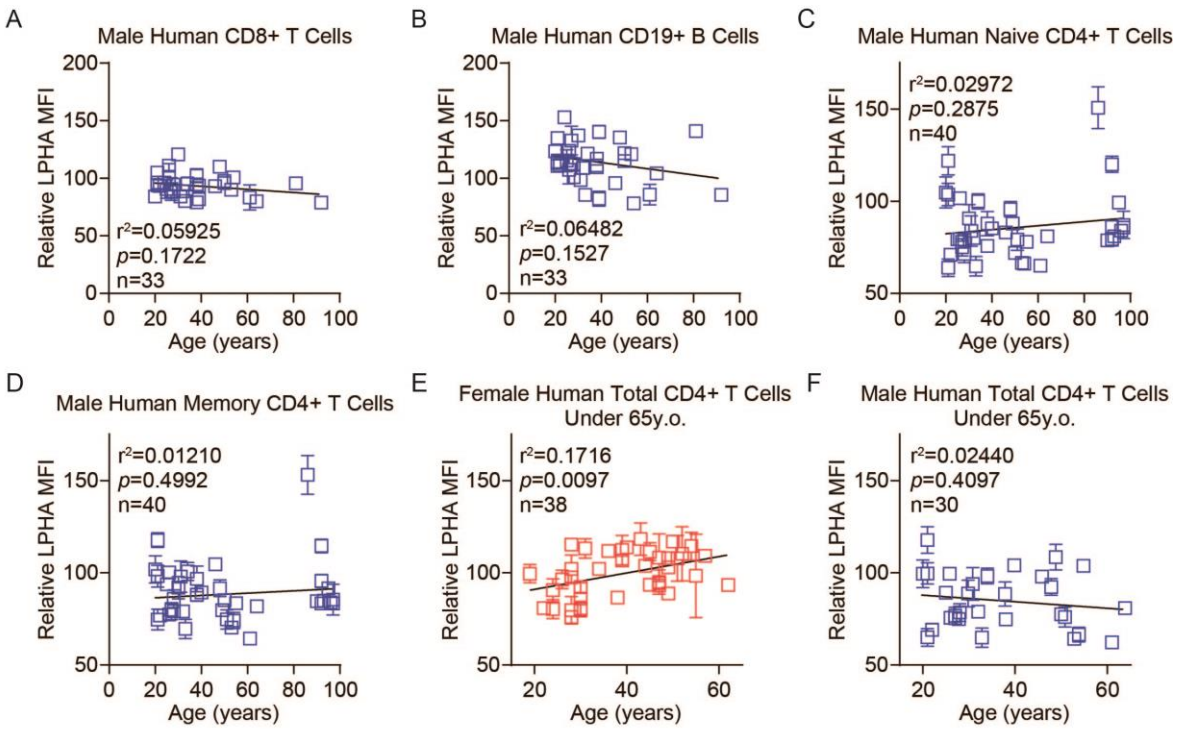
A
Male Human CD8+ T Cells
Relative LPHA MFI
r²=0.05925
p=0.1722
n=33
Age (years)
B
Male Human CD19+ B Cells
Relative LPHA MFI
r²=0.06482
p=0.1527
n=33
Age (years)
C
Male Human Naive CD4+ T Cells
Relative LPHA MFI
r²=0.02972
p=0.2875
n=40
Age (years)
D
Male Human Memory CD4+ T Cells
Relative LPHA MFI
r²=0.01210
p=0.4992
n=40
Age (years)
E
Female Human Total CD4+ T Cells
Under 65y.o.
Relative LPHA MFI
r²=0.1716
p=0.0097
n=38
Age (years)
F
Male Human Total CD4+ T Cells
Under 65y.o.
Relative LPHA MFI
r²=0.02440
p=0.4097
n=30
Age (years)

Figure 2.10

Figure 2.11 IL-7 synergizes with age-dependent increase in endogenous N-acetylglucosamine to increase N-glycan branching in humans

(A and B) Serum from humans were analyzed for levels of GlcNAc by LC-MS/MS. (C and D) PBMC's taken at the same time were analyzed by LPHA flow cytometry of naïve CD4+ T cells from (C) female and (D) male donors. (E and F) PBMCs from a 28 years old female Caucasian were treated with or without GlcNAc (40mM) and/or rhIL-7 (50ng/ml) then analyzed by LPHA flow cytometry. P-values were determined using (A-D) linear regression or (E-F) unpaired one-tailed t-test analysis. Error bars indicate mean ± s.e.m.

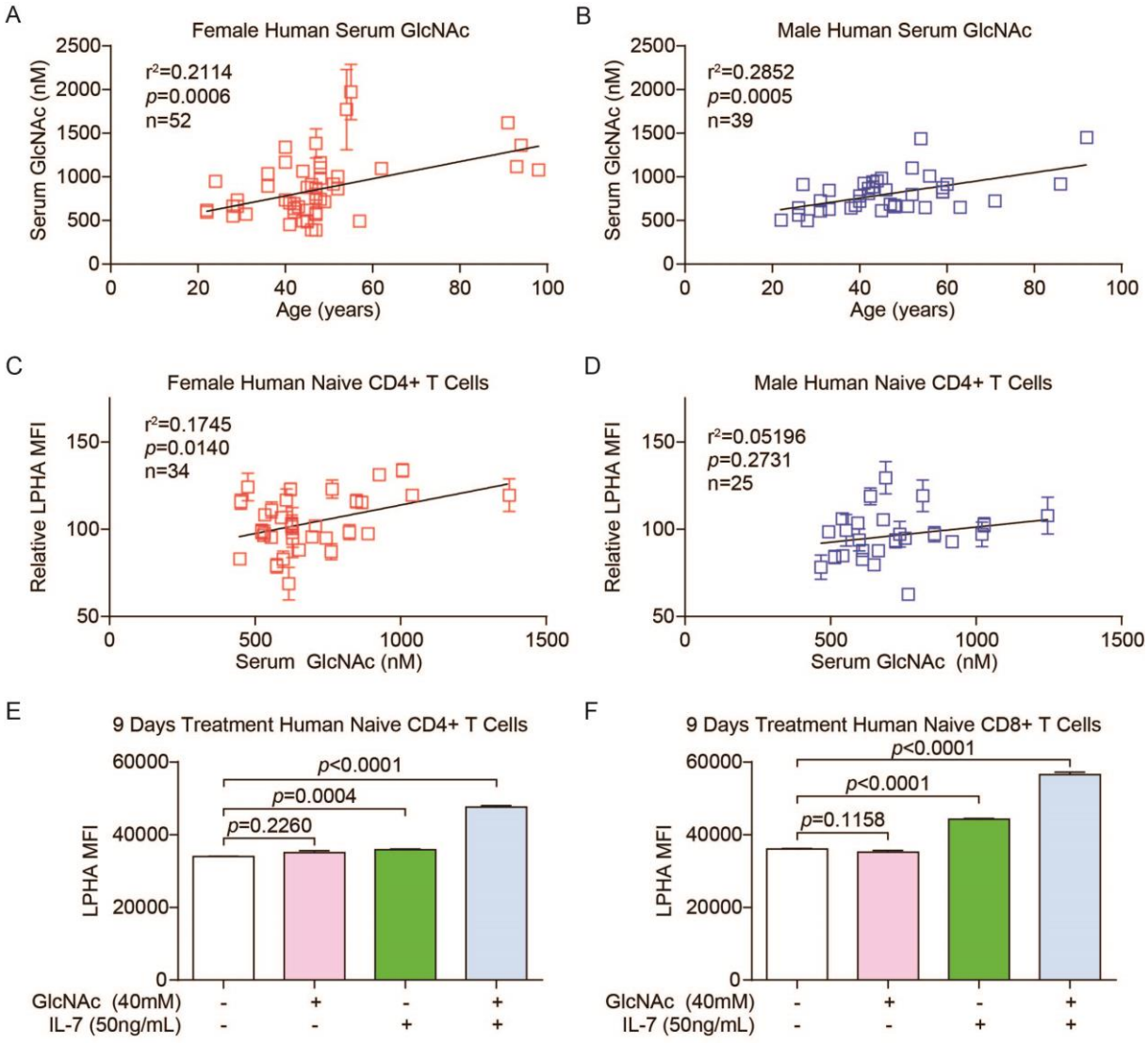
A
Female Human Serum GlcNAc
r²=0.2114
p=0.0006
n=52
Serum GlcNAc (nM)
Age (years)
B
Male Human Serum GlcNAc
r²=0.2852
p=0.0005
n=39
Serum GlcNAc (nM)
Age (years)
C
Female Human Naive CD4+ T Cells
r²=0.1745
p=0.0140
n=34
Relative LPHA MFI
Serum GlcNAc (nM)
D
Male Human Naive CD4+ T Cells
r²=0.05196
p=0.2731
n=25
Relative LPHA MFI
Serum GlcNAc (nM)
E
9 Days Treatment Human Naive CD4+ T Cells
p<0.0001
p=0.0004
p=0.2260
LPHA MFI
GlcNAc (40mM)
IL-7 (50ng/mL)
F
9 Days Treatment Human Naive CD8+ T Cells
p<0.0001
p<0.0001
p=0.1158
LPHA MFI
GlcNAc (40mM)
IL-7 (50ng/mL)

Figure 2.11

Figure 2.12 Inhibiting N-glycosylation in human cells reverse age-induced suppression of T cell activity by N-glycan branching

(A and B) Flow cytometric analysis of female human PBMCs stimulated by anti-CD3 in the presence or absence of 5μM kifunensine as indicated for (A) 24 hours to analyze for activation marker CD69 or (B) 72 hours to assess proliferation by CFSE dilution. (C-F) PBMCs from a 28 years old female Caucasian were treated with or without GlcNAc (40mM) and/or rhIL-7 (50ng/ml) for (C-E) 6 days or (F) 9 days then analyzed by LPHA flow cytometry. Data show one experiment representative of at least three independent experiments. Error bars indicate mean ± s.e.m.

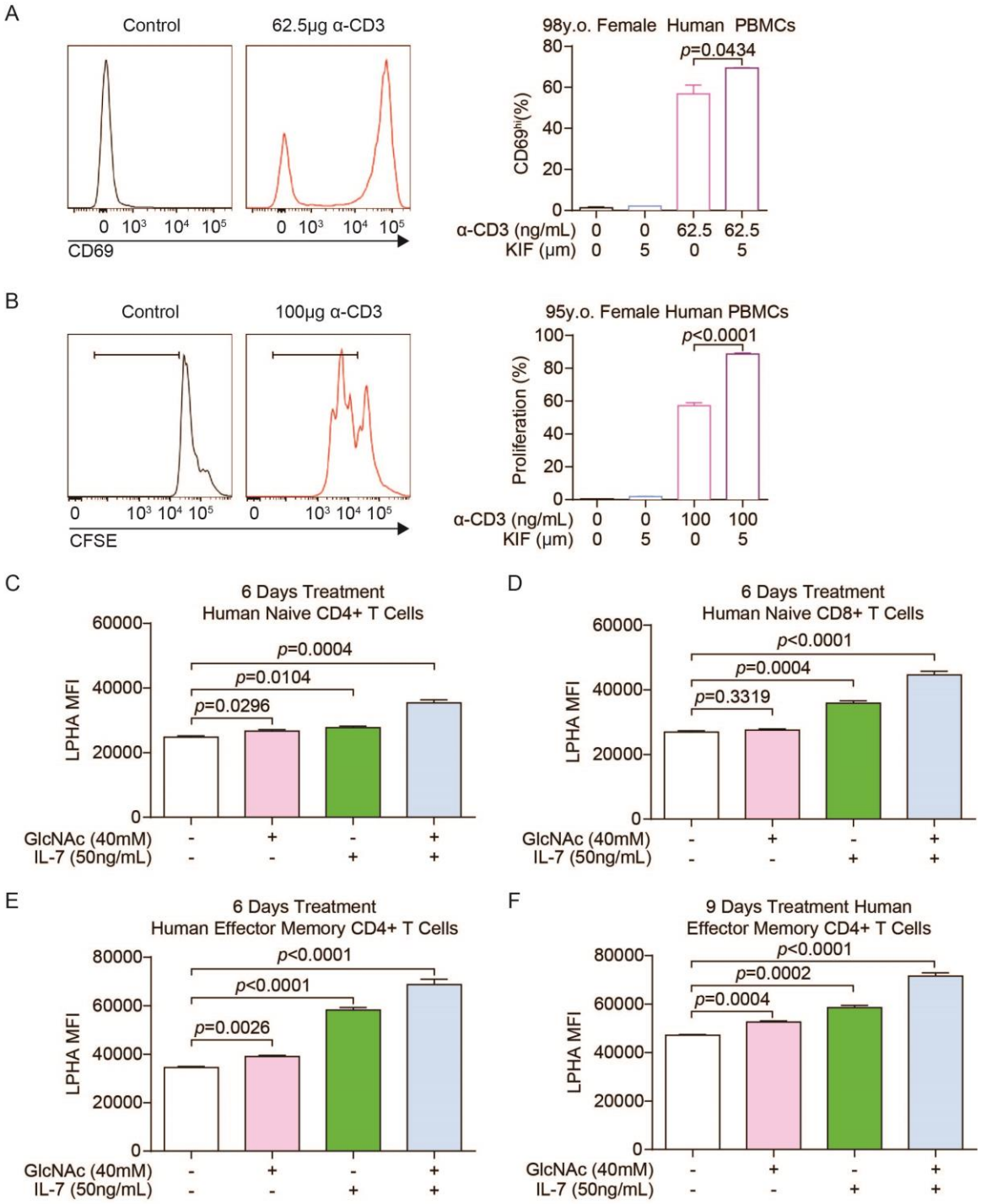
A
Control
62.5μg α-CD3
CD69
98y.o. Female Human PBMCs
p=0.0434
CD69hi(%)
α-CD3 (ng/mL) 0 0 62.5 62.5
KIF (μm) 0 5 0 5
B
Control
100μg α-CD3
CFSE
95y.o. Female Human PBMCs
p<0.0001
Proliferation (%)
α-CD3 (ng/mL) 0 0 100 100
KIF (μm) 0 5 0 5
C
6 Days Treatment
Human Naive CD4+ T Cells
LPHA MFI
p=0.0004
p=0.0104
p=0.0296
GlcNAc (40mM)
IL-7 (50ng/mL)
D
6 Days Treatment
Human Naive CD8+ T Cells
LPHA MFI
p<0.0001
p=0.0004
p=0.3319
GlcNAc (40mM)
IL-7 (50ng/mL)
E
6 Days Treatment
Human Effector Memory CD4+ T Cells
LPHA MFI
p<0.0001
p<0.0001
p=0.0026
GlcNAc (40mM)
IL-7 (50ng/mL)
F
9 Days Treatment Human
Effector Memory CD4+ T Cells
LPHA MFI
p<0.0001
p=0.0002
p=0.0004
GlcNAc (40mM)
IL-7 (50ng/mL)

Figure 2.12

Table 2.1 Female and Male IL7 Signaling Pathway DEGs

		Female		Male	
Gene Symbol	Gene Description	Adj p Value	Log2 Fold Change	Adj p Value	Log2 Fold Change
Socs3	Suppressor of cytokine signaling 3	4.49E-21	-2.5633	6.84E-01	-0.8798
Jak3	Janus kinase 3	6.67E-15	-1.4272	1.20E-01	-0.5597
IL7ra	Interleukin 7 receptor alpha	1.80E-02	0.6727	7.42E-01	0.2146
Stat5a	Signal transducer and activator of transcription 5A	6.36E-01	-0.3568	9.27E-01	-0.1486
Jak1	Janus kinase 1	6.62E-01	0.4007	9.77E-01	-0.0647
Il2rg	Interleukin 2 receptor gamma	7.52E-01	-0.2393	9.49E-01	-0.0762
Stat5b	Signal transducer and activator of transcription 5B	9.93E-01	-0.0097	8.54E-01	0.1410

Table 2.2 Female Only Young vs Old Naïve DEGs

Gene Symbol	Gene Description	Adj. p value	Log2 Fold Change
1700066B19Rik	RIKEN cDNA 1700066B19 gene	1.53E-02	-2.0579
5830416I19Rik	RIKEN cDNA 5830416I19 gene	1.66E-07	-6.8686
Abi3	ABI gene family, member 3	1.22E-02	-0.8102
Acot7	acyl-CoA thioesterase 7	1.70E-03	-1.1811
Adcy7	Adenylate cyclase 7	2.71E-02	0.6169
Anxa2	Annexin A2	4.80E-02	-1.1599
Apobec3	Apolipoprotein B mRNA editing enzyme, catalytic polypeptide 3	6.91E-03	-0.8127
B430306N03Rik	RIKEN cDNA B430306N03 gene	2.10E-02	-1.2834
Bcl3	B cell leukemia/lymphoma 3	1.26E-19	-2.2804
Bhlhe40	Basic helix-loop-helix family, member e40	1.35E-02	-2.3633
Camk2b	Calcium/Calmodulin-dependent protein kinase II, beta	1.07E-10	3.0108
Ccr5	Chemokine (C-C motif) receptor 5	1.20E-02	-3.7143
Cd55	CD55 molecule, decay accelerating factor for complement	8.26E-03	0.8636
Cd74	CD74 antigen	2.62E-22	-2.9560
Cdk5rap1	CDK5 regulatory subunit associated protein 1	9.81E-08	1.5333
Cdkn2d	Cyclin dependent kinase inhibitor 2D	1.96E-03	-0.7664
Chchd10	Coiled-coil-helix-coiled-coil-helix domain containing 10	1.23E-03	-1.1373
Cirbp	Cold inducible RNA binding protein	9.58E-03	-1.0224
Ckb	Creatine kinase, brain	2.88E-03	-0.8103
Cldn10	Claudin 10	3.42E-07	-2.2617
Cnn3	Calponin 3, acidic	1.50E-02	-0.6822
Crim1	Cysteine rich transmembrane BMP regulator 1 (chordin like)	6.11E-03	0.9050
Ctsa	Cathepsin A	1.02E-04	-0.8668
Cttn	Cortactin	3.99E-02	-3.5398
Cxcr1	Chemokine (C-X-C motif) receptor 1	4.26E-04	-2.1348
Cxcr3	Cheomkine (C-X-C motif) receptor 3	2.03E-02	-2.3439
Cxcr5	Chemokine (C-X-C motif) receptor 5	3.85E-07	-2.7931
Cysltr2	Cysteinyl leukotriene receptor 2	1.96E-03	-4.5641
Dse	Dermatan sulfate epimerase	5.44E-04	1.1449
E2f2	E2F transcription factor 2	5.07E-03	-0.7820
Egln3	egl-9 family hypoxia-inducible factor 3	3.30E-02	-1.9053
Elovl6	ELOVL fatty acid elongase 6	2.60E-03	-1.1859
Elovl7	ELOVL fatty acid elongase 7	4.60E-02	1.0645
Eomes	Eomesodermin	1.25E-02	-1.7488
Erdr1	Erythroid differentiation regulator 1	4.63E-03	-1.4042
Eri2	Exoribonuclease 2	1.72E-02	0.9227
Etv6	ETS variant transcription factor 6	1.57E-03	-1.2455
Fam212b	Inka box actin regulator 2	3.31E-02	1.2568
Fasl	Fas ligand (TNF superfamily, member 6)	3.09E-02	1.2776
Gadd45g	Growth arrest and DNA-damage-inducible 45 gamma	1.07E-06	-3.4287
Gatsl3	Cytosolic arginine sensor for mTORC1 subunit 1	6.25E-03	-0.9378
Gbp3	Guanylate binding protein 3	3.53E-02	-0.9029
Gm4956	Predicted gene 4956	3.91E-06	-2.8674
Gngt2	G protein subunit gamma transducing 2	1.22E-02	-1.1063
Gpd2	Glycerol phosphate dehydrogenase 2, mitochondrial	2.25E-06	1.5306
H2-Aa	Histocompatibility 2, class II antigen A, alpha	2.88E-03	-2.8507
H2-Ab1	Histocompatibility 2, class II antigen A, beta 1	9.99E-03	-3.4321
H2-Eb1	Histocompatibility 2, class II antigen E beta	3.16E-02	-2.5872
H2-Oa	Histocompatibility 2, O region alpha locus	2.69E-02	-1.1386
Hspa1a	Heat shock protein 1A	1.17E-03	2.5859
Hsph1	Heat shock 105kDa/110kDa protein 1	1.42E-04	1.1183
Igfbp4	Insulin-like growth factor binding protein 4	1.09E-04	-0.9894
Iigp1	Interferon inducible GTPase 1	2.02E-09	-1.4493
Ikzf4	IKAROS family zinc finger 4	2.61E-02	-1.2427
Il18bp	Interleukin 18 binding protein	2.48E-03	-2.4191
Il7r	Interleukin 7 receptor	1.76E-02	0.6727
Irf8	Interferon regulatory factor 8	1.07E-03	-1.3325
Itga6	Integrin alpha 6	9.12E-03	0.9563
Itih5	Inter-alpha (globulin) inhibitor H5	1.49E-03	-1.3769
Itk	IL2 inducible T cell kinase	3.53E-02	0.6286
Jak3	Janus kinase 3	6.67E-15	-1.4272
Jund	JunD proto-oncogene	3.43E-02	-0.5916
Jup	Junction plakoglobin	3.53E-02	-1.2538
Lag3	Lymphocyte-activation gene 3	4.71E-07	-3.7146
Mbnl3	Muscleblind like splicing factor 3	2.89E-02	0.6476
Moxd1	Monooxygenase, DBH-like 1	2.15E-02	-5.9660

Myb	Myeloblastosis oncogene	3.30E-02	-1.1794
Nebl	Nebulette	2.61E-02	3.3010
Nfkbia	NFKB inhibitor alpha	4.16E-02	-0.7300
Nkg7	Natural killer cell group 7 sequence	2.29E-11	-4.4538
Nr4a1	Nuclear receptor subfamily 4, group A, member 1	4.94E-02	-0.7616
Nrn1	Neuritin 1	6.54E-03	-1.5580
Ntrk3	Neurotrophic tyrosine kinase, receptor, type 3	3.19E-02	0.9271
Pcdhgc3	Protocadherin gamma subfamily C, 3	4.63E-03	-3.2355
Pdcd1	Programmed cell death 1 (PD-1)	3.09E-02	-1.0694
Pde2a	Phosphodiesterase 2A, cGMP-stimulated	4.92E-02	0.6572
Pde3b	Phosphodiesterase 3B, cGMP-inhibited	1.08E-08	1.1025
Pdlim4	PDZ and LIM domain 4	1.07E-06	1.4591
Pim2	Proviral integration site 2	1.07E-03	-0.7646
Plek	Pleckstrin	1.35E-02	-2.9786
Ptms	Parathymosin	3.42E-03	-0.7579
Relb	Avian reticuloendotheliosis viral (v-rel) oncogene related B	3.44E-02	-0.6937
Rgcc	Regulator of cell cycle	2.25E-02	0.7478
Rragd	Ras-related GTP binding D	3.09E-02	-1.4669
S100a4	S100 calcium binding protein A4	1.89E-02	-2.7483
S100a6	S100 calcium binding protein A6 (calcyclin)	3.09E-02	-2.5779
Sbno2	Strawberry Notch 2	6.53E-06	-1.1509
Scand1	SCAN domain-containing 1	1.96E-02	-0.9716
Sdhaf1	Succinate dehydrogenase complex assembly factor 1	1.09E-02	-0.9208
Sema4f	Semaphorin 4F	9.82E-04	0.9065
Sema7a	Semaphorin 7A	3.25E-02	-4.1315
Sgk1	Serum/glucocorticoid regulated kinase 1	1.96E-03	-0.7464
Skap2	src family associated phosphoprotein 2	3.78E-05	-1.3032
Sntb1	Syntrophin, basic 1	1.10E-03	1.4221
Sntb2	Syntrophin, basic 2	1.62E-03	1.9643
Socs1	Suppressor of cytokine signaling 1	6.00E-06	-1.4015
Socs3	Suppressor of cytokine signaling 3	4.49E-21	-2.5633
Ssbp4	Single stranded DNA binding protein 4	1.23E-03	-0.8345
Susd3	Sushi domain containing 3	3.74E-02	-0.7478
Synpo	Synaptopodin	3.30E-02	-3.2933
Tgm2	Transglutaminase 2, C polypeptide	4.66E-02	-5.2961
Tgtp1	T cell specific GTPase 1	1.96E-02	-0.7238
Tha1	Threonine aldolase 1	2.42E-05	-1.7877
Tlr12	Toll-like receptor 12	1.35E-02	-1.0229
Tm6sf1	Transmembrane 6 superfamily member 1	1.22E-02	-1.1883
Tnfaip8	Tumor necrosis factor, alpha-induced protein 8	1.84E-03	0.7255
Tnfrsf19	Tumor necrosis factor receptor superfamily, member 19	4.16E-02	2.6928
Tnfrsf4	Tumor necrosis factor receptor superfamily, member 4	7.79E-03	-1.1326
Tnfrsf9	Tumor necrosis factor receptor superfamily, member 9	8.79E-05	-1.3290
Tppp	Tubulin polymerization promoting protein	2.25E-02	5.6820
Tspan3	Tetraspanin 3	4.60E-02	-0.6839
Ttc28	Tetratricopeptide repeat domain 28	2.61E-02	1.1526
Tubb2b	Tubulin, beta 2B class IIB	8.60E-06	-1.7083
Vamp2	Vesicle-associated membrane protein 2	3.53E-02	-0.6872

Table 2.3 Male Only Young vs Old Naïve DEGs

Gene Symbol	Gene Description	Adj. p Value	Log2 Fold Change
1110032F04Rik	Riken cDNA 1110032F04 gene	1.46E-05	1.1845
2310022B05Rik	Riken cDNA 2310022B05 gene	4.62E-02	0.8614
2410006H16Rik	Riken cDNA 2410006H16 gene	3.56E-03	-0.8239
5830416I19Rik	Riken cDNA 5830416I19 gene	2.14E-12	-5.1989
Abca1	ATP-binding cassette, sub-family A (ABC1), member 1	1.84E-03	1.2653
Abcb9	ATP-binding cassette, sub-family B (MDR/TAP), member 9	3.35E-02	0.5156
Acsf2	Acyl-CoA synthetase family member 2	1.47E-02	0.8510
Ahnak	AHNAK nucleoprotein (desmoyokin)	4.87E-02	-1.3980
Aim2	Absent in melanoma 2	8.23E-03	-1.0271
Aqp3	Aquaporin 3	3.35E-02	0.8785
Arsb	Arylsulfatase B	1.02E-02	0.5862
Atp5o	ATP synthase, H+ transporting, mitochondrial F1 complex, O subunit	3.09E-02	-0.3667
B4galt5	UDP-Gal:betaGlcNAc beta 1,4-galactosyltransferase, polypeptide 5	3.18E-02	0.6390
Bach2	BTB and CNC homology, basic leucine zipper transcription factor 2	2.23E-02	0.5546
Cd52	CD52 antigen	4.04E-02	-0.3856
Cd7	CD7 antigen	3.79E-03	0.8743
Cd72	CD72 antigen	3.17E-03	-1.1841
Cmpk2	Cytidine monophosphate (UMP-CMP) kinase 2, mitochondrial	3.35E-02	0.6314
Cox7a2l	Cytochrome c oxidase subunit 7A2 like	3.32E-02	-0.4024
Cst7	Cystatin F (leukocystatin)	2.01E-07	-1.4238
Ctdsp2	CTD small phosphatase 2	2.37E-02	0.4188
Cyp4v3	Cytochrome P450, family 4, subfamily v, polypeptide 3	3.56E-03	-0.8192
Cyp51	Cytochrome P450, family 51	1.42E-03	-0.7610
Dbi	Diazepam binding inhibitor	4.63E-02	-0.7428
Dnajc15	DnaJ heat shock protein family (Hsp40) member C15	2.83E-02	-0.5734
Dos	Calcium channel, beta subunit associated regulatory protein	3.06E-02	1.1173
Dusp2	Dual specificity phosphatase 2	1.26E-02	0.6474
Eef1a1	Eukaryotic translation elongation factor 1 alpha 1	3.85E-02	-0.3604
Eef1d	Eukaryotic translation elongation factor 1 delta	4.04E-02	-0.4543
Eef1g	Eukaryotic translation elongation factor 1 gamma	2.78E-02	-0.3684
Eif3k	Eukaryotic translation initiation factor 3, subunit K	1.35E-02	-0.3968
Eif3m	Eukaryotic translation initiation factor 3, subunit M	3.35E-02	-0.4399
Fam46a	Family with sequence similarity 46, member A	8.49E-03	-0.4775
Fau	FBR-MuSV ubiquitously expressed (fox derived)	4.69E-02	-0.4788
Fdft1	Farnesyl diphosphate farnesyl transferase 1	2.58E-02	-0.6958
Fdps	Farnesyl diphosphate synthetase	1.16E-02	-0.6462
Gapdh	Glyceraldehyde-3-phosphate dehydrogenase	4.55E-02	-0.3065
Ggta1	Glycoprotein galactosyltransferase alpha 1, 3	3.44E-02	-0.6031
Gltscr2	NOP53 ribosome biogenesis factor	4.77E-02	-0.4197
Gm128	Predicted gene 128	4.43E-02	-5.2156
Gpc1	Glypican 1	1.48E-03	-1.3638
Gpr34	G protein-coupled receptor 34	2.48E-03	-1.1009
Gpr68	G protein-coupled receptor 68	1.51E-03	-1.4243
Gpx4	Glutathione peroxidase 4	7.45E-03	-0.4584
Gucy1a3	Guanylate cyclase 1, soluble, alpha 1	5.11E-03	-1.7567
H2-Q10	Histocompatibility 2, Q region locus 10	2.23E-02	-2.7733
Hmgcs1	3-hydroxy-3-methylglutaryl-Coenzyme A synthase 1	1.53E-02	-0.6002
Hnrnpdl	Heterogeneous nuclear ribonucleoprotein D-like	3.06E-02	0.6533
Hs3st3b1	Heparan sulfate (glucosamine) 3-O-sulfotransferase 3B1	3.91E-02	0.5637
Hsp90ab1	Heat shock protein 90 alpha (cytosolic), class B member 1	1.15E-03	-0.6139
Idi1	Isopentenyl-diphosphate delta isomerase	1.02E-02	-0.7977
Ifi27l2a	Interferon, alpha-inducible protein 27 like 2A	3.43E-06	0.7556
Ifit1	Interferon-induced protein with tetratricopeptide repeats 1	1.47E-04	1.0389
Ifit3	Interferon-induced protein with tetratricopeptide repeats 3	1.29E-04	1.1835
Igbp1	Immunoglobulin (CD79A) binding protein 1	4.04E-02	-0.4280
Igf2bp3	Insulin-like growth factor 2 mRNA binding protein 3	1.44E-02	5.8260
Impdh2	Inosine monophosphate dehydrogenase 2	1.62E-03	-0.4951
Irf2bp2	Interferon regulatory factor 2 binding protein 2	3.51E-02	0.5202
Irf7	Interferon regulatory factor 7	6.19E-03	0.6545
Klf2	Kruppel-like factor 2 (lung)	2.30E-02	0.4169
Klf3	Kruppel-like factor 3 (basic)	1.10E-02	0.5150
Klhdc3	Kelch domain containing 3	4.15E-02	0.4574
Ldlr	Low density lipoprotein receptor	4.48E-03	-0.8302
Lpxn	Leupaxin	1.35E-02	-0.5700
Ly6k	Lymphocyte antigen 6 complex, locus K	1.26E-03	-1.7027
Mapk11	Mitogen-activated protein kinase 11	4.62E-02	-0.7311

Mex3b	Mex3 RNA binding family member B	1.12E-02	0.9307
Mex3c	Mex3 RNA binding family member C	1.00E-02	0.6569
Mrps16	Mitochondrial ribosomal protein S16	3.16E-02	-0.5350
Mthfd2	Methylenetetrahydrofolate dehydrogenase	4.63E-02	-0.4824
Myeov2	Myeloma overexpressed 2 homolog	2.27E-02	-0.5461
Mylip	Myosin regulatory light chain interacting protein	4.87E-02	0.4050
Myo6	Myosin VI	1.45E-05	-1.0580
Nme2	NME/NM23 nucleoside diphosphate kinase 2	3.56E-03	-0.5086
Npm1	Nucleophosmin 1	4.18E-02	-0.3434
Nsa2	NSA2 ribosome biogenesis homolog	6.32E-03	-0.4449
Oas2	2'-5' oligoadenylate synthetase 2	4.87E-02	2.0424
Oasl2	2'-5' oligoadenylate synthetase-like 2	7.14E-04	1.3155
Pag1	Phosphoprotein associated with glycosphingolipid microdomains 1	1.28E-02	0.4532
Pfdn5	Prefoldin 5	1.89E-03	-0.5263
Phgdh	3-phosphoglycerate dehydrogenaseprovided	2.78E-02	-0.4446
Pid1	Phosphotyrosine interaction domain containing 1	1.23E-03	-2.1133
Plagl2	Pleiomorphic adenoma gene-like 2	2.30E-02	0.5996
Plp2	Proteolipid protein 2	1.89E-03	-0.6411
Prf1	Perforin 1 (pore forming protein)	4.97E-03	-0.5866
Pros1	Protein S (alpha)	1.34E-02	-1.8707
Ptgfrn	Prostaglandin F2 receptor negative regulator	1.10E-02	0.9535
Ptpn6	Protein tyrosine phosphatase, non-receptor type 6	4.39E-02	-0.3542
Rab11fip4	RAB11 family interacting protein 4 (class II)	2.23E-02	0.7785
Ranbp10	RAN binding protein 10	8.32E-03	0.5987
Rasal1	RAS protein activator like 1 (GAP1 like)	4.64E-03	1.4741
Rnf122	Ring finger protein 122	2.48E-03	-0.8446
Rpl10	Ribosomal protein L10	1.90E-03	-0.4722
Rpl11	Ribosomal protein L11	1.83E-02	-0.4325
Rpl13a	Ribosomal protein L13A	2.00E-02	-0.4755
Rpl14	Ribosomal protein L14	6.75E-03	-0.4597
Rpl17	Ribosomal protein L17	4.48E-03	-0.4799
Rpl3	Ribosomal protein L3	1.88E-02	-0.4605
Rpl32	Ribosomal protein L32	2.39E-02	-0.4525
Rpl35	Ribosomal protein L35	3.44E-02	-0.4375
Rpl35a	Ribosomal protein L35A	4.87E-02	-0.4262
Rpl36a	Ribosomal protein L36A	2.00E-02	-0.5360
Rpl37a	Ribosomal protein L37a	3.09E-02	-0.4574
Rpl38	Ribosomal protein L38	2.86E-02	-0.5145
Rpl39	Ribosomal protein L39	2.78E-02	-0.5456
Rpl4	Ribosomal protein L4	2.17E-02	-0.3358
Rpl5	Ribosomal protein L5	7.06E-03	-0.4216
Rpl6	Ribosomal protein L6	2.39E-02	-0.3729
Rpl7a	Ribosomal protein L7A	4.80E-02	-0.3587
Rps13	Ribosomal protein S13	4.43E-02	-0.4188
Rps15a	Ribosomal protein S15A	4.15E-02	-0.4271
Rps20	Ribosomal protein S20	3.10E-02	-0.4667
Rps21	Ribosomal protein S21	3.20E-02	-0.5277
Rps29	Ribosomal protein S29	1.21E-02	-0.6317
Rps3	Ribosomal protein S3	2.95E-02	-0.4492
Rps6	Ribosomal protein S6	1.90E-02	-0.4244
Rps8	Ribosomal protein S8	4.69E-02	-0.3784
Rps9	Ribosomal protein S9	1.68E-02	-0.5002
Rsad2	Radical S-adenosyl methionine domain containing 2	1.19E-03	1.5841
Rtp4	Receptor transporter protein 4	3.30E-05	0.8465
Sdc3	Syndecan 3	8.53E-03	1.0743
Sec61g	SEC61, gamma subunit	3.09E-02	-0.5096
Sema4a	Semaphorin 4A	2.30E-02	-0.4651
Skil	SKI-like	4.87E-02	0.3824
Slc25a39	Solute carrier family 25, member 39provided	2.79E-02	0.5353
Slc35g1	Solute carrier family 35, member G1	1.90E-03	0.8306
Snrpg	Small nuclear ribonucleoprotein polypeptide G	1.67E-02	-0.4938
Sp140	Sp140 nuclear body protein	6.75E-03	-0.6385
Sqle	Squalene epoxidase	2.06E-03	-0.9184
Srpk2	Serine/arginine-rich protein specific kinase 2	1.12E-02	0.5446
Sugt1	SGT1, suppressor of G2 allele of SKP1 (S. cerevisiae)	4.25E-03	-0.5729
Tapbpl	TAP binding protein-like	1.42E-03	-0.6756
Tbc1d30	TBC1 domain family, member 30	4.64E-03	-1.0111
Tet3	Tet methylcytosine dioxygenase 3	6.75E-03	0.7656
Tmem184b	Transmembrane protein 184b	4.14E-02	0.6102
Tnfrsf26	Tumor necrosis factor receptor superfamily, member 26	3.43E-02	0.5553

Tnfsf8	Tumor necrosis factor (ligand) superfamily, member 8	1.02E-03	-0.7095
Tob1	Transducer of ErbB-2.1	1.02E-03	0.8293
Tomm7	Translocase of outer mitochondrial membrane 7	1.65E-03	-0.7633
Traf1	TNF receptor-associated factor 1	1.66E-02	-0.6020
Trim25	Tripartite motif-containing 25	3.56E-03	0.5644
Trim59	Tripartite motif-containing 59	4.14E-02	0.4341
Tspan31	Tetraspanin 31	1.82E-03	-0.8866
Unc5a	Unc-5 netrin receptor A	2.99E-02	-1.9817
Uqcrh	Ubiquinol-cytochrome c reductase hinge protein	4.87E-02	-0.4087
Use1	Unconventional SNARE in the ER 1 homolog (S. cerevisiae)	3.28E-02	-0.4644
Usp18	Ubiquitin specific peptidase 18	4.64E-03	0.7152
Zfp36l2	Zinc finger protein 36, C3H type-like 2	3.82E-03	0.5878

Table 2.4 Female and Male Overlapping DEGs

	Female		Male	
Gene Symbol	Adj p Value	Log2 Fold Change	Adj p Value	Log2 Fold Change
1500012F01Rik	4.94E-03	-1.0524	1.46E-05	-1.1708
2410006H16Rik	4.38E-04	-1.0788	1.07E-03	-1.1059
Adss	3.58E-04	-0.7469	5.06E-08	-0.6860
Aldh1l1	9.61E-03	-1.6002	1.79E-05	-2.6125
Apol10b	1.57E-08	-3.6822	9.09E-16	-4.3784
Appl2	3.79E-03	1.1352	1.83E-02	1.1032
Arhgap29	7.84E-06	1.5590	9.05E-03	0.6801
AW112010	5.79E-06	-1.0852	1.69E-11	-1.1010
Bmpr1a	4.49E-21	-3.8931	2.00E-18	-3.1579
Cacnb3	5.86E-08	-2.8478	4.63E-02	-1.4560
Casp1	3.15E-11	-3.0164	2.69E-03	-3.5607
Casp4	3.42E-07	-3.5999	1.43E-09	-3.4210
Ccl5	4.49E-21	-5.4775	9.36E-03	-2.8902
Cd200r4	1.80E-06	-2.6842	2.36E-06	-2.0723
Cd86	2.09E-03	1.7294	2.10E-02	1.5134
Dtx1	1.04E-02	0.7035	8.73E-06	0.8036
Enc1	1.49E-03	0.8184	1.53E-03	0.6091
Fbxo17	1.02E-05	-2.3884	1.73E-03	-1.7169
Gas5	2.71E-02	-0.7366	2.40E-06	-0.9060
Gbp2	2.16E-02	-0.7099	3.95E-03	-0.6231
Gm4841	1.02E-04	-5.7597	8.12E-04	-3.6705
Gm4951	1.49E-04	-6.4540	1.59E-04	-4.3977
Gm7120	1.22E-02	-1.2963	4.64E-03	-1.3632
Gm7609	3.42E-07	-2.9338	1.66E-12	-4.0232
Gzmk	1.08E-08	-8.7232	2.86E-02	-4.4424
H2-DMa	2.15E-04	-0.9710	1.12E-05	-0.9216
Icam1	1.10E-03	-1.0113	1.81E-02	-0.7490
Ildr1	2.07E-02	2.4758	1.67E-03	2.6255
Insl6	2.83E-04	-1.3229	3.84E-05	-1.3871
Klrd1	1.10E-03	1.4582	3.84E-05	1.4034
Mrpl52	4.94E-02	-0.7541	3.80E-02	-0.5990
Nacc2	1.71E-04	0.9090	1.38E-08	1.1583
Ndrg3	1.81E-05	-0.8692	4.14E-02	-0.4223
Nnt	1.17E-08	1.3178	3.40E-12	1.2261
Pdcd4	3.52E-03	0.7233	1.10E-02	0.4678
Rab4a	1.57E-14	3.8931	5.28E-15	4.6030
Raver2	1.66E-02	-1.0172	3.56E-03	-1.0146
Rell1	2.05E-05	-1.7039	3.14E-10	-2.1798
Sox4	4.81E-02	-0.7521	4.87E-02	0.8960
Synj2	3.52E-03	-1.4869	5.04E-11	-1.6958
Syt11	5.47E-06	-1.0334	2.95E-02	-0.7932
Tdrp	1.98E-04	0.7991	1.49E-02	0.5720
Tspan9	3.42E-07	1.8474	7.99E-13	2.4207
Wdfy1	3.06E-16	3.4306	1.86E-17	2.7677

Table 2.5 Female Glycosylation Genes and Other DEGs

Gene Symbol	Gene Description	Adj. p value	Log2 Fold Change
Adpgk	ADP-dependent glucokinase	0.2667	0.4553
B3gnt1	UDP-GlcNAc:betaGal beta-1,3-N-acetylglucosaminyltransferase 1	0.9492	-0.0719
B3gnt2	UDP-GlcNAc:betaGal beta-1,3-N-acetylglucosaminyltransferase 2	0.9933	-0.0089
B3gnt3	UDP-GlcNAc:betaGal beta-1,3-N-acetylglucosaminyltransferase 3	0.1635	-1.1030
B3gnt4	UDP-GlcNAc:betaGal beta-1,3-N-acetylglucosaminyltransferase 4	NA	NA
B3gnt5	UDP-GlcNAc:betaGal beta-1,3-N-acetylglucosaminyltransferase 5	0.8926	0.2225
B3gnt6	UDP-GlcNAc:betaGal beta-1,3-N-acetylglucosaminyltransferase 6	NA	NA
B3gnt7	UDP-GlcNAc:betaGal beta-1,3-N-acetylglucosaminyltransferase 7	NA	NA
B3gnt8	UDP-GlcNAc:betaGal beta-1,3-N-acetylglucosaminyltransferase 8	0.8538	-1.3941
B3gnt9	UDP-GlcNAc:betaGal beta-1,3-N-acetylglucosaminyltransferase 9,	0.7621	-0.8225
B3gntl1	UDP-GlcNAc:betaGal beta-1,3-N-acetylglucosaminyltransferase-like 1	0.7954	-0.4591
B4galnt4	Beta-1,4-N-acetyl-galactosaminyl transferase 4	NA	-2.1628
B4galt1	UDP-Gal:betaGlcNAc beta 1,4-galactosyltransferase, polypeptide 1	0.8171	0.1699
B4galt2	UDP-Gal:betaGlcNAc beta 1,4-galactosyltransferase, polypeptide 2	NA	NA
B4galt3	UDP-Gal:betaGlcNAc beta 1,4-galactosyltransferase, polypeptide 3	0.9838	-0.0304
B4galt4	UDP-Gal:betaGlcNAc beta 1,4-galactosyltransferase, polypeptide 4	NA	0.6647
B4galt5	UDP-Gal:betaGlcNAc beta 1,4-galactosyltransferase, polypeptide 5	0.8672	0.1776
B4galt6	UDP-Gal:betaGlcNAc beta 1,4-galactosyltransferase, polypeptide 6	NA	NA
B4galt7	Beta1,4-galactosyltransferase	0.9916	0.0163
Eno1	Enolase 1, alpha-non-neuron	NA	NA
Eno1b	Enolase 1B, retrotransposed	0.9874	-0.0574
Eno2	Enolase 2	0.9951	-0.0548
Eno3	Enolase 3	0.9750	-0.0723
Eno4	Enolase 4	NA	NA
G6pdx	Glucose 6-phosphate dehydrogenase X-linked	0.8639	-0.1468
Gale	Galactose-4-epimerase, UDP	0.9290	-0.1841
Gck	Glucokinase	NA	NA
Gfpt1	Glutamine fructose-6-phosphate transaminase 1	0.8732	0.1748
Gfpt2	Glutamine fructose-6-phosphate transaminase 2	NA	-1.7757
Gls	Glutaminase	0.7603	0.2730
Glud1	Glutamate dehydrogenase 1	0.8985	0.0978
Gne	UDP-N-acetylglucosamine 2-epimerase/N-acetylmannosamine kinase	0.6054	0.3886
Gnpda1	Glucosamine-6-phosphate deaminase 1	0.8257	-0.1663
Gnpda2	Glucosamine-6-phosphate deaminase 2	0.9777	-0.0309
Gnpnat1	Glucosamine-phosphate N-acetyltransferase 1	0.7259	-0.2546
Got1	Glutamic-oxaloacetic transaminase 1	0.9740	-0.0327
Got1l1	Glutamic-oxaloacetic transaminase 1 like 1	NA	NA
Got2	Glutamic-ocaloacetic transaminase 2	0.6621	-0.2742
Gpi1	Glucose phosphate isomerase 1	0.5984	-0.3103
Gpt	Glutamic pyruvic transaminase, soluble	0.8542	-0.2380
Gpt2	Glutamic pyruvic transaminase (alaline aminotransferase) 2	0.9966	0.0295
Hk1	Hexokinase 1	0.9094	0.1194
Hk2	Hexokinase 2	NA	1.1863
Hk3	Hexokinase 3	NA	1.6616
Ldha	Lactate dehydrogenase A	0.8161	-0.1629
Man1a	Mannosidase 1, alpha	0.8152	0.2135
Man1a2	Mannosidase, alpha, class 1A, member 2	0.7477	0.2740
Man1b1	Mannosidase, alpha, class 1B, member 1	0.7946	0.1982
Man1c1	Mannosidase, alpha, class 1C, member 1	0.8367	0.3325
Man2a1	Mannosidase 2, alpha 1	0.6904	0.4323
Man2a2	Mannosidase 2, alpha 2	0.6098	0.4007
Man2b1	Mannosidase 2, alpha B1	0.9458	-0.0666
Man2b2	Mannosidase 2, alpha B2	0.9094	-0.1241
Man2c1	Mannosidase, alpha, class 2C, member 1	0.9147	0.1061
Mgat1	Mannoside acetylglucosaminyltransferase 1	0.9951	-0.0066
Mgat2	Mannoside acetylglucosaminyltransferase 2	0.9848	0.0200
Mgat3	Mannoside acetylglucosaminyltransferase 3	NA	NA
Mgat4a	Mannoside acetylglucosaminyltransferase 4, isoenzyme A	0.9886	0.0181
Mgat4b	Mannoside acetylglucosaminyltransferase 4, isoenzyme B	0.8412	-0.4425
Mgat4c	Alpha-1,3-mannosyl-glycoprotein beta-1,4-N-acetylglucosaminyltransferase, isozyme C (putative)	NA	NA
Mgat5	Mannoside acetylglucosaminyltransferase 5	0.9951	0.0155
Mgat5b	Mannoside acetylglucosaminyltransferase 5, isoenzyme B	NA	NA
Nagk	N-acetylglucosamine kinase	0.9725	-0.0562
Nat9	N-acetyltransferase 9 (GCN5-related, putative)	0.8148	-0.3844
Pfkfb1	6-phosphofructo-2-kinase/fructose-2,6-biphosphatase 1	0.9926	-0.0792

Pfkfb2	6-phosphofructo-2-kinase/fructore-2,6-biphosphatase 2	0.9352	0.1375
Pfkfb3	6-phosphofructo-2-kinase/fructore-2,6-biphosphatase 3	0.8717	0.1664
Pfkfb4	6-Phosphofructo-2-kinase/fructose-2,6-biphosphatase 4	0.9886	0.0325
Pfkl	Phosphofructokinase, liver, B-type	0.8665	0.1334
Pfkm	Phosphofructokinase, muscle	0.8862	-0.1830
Pfkp	Phosphofructokinase, platlet	0.9872	0.0170
Pgd	6-phosphogluconate dehydrogenase	0.8995	0.1036
Pgls	6-phosphogluconolactonase	0.1747	-0.6230
Pgm1	Phosphoglucomutase 1	0.6213	-0.3442
Pgm2	Phosphoglucomutase 2	0.5783	-0.3919
Pgm2l1	Phosphoglucomutase 2-like 1	0.5350	0.5911
Pgm3	Phosphoglucomutase 3	0.9454	0.0952
Pgm5	Phosphoglucomutase 5	NA	NA
Pklr	Pyruvate kinase liver and red blood cell	NA	NA
Pkm	Pyruvate kinase, muscle	0.7581	-0.1902
Rpe	Ribulase-5-phosphase-3-epimerase	0.8242	0.1568
Rpia	Ribose 5-phosphate isomerase A	0.9838	0.0237
Slc1a5	Solute carrier family 1 (neutral amino acid transporter), member 5	0.6652	-0.3384
Slc2a1	Solute carrier family 2 (facilitated glucose transporter), member 1	0.9792	-0.0278
Slc2a2	Solute carrier family 2 (facilitated glucose transporter), member 2	NA	-0.8863
Slc2a4	Solute carrier family 2 (facilitated glucose transporter), member 4	NA	NA
Slc2a4rg-ps	Slc2a4 regulator, pseudogene	0.7881	-0.5256
Slc35a3	Solute carrier family 35 (UDP-GlcNAc transporter), member 3	0.8936	0.1578
Slc35d1	Solute carrier family 35, member D1	0.9472	0.1239
Slc35d2	Solute carrier family 35, member D2	0.9777	0.0458
Slc35d3	Solute carrier family 35, member D3	NA	NA
Slc38a1	Solute carrier family 38, member 1	0.8412	0.1757
Slc38a2	Solute carrier family 38, member 2	0.9630	0.0507
Slc38a3	Solute carrier family 38, member 3	NA	NA
Slc38a5	Solute carrier family 38, member 5	NA	NA
Slc38a7	Solute carrier family 38, member 7	0.7895	-0.2652
Slc6a14	Solute carrier family 6, member 14	NA	NA
Slc6a15	Solute carrier family 6 (neurotransmitter transporter), member 15	NA	NA
Slc6a19	Solute carrier family 6 (neurotransmitter transporter), member 19	0.9964	-0.0423
Slc7a5	Solute carrier family 7 member 5	0.3858	-0.4038
Slc7a6	Solute carrier family 7 member 6	0.9995	-0.0005
Slc7a8	Solute carrier family 7 member 8	NA	0.5053
Taldo1	Transaldolase 1	0.7591	-0.2029
Tkt	Transketolase	0.7546	-0.2091
Uap1	UDP-N-acetylglucosamine pyrophosphorylase 1	0.7297	0.2763
Uap1l1	UDP-N-acteylglucosamine pyrophosphorylase 1-like 1	0.9271	-0.1403

References

1 Simonsen, L. *et al.* Impact of influenza vaccination on seasonal mortality in the US elderly population. *Arch Intern Med* **165**, 265-272, doi:10.1001/archinte.165.3.265 (2005).

2 Thompson, W. W. *et al.* Estimating influenza-associated deaths in the United States. *Am J Public Health* **99 Suppl 2**, S225-230, doi:10.2105/AJPH.2008.151944 (2009).

3 Thompson, W. W. *et al.* Mortality associated with influenza and respiratory syncytial virus in the United States. *JAMA* **289**, 179-186, doi:10.1001/jama.289.2.179 (2003).

4 Thompson, W. W. *et al.* Estimates of US influenza-associated deaths made using four different methods. *Influenza Other Respir Viruses* **3**, 37-49, doi:10.1111/j.1750-2659.2009.00073.x (2009).

5 Nikolich-Zugich, J. *et al.* SARS-CoV-2 and COVID-19 in older adults: what we may expect regarding pathogenesis, immune responses, and outcomes. *Geroscience* **42**, 505-514, doi:10.1007/s11357-020-00186-0 (2020).

6 Chen, P. L. *et al.* Non-typhoidal Salmonella bacteraemia in elderly patients: an increased risk for endovascular infections, osteomyelitis and mortality. *Epidemiol Infect* **140**, 2037-2044, doi:10.1017/S0950268811002901 (2012).

7 Maue, A. C. *et al.* T-cell immunosenescence: lessons learned from mouse models of aging. *Trends Immunol* **30**, 301-305, doi:10.1016/j.it.2009.04.007 (2009).

8 Palmer, S., Albergante, L., Blackburn, C. C. & Newman, T. J. Thymic involution and rising disease incidence with age. *Proc Natl Acad Sci U S A* **115**, 1883-1888, doi:10.1073/pnas.1714478115 (2018).

9 Han, S. N. *et al.* Age and vitamin E-induced changes in gene expression profiles of T cells. *J Immunol* **177**, 6052-6061, doi:10.4049/jimmunol.177.9.6052 (2006).

10 Mirza, N., Pollock, K., Hoelzinger, D. B., Dominguez, A. L. & Lustgarten, J. Comparative kinetic analyses of gene profiles of naive CD4+ and CD8+ T cells from young and old animals reveal novel age-related alterations. *Aging Cell* **10**, 853-867, doi:10.1111/j.1474-9726.2011.00730.x (2011).

11 Taylor, J. *et al.* Transcriptomic profiles of aging in naive and memory CD4(+) cells from mice. *Immun Ageing* **14**, 15, doi:10.1186/s12979-017-0092-5 (2017).

12 Bektas, A. *et al.* Age-associated changes in basal NF-kappaB function in human CD4+ T lymphocytes via dysregulation of PI3 kinase. *Aging (Albany NY)* **6**, 957-974, doi:10.18632/aging.100705 (2014).

13 Miller, M. L. *et al.* Basal NF-kappaB controls IL-7 responsiveness of quiescent naive T cells. *Proc Natl Acad Sci U S A* **111**, 7397-7402, doi:10.1073/pnas.1315398111 (2014).

14 Reynolds, L. M. *et al.* Transcriptomic profiles of aging in purified human immune cells. *BMC Genomics* **16**, 333, doi:10.1186/s12864-015-1522-4 (2015).

15 Demetriou, M., Granovsky, M., Quaggin, S. & Dennis, J. W. Negative regulation of T-cell activation and autoimmunity by Mgat5 N-glycosylation. *Nature* **409**, 733-739, doi:10.1038/35055582 (2001).

16 Lau, K. S. *et al.* Complex N-glycan number and degree of branching cooperate to regulate cell proliferation and differentiation. *Cell* **129**, 123-134, doi:10.1016/j.cell.2007.01.049 (2007).

17 Mkhikian, H. *et al.* Genetics and the environment converge to dysregulate N-glycosylation in multiple sclerosis. *Nat Commun* **2**, 334, doi:10.1038/ncomms1333 (2011).

18 Mkhikian, H. *et al.* Golgi self-correction generates bioequivalent glycans to preserve cellular homeostasis. *Elife* **5**, doi:10.7554/eLife.14814 (2016).

19 Zhou, R. W. *et al.* N-glycosylation bidirectionally extends the boundaries of thymocyte positive selection by decoupling Lck from Ca(2)(+) signaling. *Nat Immunol* **15**, 1038-1045, doi:10.1038/ni.3007 (2014).

20 Araujo, L., Khim, P., Mkhikian, H., Mortales, C. L. & Demetriou, M. Glycolysis and glutaminolysis cooperatively control T cell function by limiting metabolite supply to N-glycosylation. *eLife* **6**, doi:10.7554/eLife.21330 (2017).

21 Grigorian, A. *et al.* N-acetylglucosamine inhibits T-helper 1 (Th1)/T-helper 17 (Th17) cell responses and treats experimental autoimmune encephalomyelitis. *J Biol Chem* **286**, 40133-40141, doi:10.1074/jbc.M111.277814 (2011).

22 Grigorian, A. *et al.* Control of T Cell-mediated autoimmunity by metabolite flux to N-glycan biosynthesis. *J Biol Chem* **282**, 20027-20035, doi:10.1074/jbc.M701890200 (2007).

23 Lee, S. U. *et al.* N-glycan processing deficiency promotes spontaneous inflammatory demyelination and neurodegeneration. *J Biol Chem* **282**, 33725-33734, doi:10.1074/jbc.M704839200 (2007).

24 Morgan, R. *et al.* N-acetylglucosaminyltransferase V (Mgat5)-mediated N-glycosylation negatively regulates Th1 cytokine production by T cells. *J Immunol* **173**, 7200-7208, doi:10.4049/jimmunol.173.12.7200 (2004).

25 Grigorian, A. & Demetriou, M. Manipulating cell surface glycoproteins by targeting N-glycan-galectin interactions. *Methods Enzymol* **480**, 245-266, doi:10.1016/S0076-6879(10)80012-6 (2010).

26 Grigorian, A., Torossian, S. & Demetriou, M. T-cell growth, cell surface organization, and the galectin-glycoprotein lattice. *Immunol Rev* **230**, 232-246, doi:10.1111/j.1600-065X.2009.00796.x (2009).

27 Mortales, C. L., Lee, S. U. & Demetriou, M. N-Glycan Branching Is Required for Development of Mature B Cells. *J Immunol* **205**, 630-636, doi:10.4049/jimmunol.2000101 (2020).

28 Dennis, J. W., Nabi, I. R. & Demetriou, M. Metabolism, cell surface organization, and disease. *Cell* **139**, 1229-1241, doi:10.1016/j.cell.2009.12.008 (2009).

29 Abdel Rahman, A. M., Ryczko, M., Pawling, J. & Dennis, J. W. Probing the hexosamine biosynthetic pathway in human tumor cells by multitargeted tandem mass spectrometry. *ACS Chem Biol* **8**, 2053-2062, doi:10.1021/cb4004173 (2013).

30 Aspinall, R. & Andrew, D. Thymic involution in aging. *J Clin Immunol* **20**, 250-256, doi:10.1023/a:1006611518223 (2000).

31 Haynes, B. F., Sempowski, G. D., Wells, A. F. & Hale, L. P. The human thymus during aging. *Immunol Res* **22**, 253-261, doi:10.1385/IR:22:2-3:253 (2000).

32 Lazuardi, L. *et al.* Age-related loss of naive T cells and dysregulation of T-cell/B-cell interactions in human lymph nodes. *Immunology* **114**, 37-43, doi:10.1111/j.1365-2567.2004.02006.x (2005).

33 Blaschitz, C. & Raffatellu, M. Th17 cytokines and the gut mucosal barrier. *J Clin Immunol* **30**, 196-203, doi:10.1007/s10875-010-9368-7 (2010).

34 Liu, J. Z., Pezeshki, M. & Raffatellu, M. Th17 cytokines and host-pathogen interactions at the mucosa: dichotomies of help and harm. *Cytokine* **48**, 156-160, doi:10.1016/j.cyto.2009.07.005 (2009).

35 Ren, Z. *et al.* Effect of age on susceptibility to Salmonella Typhimurium infection in C57BL/6 mice. *J Med Microbiol* **58**, 1559-1567, doi:10.1099/jmm.0.013250-0 (2009).

36 Carrette, F. & Surh, C. D. IL-7 signaling and CD127 receptor regulation in the control of T cell homeostasis. *Semin Immunol* **24**, 209-217, doi:10.1016/j.smim.2012.04.010 (2012).

37 Juffroy, O. *et al.* Dual mechanism of impairment of interleukin-7 (IL-7) responses in human immunodeficiency virus infection: decreased IL-7 binding and abnormal activation of the JAK/STAT5 pathway. *J Virol* **84**, 96-108, doi:10.1128/JVI.01475-09 (2010).

38 Martin, C. E. *et al.* IL-7/anti-IL-7 mAb complexes augment cytokine potency in mice through association with IgG-Fc and by competition with IL-7R. *Blood* **121**, 4484-4492, doi:10.1182/blood-2012-08-449215 (2013).

39 Valenzona, H. O., Dhanoa, S., Finkelman, F. D. & Osmond, D. G. Exogenous interleukin 7 as a proliferative stimulant of early precursor B cells in mouse bone

marrow: efficacy of IL-7 injection, IL-7 infusion and IL-7-anti-IL-7 antibody complexes. *Cytokine* **10**, 404-412, doi:10.1006/cyto.1997.0312 (1998).

40 Dorshkind, K., Montecino-Rodriguez, E. & Signer, R. A. The ageing immune system: is it ever too old to become young again? *Nat Rev Immunol* **9**, 57-62, doi:10.1038/nri2471 (2009).

41 Surh, C. D. & Sprent, J. Homeostatic T cell proliferation: how far can T cells be activated to self-ligands? *J Exp Med* **192**, F9-F14, doi:10.1084/jem.192.4.f9 (2000).

42 Goronzy, J. J. & Weyand, C. M. Mechanisms underlying T cell ageing. *Nat Rev Immunol* **19**, 573-583, doi:10.1038/s41577-019-0180-1 (2019).

43 Fairweather, D., Frisancho-Kiss, S. & Rose, N. R. Sex differences in autoimmune disease from a pathological perspective. *Am J Pathol* **173**, 600-609, doi:10.2353/ajpath.2008.071008 (2008).

44 Fairweather, D. & Rose, N. R. Women and autoimmune diseases. *Emerg Infect Dis* **10**, 2005-2011, doi:10.3201/eid1011.040367 (2004).

45 Jin, J. M. *et al.* Gender Differences in Patients With COVID-19: Focus on Severity and Mortality. *Front Public Health* **8**, 152, doi:10.3389/fpubh.2020.00152 (2020).

46 Fink, A. L. & Klein, S. L. Sex and Gender Impact Immune Responses to Vaccines Among the Elderly. *Physiology (Bethesda)* **30**, 408-416, doi:10.1152/physiol.00035.2015 (2015).

47 Ryan, M. R. *et al.* An IL-7-dependent rebound in thymic T cell output contributes to the bone loss induced by estrogen deficiency. *Proc Natl Acad Sci U S A* **102**, 16735-16740, doi:10.1073/pnas.0505168102 (2005).

48 Weitzmann, M. N., Roggia, C., Toraldo, G., Weitzmann, L. & Pacifici, R. Increased production of IL-7 uncouples bone formation from bone resorption during estrogen deficiency. *J Clin Invest* **110**, 1643-1650, doi:10.1172/JCI15687 (2002).

49 Decaroli, M. C. & Rochira, V. Aging and sex hormones in males. *Virulence* **8**, 545-570, doi:10.1080/21505594.2016.1259053 (2017).

50 Nikolich-Zugich, J. The twilight of immunity: emerging concepts in aging of the immune system. *Nat Immunol* **19**, 10-19, doi:10.1038/s41590-017-0006-x (2018).

51 Li, G. *et al.* Decline in miR-181a expression with age impairs T cell receptor sensitivity by increasing DUSP6 activity. *Nat Med* **18**, 1518-1524, doi:10.1038/nm.2963 (2012).

52 Lev, A. *et al.* Reduced Function and Diversity of T Cell Repertoire and Distinct Clinical Course in Patients With IL7RA Mutation. *Front Immunol* **10**, 1672, doi:10.3389/fimmu.2019.01672 (2019).

53 Muegge, K., Vila, M. P. & Durum, S. K. Interleukin-7: a cofactor for V(D)J rearrangement of the T cell receptor beta gene. *Science* **261**, 93-95, doi:10.1126/science.7686307 (1993).

54 Lundstrom, W., Fewkes, N. M. & Mackall, C. L. IL-7 in human health and disease. *Semin Immunol* **24**, 218-224, doi:10.1016/j.smim.2012.02.005 (2012).

55 Andrew, D. & Aspinall, R. Il-7 and not stem cell factor reverses both the increase in apoptosis and the decline in thymopoiesis seen in aged mice. *J Immunol* **166**, 1524-1530, doi:10.4049/jimmunol.166.3.1524 (2001).

56 Henson, S. M., Snelgrove, R., Hussell, T., Wells, D. J. & Aspinall, R. An IL-7 fusion protein that shows increased thymopoietic ability. *J Immunol* **175**, 4112-4118, doi:10.4049/jimmunol.175.6.4112 (2005).

Chapter 3

Conclusions and Future Directions

Aging is inevitable, resulting in a time-dependent decline in immune function. With advances in modern technology in healthcare, life expectancy is increasing and populations in the most developed countries of the world are rapidly aging. In recent years however, there have been growing empirical evidence, based on animal models, suggesting that the aging process could be delayed and immune function can be rejuvenated among the elderly[1]. Indeed, we have demonstrated that age-associated increase of N-glycan branching, via increased supply of GlcNAc and IL-7 signaling, contributes to impaired T cell immunity in females. Reversing this phenotype rejuvenates T cell responses, providing a novel therapeutic target for immune senescence and diseases that target the elderly.

An important question is what leads to the age associated increases in serum GlcNAc. Serum GlcNAc is excreted in the kidney and therefore this may track with kidney function. However, this will require formal testing. Serum GlcNAc and/or $CD4^+$ T_N cell N-glycan branching level may serve as useful biomarkers of T cell aging. In future work it will be important to determine whether variability in serum GlcNAc and/or N-glycan branching correlates with variability in clinical immune function or vaccine responses in the elderly.

Aging and N-glycosylation in cancer immunotherapy

Along with an increase in life expectancy is a shift of an increasing proportion of individuals with cancer[2]. Among cancer immunotherapies, neutralizing antibodies that target immune checkpoints CTLA-4 and PD-1 are particularly successful[3,4]. Although these antibodies have resulted in dramatic improvements in disease outcome, a majority

of advanced stage cancer patients do not response or will relapse. Although cancer is known as a disease of old age where most cancer diagnoses are from elderly patients above the age of 65[5-7], a majority of studies have shown that age limits activity of anti-PD1 and anti-CTLA-4 immunotherapy, diminishing their efficiency and effect[8,9]. N-glycan branching promotes PD-1 and CTLA-4 surface expression on blasting T cells[10]. Age-dependent increase in N-glycan branching would suggest an antagonistic effect against immune check point inhibitors such as anti-PD1 and anti-CTLA-4. Supplementing these immune check point blocking treatments with agents that target N-glycan branching may improve efficiency. We have previously shown that age-induced increases in N-glycan branching functionally suppresses T cell activity. Reversing age-dependent increase in N-glycan branching will restore T cell function by promoting TCR clustering and signaling, reduce surface expression of PD-1 and CTLA-4, and promote pro-inflammatory T_H1 and T_H17 differentiation over anti-inflammatory T_H2 and Treg. Together with our findings of age-dependent increase in N-glycan branching merits exploring the effect of these agents in coordination with immune check point therapy.

Aging, IL-7, and N-glycosylation: how it impacts COVID-19 symptoms

Introductory studies produced in identifying conditions common among patients with the most severe COVID-19 symptoms narrowed down to those who are older (above 65 years in age)[11], male[12], or with lung conditions including asthma[13,14]. An early analysis that investigated a little more than 1500 patients concluded that patients with asthma were no more likely than those without asthma to be hospitalized[14]. However, the study didn't investigate whether different types of asthma have different levels of risk. Thus another

recent study analyzed two asthma subtypes – allergic and non-allergic asthma – as separate risk factors[13]. The population-based study which analyzed medical records from 492,768 individuals found that non-allergic asthma significantly heightened the likelihood of severe COVID-19 whereas allergic asthma had no statistically significance associated with severe COVID-19[13].

IL-2 and IL-7, which are responsible for expansion and differentiation of various T cell subsets, are increased in the sera of patients with COVID-19[15], possibly due to lymphopenia increasing cytokine availability[16-18]. Recent studies have identified TSLP as a novel molecular player in non-allergen induced inflammatory conditions[19,20]. Our studies suggest that, when comparing to elderly women, men have less IL-7 signaling in T cells which results in a lack of negative feedback of IL-7Rα surface expression which may increase TSLP signaling to both suppress the development of tolerance to allergens within the lungs while enhancing pro-inflammatory T_H2 responses[21-23].

Currently research is being focused primarily on the coronavirus transmembrane spike (S) glycoprotein, which extends from the viral surface to mediate host cell entry. This results in a crosstalk between the virus S-glycoprotein to the ACE2 receptor on the surface of human cells. With 66 N-linked glycosylation sites on the S-glycoprotein, the glycan diversity allows the pathogen to escape immune system response[24,25]. Controversial antimalarial drug chloroquine, and its alternative hydroxychloroquine, have shown effectiveness *in vitro* in inhibiting SARS-CoV-2 infection by altering glycosylation profiles of the ACE2 receptor, thus interfering with host-cell binding and entry and its subsequent viral replication, although no effect is seen among actual COVID-19 patients[26,27]. Perhaps higher levels of N-glycosylation on naïve immune cells in elderly

women may be responsible in interfering with the viral S-glycoprotein binding to the host ACE2 receptor, thus resulting in less severe infection and symptoms when compared to men. Further studies are required to understand the role of glycosylation on these viral and host proteins if we are to successfully diagnose, treat, and eventually prevent COVID-19.

Summary

It is now prevalent that N-glycan branching is dynamically regulated with age and plays a role in immune senescence, however further studies are required to understand the extent of N-glycosylation and its role in regulating viral and vaccine response, cancer immunotherapy, and general immune response. Indeed, there are many age-related diseases and disorders in which we do not have a good understanding of what causes it or how it progresses. With the discovery that N-glycan branching increases with age secondary to up-regulation of IL-7 availability to naïve CD4+ T cells in females, it is increasingly important to explore glycosylation as a factor in age-related diseases and disorders. Furthermore, these treatments must take into consideration differences in sex in order to appropriately customize treatment to individuals.

References

1 Beltran-Sanchez, H., Soneji, S. & Crimmins, E. M. Past, Present, and Future of Healthy Life Expectancy. *Cold Spring Harb Perspect Med* **5**, doi:10.1101/cshperspect.a025957 (2015).

2 Aunan, J. R., Cho, W. C. & Soreide, K. The Biology of Aging and Cancer: A Brief Overview of Shared and Divergent Molecular Hallmarks. *Aging Dis* **8**, 628-642, doi:10.14336/AD.2017.0103 (2017).

3 Seidel, J. A., Otsuka, A. & Kabashima, K. Anti-PD-1 and Anti-CTLA-4 Therapies in Cancer: Mechanisms of Action, Efficacy, and Limitations. *Front Oncol* **8**, 86, doi:10.3389/fonc.2018.00086 (2018).

4 Weber, J. Immune checkpoint proteins: a new therapeutic paradigm for cancer--preclinical background: CTLA-4 and PD-1 blockade. *Semin Oncol* **37**, 430-439, doi:10.1053/j.seminoncol.2010.09.005 (2010).

5 Weng, N. P. Aging of the immune system: how much can the adaptive immune system adapt? *Immunity* **24**, 495-499, doi:10.1016/j.immuni.2006.05.001 (2006).

6 Weyand, C. M. & Goronzy, J. J. Aging of the Immune System. Mechanisms and Therapeutic Targets. *Ann Am Thorac Soc* **13 Suppl 5**, S422-S428, doi:10.1513/AnnalsATS.201602-095AW (2016).

7 Daste, A. *et al.* Immune checkpoint inhibitors and elderly people: A review. *Eur J Cancer* **82**, 155-166, doi:10.1016/j.ejca.2017.05.044 (2017).

8 Padron, A. *et al.* Age effects of distinct immune checkpoint blockade treatments in a mouse melanoma model. *Exp Gerontol* **105**, 146-154, doi:10.1016/j.exger.2017.12.025 (2018).

9 Elias, R. *et al.* Efficacy of PD-1 & PD-L1 inhibitors in older adults: a meta-analysis. *J Immunother Cancer* **6**, 26, doi:10.1186/s40425-018-0336-8 (2018).

10 Lau, K. S. *et al.* Complex N-glycan number and degree of branching cooperate to regulate cell proliferation and differentiation. *Cell* **129**, 123-134, doi:10.1016/j.cell.2007.01.049 (2007).

11 Nikolich-Zugich, J. *et al.* SARS-CoV-2 and COVID-19 in older adults: what we may expect regarding pathogenesis, immune responses, and outcomes. *Geroscience* **42**, 505-514, doi:10.1007/s11357-020-00186-0 (2020).

12 Jin, J. M. *et al.* Gender Differences in Patients With COVID-19: Focus on Severity and Mortality. *Front Public Health* **8**, 152, doi:10.3389/fpubh.2020.00152 (2020).

13 Zhu, Z. *et al.* Association of asthma and its genetic predisposition with the risk of severe COVID-19. *J Allergy Clin Immunol* **146**, 327-329 e324, doi:10.1016/j.jaci.2020.06.001 (2020).

14 Chhiba, K. D. *et al.* Prevalence and characterization of asthma in hospitalized and nonhospitalized patients with COVID-19. *J Allergy Clin Immunol* **146**, 307-314 e304, doi:10.1016/j.jaci.2020.06.010 (2020).

15 Huang, C. *et al.* Clinical features of patients infected with 2019 novel coronavirus in Wuhan, China. *Lancet* **395**, 497-506, doi:10.1016/S0140-6736(20)30183-5 (2020).

16 Zhang, Y. *et al.* Potential contribution of increased soluble IL-2R to lymphopenia in COVID-19 patients. *Cell Mol Immunol* **17**, 878-880, doi:10.1038/s41423-020-0484-x (2020).

17 Tan, L. *et al.* Lymphopenia predicts disease severity of COVID-19: a descriptive and predictive study. *Signal Transduct Target Ther* **5**, 33, doi:10.1038/s41392-020-0148-4 (2020).

18 Henry, B. M. COVID-19, ECMO, and lymphopenia: a word of caution. *Lancet Respir Med* **8**, e24, doi:10.1016/S2213-2600(20)30119-3 (2020).

19 Lo Kuan, E. & Ziegler, S. F. Thymic stromal lymphopoietin and cancer. *J Immunol* **193**, 4283-4288, doi:10.4049/jimmunol.1400864 (2014).

20 Roan, F. *et al.* The multiple facets of thymic stromal lymphopoietin (TSLP) during allergic inflammation and beyond. *J Leukoc Biol* **91**, 877-886, doi:10.1189/jlb.1211622 (2012).

21 Nguyen, K. D., Vanichsarn, C. & Nadeau, K. C. TSLP directly impairs pulmonary Treg function: association with aberrant tolerogenic immunity in asthmatic airway. *Allergy Asthma Clin Immunol* **6**, 4, doi:10.1186/1710-1492-6-4 (2010).

22 Lei, L., Zhang, Y., Yao, W., Kaplan, M. H. & Zhou, B. Thymic stromal lymphopoietin interferes with airway tolerance by suppressing the generation of antigen-specific regulatory T cells. *J Immunol* **186**, 2254-2261, doi:10.4049/jimmunol.1002503 (2011).

23 Perrigoue, J. G. *et al.* MHC class II-dependent basophil-CD4+ T cell interactions promote T(H)2 cytokine-dependent immunity. *Nat Immunol* **10**, 697-705, doi:10.1038/ni.1740 (2009).

24 Wrapp, D. *et al.* Cryo-EM structure of the 2019-nCoV spike in the prefusion conformation. *Science* **367**, 1260-1263, doi:10.1126/science.abb2507 (2020).

25 Watanabe, Y. *et al.* Vulnerabilities in coronavirus glycan shields despite extensive glycosylation. *Nat Commun* **11**, 2688, doi:10.1038/s41467-020-16567-0 (2020).

26 Liu, J. *et al.* Hydroxychloroquine, a less toxic derivative of chloroquine, is effective in inhibiting SARS-CoV-2 infection in vitro. *Cell Discov* **6**, 16, doi:10.1038/s41421-020-0156-0 (2020).

27 Cavalcanti, A. B. *et al.* Hydroxychloroquine with or without Azithromycin in Mild-to-Moderate Covid-19. *N Engl J Med*, doi:10.1056/NEJMoa2019014 (2020).